

Master of Science Thesis

Spatially mass-, kinetic energy- and helicity-preserving mimetic discretization of 3D incompressible Euler flows

Yi Zhang

February 15, 2016



**Spatially mass-, kinetic energy- and helicity-preserving  
mimetic discretization of 3D incompressible Euler flows**

Master of Science Thesis

For obtaining the degree of Master of Science in Aerospace Engineering  
at Delft University of Technology

Yi Zhang

February 15, 2016



Copyright © Aerospace Engineering, Delft University of Technology  
All rights reserved.

DELFT UNIVERSITY OF TECHNOLOGY  
DEPARTMENT OF AERODYNAMICS

The undersigned hereby certify that they have read and recommend to the Faculty of Aerospace Engineering for acceptance the thesis entitled “**Spatially mass-, kinetic energy- and helicity-preserving mimetic discretization of 3D incompressible Euler flows**” by **Yi Zhang** in fulfillment of the requirements for the degree of **Master of Science**.

Dated: February 15, 2016

Supervisor:

---

Dr. ir. M.I. Gerritsma

Readers:

---

Prof. dr. S. Hickel

---

Dr. M. Möller

---

Dr. A. Palha



# Summary

Based on the recently developed mimetic spectral element method, we propose an effective numerical scheme for solving three-dimensional periodic incompressible Euler flows, which spatially preserves mass, kinetic energy and helicity. Preserving multiple integral invariants numerically will significantly contribute to the stability and accuracy of the numerical scheme. We start from the introduction of differential geometry and algebraic topology with which we then set up the mimetic spectral element method (the mimetic framework). With the mimetic spectral element method, physical variables can be expressed in more physical forms and the discretization error will be eliminated as much as possible.

After that, we turn to Euler equations. We first rewrite Euler equations as inner oriented Euler equations and outer oriented Euler equations in terms of differential differential forms. Meanwhile the conservation laws of mass, kinetic energy and helicity based on these new forms of Euler equations at the continuous level are proven. Then, according to expressions of kinetic energy and helicity in the mimetic framework, we convert the inner oriented and outer oriented Euler equations into two weak forms and then spatially discretize them using the mimetic spectral element method in a unit 3-cube  $([-1, 1]^3)$  domain equipped with a cell complex given by the Gauss-Lobatto-Legendre grid. Afterwards, interactions between the two spatially discretized weak forms and discretizations of time derivative terms are constructed, which eventually gives rise to a solvable, mass, kinetic energy and helicity spatially preserved, fully discretized system. The scheme then is tested with a periodic flow.

In summary, the mass conservation is automatically achieved by taking the divergence free flow condition exactly into account. In addition, with proper discretization of the momentum equation and vorticity equation both kinetic energy and helicity are spatially preserved at the discretization level.



# Acknowledgments

This master project is a great challenge for me. Without helps from many people, I can not even imagine that I could complete this journey.

First of all, I would like to express my most sincere gratitude to my supervisor Dr. ir. Marc Gerritsma who constantly supports, guides and motivates me during the whole project. Your vivid explanations and humorous discussions impress, benefit me significantly and always keep me on the right path.

I owe a big debt of gratitude to Dr. Artur Palha. The endless discussions with Artur help me to understand the theories of the mimetic spectral element method and motivate me to develop and improve my scheme, which saves many days for me.

I also greatly appreciate the daily help from all my friends, Pastor Cai, Brother Pan, Anyao, Fei, Si, Renshi, Yanchun, Haiyan, Ye, Lulu, Meixia, Yi, PH, Xiao Feifei, Ku Ou, Tianmu, Li Yan, Weishan, Siqi, Michelle, Yihui, Weiyuan, Yuanyuan, Zihao, Wan Chang, Xinting, Yining, Huiqing Wang, Teng and so many more whom I do not mention here. Your company gives me courage to carry on all the way.

At last, I would like to deeply thank my strongest backbone, my parents, who love me for nothing in return. They give me everything I need, never be impatient or pressure me. Meanwhile, I want to give a special thank to my girlfriend, Yinni Xiao. Your love, support, understanding and encouragement always give me power and make my master career a lovely one.



# Contents

<b>Summary</b>	<b>i</b>
<b>Acknowledgments</b>	<b>iii</b>
<b>Contents</b>	<b>vii</b>
<b>List of figures</b>	<b>ix</b>
<b>List of symbols</b>	<b>xi</b>
<b>1 Introduction</b>	<b>1</b>
1.1 State of art . . . . .	3
1.2 Conservation laws in incompressible Euler equations . . . . .	7
1.3 Thesis outline . . . . .	10
<b>2 Mathematical background</b>	<b>11</b>
2.1 Differential geometry . . . . .	12
2.1.1 Manifolds . . . . .	12

2.1.2	Vectors and covectors . . . . .	13
2.1.3	Orientations . . . . .	16
2.1.4	Differential forms . . . . .	18
2.1.5	True forms and pseudo-forms . . . . .	23
2.1.6	Hodge star operator and codifferential . . . . .	25
2.1.7	Lie derivative . . . . .	27
2.2	Algebraic topology . . . . .	29
2.2.1	Cell complex . . . . .	29
2.2.2	Chain and cochain . . . . .	30
2.2.3	Dual complex . . . . .	33
<b>3</b>	<b>Mimetic spectral element method</b>	<b>35</b>
3.1	Projections . . . . .	36
3.2	Discrete operators . . . . .	38
3.3	Basic functions and reconstructions of discrete forms . . . . .	39
<b>4</b>	<b>Numerical modeling</b>	<b>45</b>
4.1	Conservation laws in mimetic framework . . . . .	45
4.1.1	Inner Euler . . . . .	46
4.1.2	Outer Euler . . . . .	48
4.2	Weak forms and spatial discretizations . . . . .	51
4.2.1	Inner Euler . . . . .	55
4.2.2	Outer Euler . . . . .	57
4.3	Conservation laws at the discrete level . . . . .	59
4.3.1	Inner Euler . . . . .	59

---

4.3.2	Outer Euler . . . . .	61
4.4	Temporal discretizations . . . . .	62
4.4.1	Inner Euler . . . . .	63
4.4.2	Outer Euler . . . . .	64
<b>5</b>	<b>Test case and results</b>	<b>67</b>
<b>6</b>	<b>Conclusions and recommendations</b>	<b>75</b>
6.1	Conclusions . . . . .	76
6.2	Recommendations . . . . .	77
	<b>Reference</b>	<b>82</b>
<b>A</b>	<b>Appendix: Discretizations</b>	<b>83</b>
A.1	Inner Euler discretization . . . . .	86
A.1.1	Mass matrix $\hat{\mathbb{M}}^{(0)}$ . . . . .	87
A.1.2	Mass matrix $\hat{\mathbb{M}}^{(1)}$ . . . . .	87
A.1.3	Mass matrix $\hat{\mathbb{M}}^{(2)}$ . . . . .	88
A.1.4	Matrix $\mathbb{A}$ . . . . .	90
A.1.5	Matrix $\mathbb{B}$ . . . . .	93
A.2	Outer Euler discretization . . . . .	94
A.2.1	Mass matrix $\mathbb{M}^{(1)}$ . . . . .	95
A.2.2	Mass matrix $\mathbb{M}^{(2)}$ . . . . .	95
A.2.3	Mass matrix $\mathbb{M}^{(3)}$ . . . . .	96



# List of figures

2.1	Coordinate charts on a manifold [28]. . . . .	12
2.2	A 2-manifold in $\mathbb{R}^3$ . . . . .	13
2.3	Orientations in vector spaces. . . . .	16
2.4	The positive orientation of 2-dimensional manifold $\mathcal{M}$ . . . . .	17
2.5	Inner (red) and outer (blue) orientations of a 2-manifold in 2-dimensional (left) and 3-dimensional (right) spaces. . . . .	18
2.6	Inner and outer orientations of 0,1,2,3-manifolds in $\mathbb{R}^3$ [28]. . . . .	19
2.7	Cells of a cell complex in $\mathbb{R}^3$ . . . . .	30
2.8	A cell complex in $\mathbb{R}^2$ . . . . .	30
2.9	Coboundaries of cochains. . . . .	33
2.10	A dual complex. . . . .	34
3.1	Projection $\pi$ , reduction $\mathcal{R}$ and reconstruction $\mathcal{I}$ . . . . .	36
3.2	Projections using Gauss-Lobatto-Legendre polynomials at $N = 4$ . . . . .	41
3.3	Gauss-Lobatto-Legendre polynomials and their edge polynomials for $N = 3,4,5$ . . . . .	44

---

4.1	The Gauss-Lobatto-Legendre primal grid (black) and the extended Gauss-Legendre dual grid (red) for $N = 2$ . . . . .	52
4.2	A discrete inner velocity on a Gauss-Lobatto-Legendre grid at $N = 2$ . . . . .	53
4.3	Spatially mass-, kinetic energy- and helicity-preserving numerical scheme. . . . .	65
5.1	Projections of $\cos(\pi x)$ on Gauss-Lobatto-Legendre grids for $N = 3, 5, 7$ . . . . .	67
5.2	Projections of $\sin(\pi x)$ on Gauss-Lobatto-Legendre grids for $N = 3, 5, 7$ . . . . .	68
5.3	Results at $N = 3$ , $\Delta t = 0.0001$ , $t = 2s$ . . . . .	70
5.4	Results at $N = 5$ , $\Delta t = 0.0001$ , $t = 2s$ . . . . .	71
5.5	Results at $N = 7$ , $\Delta t = 0.0001$ , $t = 2s$ . . . . .	72
5.6	Results at $N = 5$ , $\Delta t = 0.0001$ , $t = 20s$ . . . . .	73

## List of symbols

$K$	Kinetic energy
$k$	Kinetic energy density
$E$	Enstrophy
$H$	Helicity
$h$	Helicity density
$\mathcal{M}, \mathcal{N}, \mathcal{U}$	Manifolds
$\mathbb{R}^n$	$n$ -dimensional Euclidean space
$T_p\mathcal{M}$	Tangent space of manifold $\mathcal{M}$
$T_p^\perp\mathcal{M}$	Normal space of manifold $\mathcal{M}$
$T\mathcal{M}$	Tangent bundle of manifold $\mathcal{M}$
$T_p^*\mathcal{M}$	Dual space of tangent space $T_p\mathcal{M}$
$T^*\mathcal{M}$	Cotangent bundle of manifold $\mathcal{M}$
$\flat$	Flat operator
$\sharp$	Sharp operator
$g_{i,j}$	Metric tensor
$\alpha^{(k)}, \beta^{(l)}, \gamma^{(m)}$	Differential forms
$\wedge$	Wedge product
$d$	Exterior derivative
$\langle \alpha^{(k)}, \mathcal{M} \rangle$	Duality pairing between differential form $\alpha^{(k)}$ and manifold $\mathcal{M}$

---

$\star$	Hodge star operator
$(\cdot, \cdot)$	Inner product
$(\cdot, \cdot)_{\mathcal{M}}$	$L^2$ -inner product in manifold $\mathcal{M}$
$\Lambda^k(\mathcal{M})$	Space of $k$ -forms in manifold $\mathcal{M}$
$L^2\Lambda^k(\mathcal{M})$	Hilbert Space of $k$ -forms in manifold $\mathcal{M}$
$d^*$	codifferential
$\mathcal{L}_u$	Lie derivative in vector field $u$
$L_u$	Adjoint operator of Lie derivative in vector field $u$
$\iota_u$	Interior product in vector field $u$
$j_u$	Adjoint operator of interior product $\iota_u$ in vector field $u$
$\sigma_{(k)}$	$k$ -cell
$D$	cell complex
$c^{(k)}$	$k$ -chain
$c_k$	Vector form of $k$ -chain
$C_k(D)$	$k$ -chain space in cell complex $D$
$c^{(k)}$	$k$ -cochain
$c^k$	Vector form of $k$ -cochain
$C^k(D)$	$k$ -cochain space in cell complex $D$
$\langle c^{(k)}, c_{(k)} \rangle$	Duality pairing between $k$ -cochain $c^{(k)}$ and $k$ -chain $c_{(k)}$
$\delta$	Coboundary operator
$\mathbb{E}$	Incidence matrix
$I^n$	unit $n$ -cube
$\pi$	Projection operator
$\mathcal{R}$	Reduction operator
$\mathcal{I}$	Reconstruction operator
$\cdot_h$	Discrete form or discrete operator
$\psi_i^j(x)$	$j = 0, 1$ , basis functions
$l_i^{gl}(x)$	Gauss-Lobatto-Legendre polynomials
$e_i^{gl}(x)$	Edge polynomials of Gauss-Lobatto-Legendre polynomials
$\ \cdot\ _{L^2}$	$L^2$ -norm.

# Introduction

It is well known that incompressible Navier-Stokes equations conserve mass and, in absence of viscosity (Euler equations), kinetic energy ( $K = \frac{1}{2} \int_{\Omega} |u|^2 d\Omega$ ) simultaneously. These conservation laws are critical elements for numerical schemes. Satisfying the conservation laws not only significantly contributes to the numerical stability and convergence, but also is a crucial factor for getting physically relevant solutions [31]. For Euler equations, in addition to mass and kinetic energy, there are other integral invariants that are of fundamental importance, the *enstrophy* ( $E = \frac{1}{2} \int_{\Omega} |\nabla \times \mathbf{u}|^2 d\Omega$ ) for two-dimensional flows and the *helicity* ( $H = \int_{\Omega} \mathbf{u} \cdot (\nabla \times \mathbf{u}) d\Omega$ ) for three-dimensional flows. Preserving enstrophy and helicity in numerical schemes is as important as preserving mass or kinetic energy. However, most existing numerical schemes just preserve mass. Satisfying more physical conservation laws is usually difficult.

Local helicity (helicity density) is given as  $h = \mathbf{u} \cdot (\nabla \times \mathbf{u})$ . The conservation law of helicity (1.0.1) states that for inviscid flows when the net helicity flux through the boundary is zero, the helicity of the domain does not change over time.

$$\frac{dH}{dt} = \frac{d}{dt} \int_{\Omega} h = 0. \quad (1.0.1)$$

For viscous flows, the helicity conservation law is replaced by the helicity balance equation (1.0.2), see [37].

$$H(T) + 2\nu \int_0^T (\nabla \mathbf{u}(t), \nabla \boldsymbol{\omega}(t)) dt = H(0). \quad (1.0.2)$$

This relation is equivalent to the helicity conservation law (1.0.1) when  $\nu = 0$ .

Although the conservation law of helicity was discovered as early as in 1961 by Moreau and was emphasized by Moffatt and Tsinober in their famous paper [35] in 1992, there was not even one numerical scheme that specializes in conserving helicity besides mass and kinetic

energy until 2004 when Liu and Wang [31] constructed the first numerical scheme which conserves mass, kinetic energy and helicity simultaneously.

Moffatt and Tsinober [35] revealed that the helicity has an interesting topological interpretation in terms of total circulation and Gauss linking number of two interlocking vortex filaments, which indicates that the helicity could be strongly related to vortical flow structures. Structure-preserving discretization techniques that preserve properties of basic differential operators and hence can capture the physics more accurately have natural advantages for developing helicity-preserving schemes. The structure-preserving discretization technique that will be used in this project is called the mimetic discretization or compatible discretization.

From a physical phenomenon to its physical model (e.g. partial differential equations or integral equations), error will be introduced, which always lies in the so called constitutive relations or material relations or closure relations. This is because humans can not totally understand some points of the phenomenon and then they use approximate relations to represent that. This kind of approximations is unavoidable. So it has to be taken into account in the numerical schemes. However, for remaining relations, for example the divergence free condition of Stokes problems, can they be represented in the numerical schemes exactly? The answer is yes. To achieve this, it is crucial to understand the essence of physical variables.

Classical approaches introduce error everywhere. This is because that, when they use scalars or vectors to represent physical variables, they obscure the topological and geometrical information of variables. For example, in an incompressible flow field, when a velocity vector  $\mathbf{u}$  is associated with a surface, it is in fact a representation of mass flux and it is constrained by the divergence free condition  $\mathbf{div} \mathbf{u} = \mathbf{0}$ . However, when a velocity vector  $\tilde{\mathbf{u}}$  is associated with a line, it actually is related to the velocity potential  $\varphi$  of the flow field, the corresponding relation is given by  $\tilde{\mathbf{u}} = \text{grad}\varphi$ . These two velocity vector obviously are different and can not be equated to each other,  $\mathbf{u} \neq \tilde{\mathbf{u}}$ . However, not many numerical schemes consider this point. In addition, classical approaches can not even exactly discretize first-order differential operators, such as gradient, curl and divergence, which are ingredients of a wide range of partial differential equations. For example, the conventional finite difference method approximates the gradient at a node through values at this node and neighbor nodes. The conventional finite volume method approximates the divergence free condition by using the mean value of two connected volumes to represent the value on the boundary. Both of them introduce error.

Compared to classical approaches, mimetic discretizations are new numerical techniques which try to mimic the structures of the partial differential equations as much as possible. Among them, the mimetic spectral element discretization [3, 8, 10, 11, 13, 16, 17, 25, 26, 27, 36, 38, 41, 42, 43, 46] focuses on the topological and geometrical essence of the variables, distinguishes the variables associated with different geometrical objects, makes use of the strong analogy between differential geometry and algebraic topology and develops discrete analogs of differential operators with their properties preserved at the discrete level .

All these aspects in fact are also implicitly embedded in the earlier developed mimetic finite difference method [4, 6, 7, 14, 18, 19, 20, 21, 22, 23, 24, 29, 30, 34, 45]. In contrast to the mimetic finite difference method, the mimetic spectral element method uses a series of basis functions (Lagrange polynomials [5, 10, 33] or B-spline polynomials [25] or interpolator & histopolator functions [45]) to represent the unknowns, which leads to higher-order schemes.

## 1.1 State of art

From many recent papers, for example see [1, 31, 37, 44], we can conclude that Moffatt and Tsinober's work in [35] is important for the investigation of helicity. In this paper, they explain that helicity is of importance comparable to the kinetic energy for three-dimensional flows at a fundamental level in relation to flow kinematics because it admits topological interpretation in relation to the linkage or linkages of vortex lines of the flow. They also reveal the relationships between helicity and turbulence at the topological level through theoretical analysis on vorticity.

The variable similar to helicity in two-dimensional flows is enstrophy. The first scheme conserving both kinetic energy and enstrophy has existed for a long time. It was developed and published by Arakawa in 1966. That scheme was then re-organized and re-published in 1997 [1]. In this paper, with the properly designed finite difference analogue for the advection term, a kinetic energy and enstrophy preserving scheme of significant stability for long-time numerical integrations is developed. Recently, by using the newly developed mimetic spectral element method, Natale [36] and Ruijter [8] also successfully develop schemes that conserve mass, kinetic energy and enstrophy for two-dimensional incompressible Euler flows respectively.

The article of Olshanskii et. al. [37] focuses on the investigation of the helicity balance in the conventional Galerkin method. The Galerkin method is a very sound finite element method and it does not consider helicity conservation since its appearance. The work of Olshanskii et. al. shows that in the periodic setting the usual Galerkin method with explicitly skew-symmetric nonlinear terms accurately balances both a discrete kinetic energy and a discrete helicity for three-dimensional flows. But when it is extended to homogeneous Dirichlet boundary conditions, helicity is generated near the boundary. This is consistent with the helicity balance relation (1.0.2).

The first scheme specializing in satisfying helicity balance was released at 2004 by Liu and Wang [31]. This scheme is used for axisymmetric hydro- and magnetohydro-dynamics flows. For such flows, it is possible to introduce a generalized vorticity-stream formulation. Therefore the divergence free constraint for the fluid velocity is trivially satisfied. Although this scheme is very efficient because all the nonlinear terms are treated explicitly, it is not suitable for non-symmetric general flows. After that, Liu and Wang [32] give a convergence

analysis of the kinetic energy and helicity preserving scheme for axisymmetric flows. The way of analyzing the truncation error is given in this paper as well. Rebholz [44], motivated by the work of Liu and Wang, then published his finite element scheme which satisfies kinetic energy balance and helicity balance for Navier-Stokes equations in 2007. In this paper, satisfying both kinetic energy balance and helicity balance are fulfilled through the use of the projection of the vorticity and a new variational formulation of the nonlinearity which cancels when tested against either the velocity or projected vorticity.

From 1997 to 1999, Hyman and Shashkov published a series of papers [19, 20, 21, 23] to create discrete analogies of first-order differential operators, i.e. **div**, **grad** and **curl**, on logically two-dimensional rectangular, nonorthogonal, non-smooth grids, which exactly satisfies the theorems in vector calculus at the discrete level. Those discrete analogies of differential operators developed in this series of papers provide fundamental ingredients for the development of mimetic finite difference discretization techniques.

Margolin et al. published their paper [34] in 2000, in which they introduce the support operators method (SOM). The SOM is a conceptual framework that can be used to derive the discrete operator calculus with some properties of the differential operators preserved (mimicked) exactly. The application of SOM proceeds in two steps. First, the *prime* operator (one of the fundamental operators) and its discrete form are chosen. Second, according to the analytical properties one wants to preserve, one can sequentially construct discrete forms of the other fundamental operators, which are then called *derived* operators.

The SOM is the method used by Hyman and Shashkov [19]. In this article, for the discretizations of adjoint first-order differential operators, the natural discrete operators in [20] are selected as *prime* operators. With the “support” of integral identities Eq. (1.1.1) and Eq. (1.1.2), the *derived* adjoint operators then follow.

$$\int_V u \mathbf{div} \mathbf{W} dV + \int_V (\mathbf{W}, \mathbf{grad} u) dV = \oint_{\partial V} u(\mathbf{W}, \mathbf{n}) dS. \quad (1.1.1)$$

$$\int_V (\mathbf{A}, \mathbf{curl} \mathbf{B}) dV - \int_V (\mathbf{B}, \mathbf{curl} \mathbf{A}) dV = \oint_{\partial V} ([\mathbf{B} \times \mathbf{A}], \mathbf{n}) dS. \quad (1.1.2)$$

Hyman et al. [18] then develop a scheme based on mimetic finite difference methods to solve diffusion equations on non-smooth, nonorthogonal, structured and unstructured computational grids. Kuznetsov et al. [29] and Lipnikov et al. [30] furthermore extend the application of mimetic finite difference methods for diffusion problems to unstructured polygonal and polyhedral meshes on which mimetic finite difference methods constantly show a first-order convergence rate for vector unknowns (for example velocity vector) and a second-order convergence rate for scalar unknowns (for example pressure) on even non-matching and slightly distorted meshes. In addition, Brezzi et al. [4] develop a family of new inexpensive numerical schemes for diffusion problems based on the general principles of the mimetic finite difference method on generalized polyhedral meshes. With these schemes, the convergence

rate for scalar variables is slightly improved while the convergence rate for vector variables keeps at first-order.

Meanwhile, to improve the accuracy of mimetic finite difference methods on vector variables for diffusion-type problems, Gyrya et al. [14] develop a high-order mimetic difference methods in which are second-order accurate for both vector and scalar variables. Further, Veiga et al. [7] extend mimetic finite difference methods on arbitrary polygonal meshes to Stokes problems and generate a new method which results in a second-order convergence rate in a discrete  $L^2$ -norm and a first-order convergence rate in a discrete  $H^1$ -norm for the velocity variable and a first-order convergence rate in a discrete  $L^2$ -norm for the pressure variable.

After the development of mimetic finite differences methods, the idea of mimicking properties of PDEs is then associated with the least-squares spectral element method. Palha and Gerritsma [39, 40] combine the least-squares spectral element method with mimetic approaches based on differential geometry and algebraic topology and develop the mimetic least-squares spectral element method.

Bochev et al. [2] then present their mimetic least-squares method for diffusion-reaction problems. The diffusion-reaction problem is deconstructed into a first-order system including two scalar and two vector variables. These variables can convert the material properties of the differential equations into two constitutive relations (two Hodge- $\star$  relations actually). Motivated by this new first-order representation (four-field first-order system) of the diffusion-reaction problem, they develop a new least-squares functional whose minimizer satisfies the differential equations exactly.

In the common finite element methods, unknowns are always expanded with nodal functions. As a result, the discretizations of gradient, curl and divergence operators always require quite some work and meanwhile introduce some error. This is because not all variables are associated with nodal values. In [10], Gerritsma presents the higher order basis functions, edge functions, which can be used to expand variables associated with higher dimensional geometric objects, lines, surfaces and volumes etc.. These edge functions actually already have been used in the mimetic least-squares methods stated previously [12, 39, 40]. By using these edge functions, first-order differential operators can be represented in discrete domain easily and exactly. As a consequence, their properties are conserved. Based on the mimetic framework already developed, the mimetic spectral element method then appears naturally. The mimetic discretization, motivated by the strong analogy between differential geometry and algebraic topology (for example see [9]), associated with the spectral element method results in the mimetic spectral element method [8, 11, 13, 17, 25, 26, 28, 36, 38, 42].

A first comprehensive introduction of mimetic spectral element method is given by Kreeft et al. [28]. In this paper, concepts of differential geometric and algebraic topology, for example the differential forms and differential operators (i.e. exterior derivative, Hodge star operator, etc.), are presented first which is then followed by the development of mimetic

operators (i.e. reduction, reconstruction and projection operator) and discrete analogies of differential operators. These contents are ingredients of the mimetic spectral element method. Meanwhile, the method of solving flow problems in complex flow domains is also presented in this paper.

Additional introductions about the mimetic spectral element method can be found in [11, 13]. Gerritsma et al. in [13] emphasize the essential connections among physical phenomenons, their mathematical representation (partial differential equations) and geometries. Meanwhile, the way of setting up weak formulations in which all the metric-dependent differential operators are replaced by metric-free differential operators with the help of integration by parts is presented in this paper. The metric-free differential operators in fact are the natural operators considered in [20]. While the metric-dependent differential operators are the adjoint operators discussed in [19]. The integration by parts used here actually is a different expression of the integral identities (1.1.1) (1.1.2) mentioned in [19, 22, 23]. These relations are of inherent importance for both mimetic finite difference methods and mimetic spectral element methods. Another paper of the introduction about the mimetic spectral element method from Gerritsma is [11]. In this paper, the mimetic spectral element method is explained in detail from the computational and physical point of view. It is mathematically shown how to construct scheme from physical modeling to a spectral element discretization with orthogonal polynomials with respect to differential forms and algebraic topological cochains. The treatment of curvilinear grids is given in this article as well.

With this mimetic spectral method, Bouman et al. [3] then solve the Poisson equation on curvilinear dual grids. The orthogonal dual grids, consisting of a Gauss-Lobatto-Legendre grid and an extended Gauss-Legendre grid, are mapped into curvilinear grids on which  $k$ -forms are pullbacked onto the standard unit domain by the *pullback* operator. Utilizing the commutation of the *pullback* operator with the wedge product and the exterior derivative leads to a mimetic spectral element formulation that performs metric-free discretizations of divergence and gradient operators exactly on curvilinear grids. As for the metric dependent part of the Poisson equation, the Hodge star operator, the support operator method proposed by Hyman et al. [24] again is employed. This scheme displays exponential convergence rate which is then proven by a sample problem. A more comprehensive introduction about the application of mimetic spectral element method on the Poisson equation is given in [42].

Rebelo et al. [43] then apply the mimetic spectral element method to the Darcy's problem. In this paper, an anisotropic flow through a porous medium is considered and a discretization of a full permeability tensor is presented. The discretization is based on the mixed formulation of the Darcy's problem. To derive the mixed formulation, the weighted inner product for vectors associated with outer-oriented objects is defined. The performance of the application of the mimetic spectral element method on the Darcy's problem then is tested by standard test problems. The results show an exponential convergence rate for this scheme.

Recently, a lot of research using the mimetic spectral element method have been done on

Stokes problems, for example, see [16, 17, 26, 27]. Within the mimetic spectral framework, the Stokes problem is described as a mixed formulation. This mixed formulation then results in a symmetric system of linear equations. The performance of the mimetic spectral element method on the Stokes problem then is tested by lid driven cavity flows. The results show that the properties of differential operators are exactly preserved.

The most used basic functions for the mimetic spectral element method are the Lagrange polynomials and its corresponding edge polynomials. Alternatively, one can use the B-spline node functions and B-spline edge functions or interpolator & histopolator functions to interpolate (reconstruct) the unknowns. The B-spline basis functions are introduced, for instance, in [16, 17] and interpolator & histopolator functions are introduced by Rufat et al. in [45].

Besides the exterior derivative, Hodge star operator and so on, a more complicated operator, the interior product, one of the two fundamental elements of the Lie derivative that is used to represent convective terms, is not involved by mimetic spectral element method until Palha et al. publish their paper [41] in which a discretization of the linear advection of differential forms is presented. Since the other element of Lie derivative, exterior derivative, already has a very nice discrete analogy, the metric-free coboundary operator which can be represented by the incidence matrix in the discrete system. Once the discretization of the interior product is given, the Lie derivative can be discretized. Hence, with the work of Palha et al., the mimetic spectral element method is expanded to incorporate the Lie derivative. Therefore, the mimetic framework is applicable for convective term related problems like Euler problems and Navier-Stokes problems. In addition to the discretization of the interior product, a time integrator, the canonical mimetic time integrator, for solving the time evolution is also given in this paper. This time integrator, together with the discretization of the interior product, then is applied to a two-dimensional advection equation. The results show good  $p$ - and  $h$ -convergence rates.

## 1.2 Conservation laws in incompressible Euler equations

In this section, we derive three conservation laws, conservation of mass, kinetic energy and helicity, of three-dimensional incompressible Euler flows with periodic boundary conditions from the viewpoint of conventional vector calculus. We start from the velocity-vorticity form of incompressible Euler equations. It is written as

$$\left\{ \begin{array}{l} \frac{\partial \mathbf{u}}{\partial t} + (\mathbf{u} \cdot \nabla) \mathbf{u} + \nabla p = 0 \\ \frac{\partial \boldsymbol{\omega}}{\partial t} + (\mathbf{u} \cdot \nabla) \boldsymbol{\omega} = 0 \\ \nabla \cdot \mathbf{u} = 0 \end{array} \right. , \quad (1.2.1)$$

where  $\boldsymbol{\omega} = \nabla \times \mathbf{u}$ . Suppose the periodic flow domain is denoted by  $\Omega$ . Because of the periodic boundary condition, all boundary integral terms, for example see Eq. (1.2.6) and Eq. (1.2.13), are zero.

**Mass conservation** Since we are considering incompressible flows, the density is constant and  $\nabla \cdot \mathbf{u} = 0$  everywhere, according to the Gauss theorem, we can easily know that the mass is conserved not only globally and but also locally.

**Kinetic energy conservation** The kinetic energy is given as

$$K = \int_{\Omega} k \, d\Omega = \frac{1}{2} \int_{\Omega} \|\mathbf{u}\|^2 d\Omega, \quad (1.2.2)$$

where  $k = \frac{1}{2}\|\mathbf{u}\|^2$  is the kinetic energy density. To obtain the conservation law of kinetic energy, we take the inner product between the momentum equation of Eq. (1.2.1) and the velocity vector  $\mathbf{u}$  then integrate over the domain  $\Omega$ , which results in

$$\frac{dK}{dt} + \int_{\Omega} \mathbf{u} \cdot [(\mathbf{u} \cdot \nabla) \mathbf{u}] \, d\Omega + \int_{\Omega} \mathbf{u} \cdot \nabla p \, d\Omega = 0, \quad (1.2.3)$$

where the second term can be expressed as

$$\begin{aligned} \int_{\Omega} \mathbf{u} \cdot [(\mathbf{u} \cdot \nabla) \mathbf{u}] \, d\Omega &= \int_{\Omega} \mathbf{u} \cdot [\nabla \cdot (\mathbf{u} \otimes \mathbf{u})] \, d\Omega \\ &= \int_{\Omega} \nabla \cdot (k\mathbf{u}) + k\nabla \cdot \mathbf{u} \, d\Omega, \end{aligned} \quad (1.2.4)$$

and because of the integration by parts, the third term can be written as

$$\int_{\Omega} \mathbf{u} \cdot \nabla p \, d\Omega = \int_{\Omega} \nabla \cdot (p\mathbf{u}) - p\nabla \cdot \mathbf{u} \, d\Omega, \quad (1.2.5)$$

Therefore, with the Gauss theorem, Eq. (1.2.3) becomes

$$\frac{dK}{dt} + \int_{\partial\Omega} (k\mathbf{u} + p\mathbf{u}) \cdot \mathbf{n} \, d\Gamma + \int_{\Omega} (k - p) \nabla \cdot \mathbf{u} \, d\Omega = 0. \quad (1.2.6)$$

Because the flow field has the periodic boundary condition and is divergence free everywhere, the second term and third term of Eq. (1.2.6) are zero. Therefore, we obtain the conservation law of kinetic energy:

$$\frac{dK}{dt} = 0. \quad (1.2.7)$$

**Helicity conservation** The helicity of the domain  $\Omega$  is expressed as

$$H = \int_{\Omega} h \, d\Omega = \int_{\Omega} \mathbf{u} \cdot \boldsymbol{\omega} \, d\Omega, \quad (1.2.8)$$

where  $h = \mathbf{u} \cdot \boldsymbol{\omega}$  is the helicity density.

To get the conservation law of helicity, we multiply the momentum equation of Eq. (1.2.1) by the vorticity vector  $\boldsymbol{\omega}$  and multiply the vorticity equation of Eq. (1.2.1) by the velocity vector  $\mathbf{u}$  and then integrate these two equations over the domain  $\Omega$ , which gives

$$\int_{\Omega} \frac{\partial \mathbf{u}}{\partial t} \cdot \boldsymbol{\omega} \, d\Omega + \int_{\Omega} \boldsymbol{\omega} \cdot [(\mathbf{u} \cdot \nabla) \mathbf{u}] \, d\Omega + \int_{\Omega} \boldsymbol{\omega} \cdot \nabla p \, d\Omega = 0, \quad (1.2.9)$$

$$\int_{\Omega} \mathbf{u} \cdot \frac{\partial \boldsymbol{\omega}}{\partial t} \, d\Omega + \int_{\Omega} \mathbf{u} \cdot [(\mathbf{u} \cdot \nabla) \boldsymbol{\omega}] \, d\Omega = 0. \quad (1.2.10)$$

Adding above two equations yields

$$\begin{aligned} \frac{dH}{dt} &= - \int_{\Omega} \boldsymbol{\omega} \cdot [(\mathbf{u} \cdot \nabla) \mathbf{u}] \, d\Omega - \int_{\Omega} \mathbf{u} \cdot [(\mathbf{u} \cdot \nabla) \boldsymbol{\omega}] \, d\Omega - \int_{\Omega} \boldsymbol{\omega} \cdot \nabla p \, d\Omega \\ &= - \int_{\Omega} \boldsymbol{\omega} \cdot [\nabla \cdot (\mathbf{u} \otimes \mathbf{u})] + \mathbf{u} \cdot [\nabla \cdot (\mathbf{u} \otimes \boldsymbol{\omega} - \boldsymbol{\omega} \otimes \mathbf{u})] \, d\Omega - \int_{\Omega} \boldsymbol{\omega} \cdot \nabla p \, d\Omega. \end{aligned} \quad (1.2.11)$$

With the periodic boundary condition and integration by parts, we have

$$\int_{\Omega} \boldsymbol{\omega} \cdot [\nabla \cdot (\mathbf{u} \otimes \mathbf{u})] \, d\Omega = - \int_{\Omega} \mathbf{u} \cdot [\nabla \cdot (\mathbf{u} \otimes \boldsymbol{\omega})] \, d\Omega. \quad (1.2.12)$$

According to the Gauss theorem and the periodic boundary condition, we obtain

$$\int_{\Omega} \mathbf{u} \cdot [\nabla \cdot (\boldsymbol{\omega} \otimes \mathbf{u})] \, d\Omega = \int_{\Omega} \nabla \cdot [(\mathbf{u} \cdot \boldsymbol{\omega}) \mathbf{u}] \, d\Omega = \int_{\partial\Omega} hu \cdot \mathbf{n} \, d\Gamma = 0. \quad (1.2.13)$$

Because of the integration by parts, the Gauss theorem, the periodic boundary condition and the fact that the divergence of the vorticity is always zero, we can find that

$$\int_{\Omega} \boldsymbol{\omega} \cdot \nabla p \, d\Omega = 0. \quad (1.2.14)$$

Therefore, we obtain the conservation law of helicity

$$\frac{dH}{dt} = \int_{\Omega} \frac{\partial \mathbf{u}}{\partial t} \cdot \boldsymbol{\omega} \, d\Omega + \int_{\Omega} \mathbf{u} \cdot \frac{\partial \boldsymbol{\omega}}{\partial t} \, d\Omega = 0. \quad (1.2.15)$$

Besides mass, kinetic energy and helicity, you can find a lot of other integral invariants for three-dimensional incompressible Euler flows. These invariants imply essential properties of three-dimensional incompressible Euler flows. However, no numerical schemes can preserve all the invariants. There is always a trade-off. When a scheme satisfies some conservation laws, it keeps some properties, but loses some others. Therefore, once the conservation laws you want to preserve are satisfied, for example the mass conservation and the kinetic energy conservation, satisfying additional conservation laws in your scheme is always good for the scheme because these additional conservation laws bring more properties of real flows into the numerical systems, which means you can get more physical solutions. In addition, your scheme normally becomes more stable because of that.

### 1.3 Thesis outline

The outline of this thesis is as follow. In Chapter 2, the mathematical background, differential geometry and algebraic topology, will be introduced, which is then followed by the introduction of the mimetic spectral element method in Chapter 3. With these tools, we construct our scheme in Chapter 4. After that, the scheme is tested. The test case, results and corresponding discussions are given in Chapter 5. Finally, some conclusions and recommendations are given in Chapter 6. In addition, details of the discretization of each term are given in the Appendix A.

## Mathematical background

In this chapter, two main mathematical bases of the mimetic element spectral method, differential geometry and algebraic topology, will be presented. Differential geometry which probably is a novel topic for most readers actually handles similar problems as conventional vector calculus. The major difference between them is that the vector calculus discusses the geometric aspects of physical models while differential geometry plays with physical ideas as well in addition to geometric ideas. (Recall the example of velocities associated with lines and faces in Chapter 1.) This does not mean vector calculus is incorrect. As we have said, vector calculus discusses the geometric level of physical models, and it does not assign a velocity vector associated with face to a velocity vector associated with line. This happens when someone is using vector calculus on physical problems and he does not make the proper association with geometries. Hyman and Shashkov noticed this point and developed the mimetic finite difference methods, for example see [18, 22]. However, if the geometrical meaning of a variable can be expressed explicitly on the variable, it will be better. Therefore, we present differential geometry here.

Algebraic topology which has a strong analogy with differential geometry will also be presented in this chapter. By making use of the analogy, the mimetic spectral element method (the mimetic framework) is constructed, which is the topic of next chapter.

This chapter is based on the work of Kreeft, Palha, Gerritsma et al., for example see [25, 28, 38]. More details can be found in [9].

## 2.1 Differential geometry

### 2.1.1 Manifolds

In mathematics, a manifold is a topological space which extends the Euclidean space. For each point of an  $n$ -dimensional manifold, it has a neighborhood which is isomorphic to an  $n$ -dimensional Euclidean space. A formal definition of differential manifolds is given below:

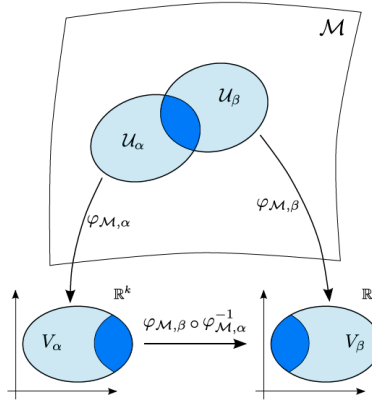


Figure 2.1: Coordinate charts on a manifold [28].

**Manifolds:** [9, 25, 28, 38] A  $k$ -dimensional manifold is a set  $\mathcal{M}$ , together with a countable collection of subset  $\mathcal{U}_\alpha$ , called coordinate charts, and one-to-one functions  $\varphi_{\mathcal{M},\alpha} : \mathcal{U}_\alpha \rightarrow V_\alpha$  onto connected open subsets  $V_\alpha$  of  $\mathbb{R}^k$  called local coordinate maps, as in Fig. 2.1, which satisfy the following properties:

- (1) The coordinate charts cover  $\mathcal{M}$ :

$$\bigcup_{\alpha} \mathcal{U}_\alpha = \mathcal{M} ;$$

- (2) On the overlap of any pair of coordinate charts  $\mathcal{U}_\alpha \cap \mathcal{U}_\beta$ , the composite map:

$$\varphi_{\mathcal{M},\beta} \circ \varphi_{\mathcal{M},\alpha}^{-1} : \varphi_{\mathcal{M},\alpha}(\mathcal{U}_\alpha \cap \mathcal{U}_\beta) \rightarrow \varphi_{\mathcal{M},\beta}(\mathcal{U}_\alpha \cap \mathcal{U}_\beta) ,$$

is a smooth (infinitely differentiable) function;

- (3) If  $x \in \mathcal{U}_\alpha$  and  $y \in \mathcal{U}_\beta$  are distinct points in  $\mathcal{M}$ , then there exist open subsets  $W_\alpha$  of  $\varphi_{\mathcal{M},\alpha}$  in  $V_\alpha$  and  $W_\beta$  of  $\varphi_{\mathcal{M},\beta}$  in  $V_\beta$  such that

$$\varphi_{\mathcal{M},\alpha}^{-1}(W_\alpha) \cap \varphi_{\mathcal{M},\beta}^{-1}(W_\beta) = \emptyset .$$

This definition looks mysterious. However, it is quite understandable in low order Euclidean spaces. For example, In  $\mathbb{R}^3$  equipped with a coordinate system  $\{x, y, z\}$ , for an arbitrary surface (2-manifold  $\mathcal{M}$ ), we can set up a local coordinate, say  $\{\xi, \eta\}$ , in the surface with which the position vector  $\boldsymbol{p}$  of each point in the surface can be expressed as  $\{p_1(\xi, \eta), p_2(\xi, \eta), p_3(\xi, \eta)\}^T$ . From this point, we can see that, for every subset  $\mathcal{U} \subseteq \mathcal{M}$ , there is a one-to-one function  $\varphi_{\mathcal{M}} : \mathcal{U} \rightarrow V$  where  $V$  is a subset of  $\mathbb{R}^2$ , for example, the one equipped with the coordinate system  $\{\xi, \eta\}$ , see Fig. 2.2.

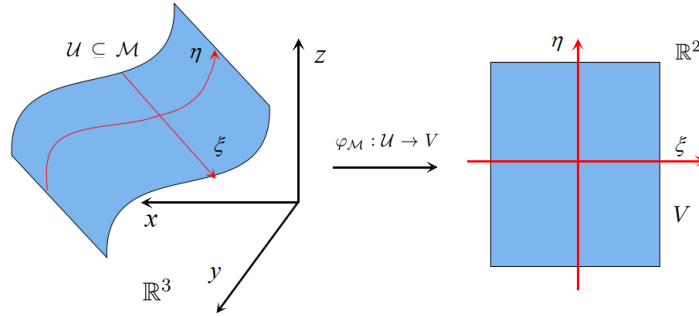


Figure 2.2: A 2-manifold in  $\mathbb{R}^3$ .

In  $\mathbb{R}^n$ , we can define  $n + 1$  types of manifolds with dimensions from 0 to  $n$ . In a  $k$ -manifold ( $0 \leq k \leq n$ ), we can find  $(k + 1)$  types of sub-manifolds with dimensions from 0 to  $k$ . For example, In  $\mathbb{R}^3$ , we can define four types of manifolds, namely, points, lines, surfaces and volumes, and in a surface (2-manifold  $\mathcal{M}$ ), you can find infinite numbers of points, lines and surfaces which are the sub-manifolds of  $\mathcal{M}$ .

The boundary of a manifold  $\mathcal{M}$  is written as  $\partial\mathcal{M}$ . The boundary of a manifold is always a boundaryless manifold, which means

$$\partial\partial\mathcal{M} = \emptyset. \quad (2.1.1)$$

For a periodic domain  $\mathcal{M}$ , it can be considered as a boundaryless domain itself,  $\partial\mathcal{M} = \emptyset$ , which is the case in this project.

### 2.1.2 Vectors and covectors

In  $\mathbb{R}^n$ , if a curve through a point  $p$  on a  $k$ -manifold  $\mathcal{M}$  is given by  $\boldsymbol{r}_p(\tau)$ ,  $a \leq \tau \leq b$ , and  $\boldsymbol{r}_p(0)$  refers to point  $p$ . The derivative of  $\boldsymbol{r}_p(0)$  is the tangent vector  $\boldsymbol{e}_p$  of the curve on the point  $p$ . Remember, the dimensions of the tangent vector  $\boldsymbol{e}_p$  is equal to the dimensions of the space in which the  $k$ -manifold  $\mathcal{M}$  is embedded. If we select  $k$  different curves,  $\boldsymbol{r}_p^1(\tau)$ ,  $\boldsymbol{r}_p^2(\tau)$ ,  $\dots$ ,  $\boldsymbol{r}_p^k(\tau)$ , through the point  $p$  and take derivative of  $\boldsymbol{r}_p^1(0)$ ,  $\boldsymbol{r}_p^2(0)$ ,  $\dots$ ,  $\boldsymbol{r}_p^k(0)$ , we get  $k$  linear

independent tangent vectors. The collection of these  $k$  tangent vectors,  $\{e_p^1, e_p^2, \dots, e_p^k\}$ , spans a vector space called the *tangent space* of the  $k$ -manifold  $\mathcal{M}$  at the point  $p$ , denoted by  $T_p\mathcal{M}$ .  $\{e_p^1, e_p^2, \dots, e_p^k\}$  is then called a *basis* of the space  $T_p\mathcal{M}$  [42]. An element of  $T_p\mathcal{M}$  is called a *vector*. Therefore, any vector  $\mathbf{u}$  in  $T_p\mathcal{M}$  can be expressed as

$$\mathbf{u} = \sum_{i=1}^k u_i e_p^i, \quad (2.1.2)$$

where  $u^i$  are the vector coefficients. Specifically, if we set up a local coordinate system  $\{x_p^1, x_p^2, \dots, x_p^k\}$  in the  $k$ -manifold  $\mathcal{M}$ , we normally use the  $k$  tangent vectors parallel to the coordinate axes to construct the basis which is denoted by  $\left\{ \frac{\partial}{\partial x_p^1}, \frac{\partial}{\partial x_p^2}, \dots, \frac{\partial}{\partial x_p^k} \right\}$  or by  $\{\partial x_p^1, \partial x_p^2, \dots, \partial x_p^k\}$ . So the vector  $\mathbf{u}$  in  $T_p\mathcal{M}$  can be written as

$$\mathbf{u} = \sum_{i=1}^k u_i \partial x_p^i. \quad (2.1.3)$$

The vector space perpendicular to the tangent space  $T_p\mathcal{M}$  is called the *normal space*, denoted by  $T_p^\perp\mathcal{M}$ , which is an  $(n - k)$ -dimensional vector space. If the  $k$ -manifold  $\mathcal{M}$  is a sub-manifold of an  $n$ -manifold  $\mathcal{N}$ , then we have

$$T_p\mathcal{M} \oplus T_p^\perp\mathcal{M} = T_p\mathcal{N}. \quad (2.1.4)$$

The establishment of the tangent space can be done for all points, the collection of all tangent spaces is called the *tangent bundle*, denoted by  $T\mathcal{M}$ :

$$T\mathcal{M} := \bigcup_{p \in \mathcal{M}} T_p\mathcal{M}. \quad (2.1.5)$$

From linear algebra, we know that for an arbitrary linear vector space  $V$ , we can always associate  $V$  with a space of linear functions, say  $V^*$ , such that

$$\forall \alpha \in V^*, \quad \alpha : V \rightarrow \mathbb{R}. \quad (2.1.6)$$

This linear function space is also called the dual space of the vector space  $V$ .

For a tangent space  $T_p\mathcal{M}$ , we can associate a dual space  $T_p^*\mathcal{M}$  to  $T_p\mathcal{M}$ , such that  $\forall \alpha, \beta \in T_p^*\mathcal{M}$

$$\alpha(\mathbf{u}) = \mathbb{R} \quad \forall \mathbf{u} \in T_p\mathcal{M}, \quad (2.1.7)$$

and

$$\alpha(a\mathbf{u} + b\mathbf{v}) = a\alpha(\mathbf{u}) + b\alpha(\mathbf{v}) \quad \forall \mathbf{u}, \mathbf{v} \in T_p\mathcal{M} \quad a, b \in \mathbb{R}, \quad (2.1.8)$$

$$(a\alpha + b\beta)(\mathbf{u}) = a\alpha(\mathbf{u}) + b\beta(\mathbf{u}) \quad \forall \mathbf{u} \in T_p\mathcal{M} \quad a, b \in \mathbb{R}, \quad (2.1.9)$$

where  $T_p^*\mathcal{M}$  is called the *cotangent space*, an element of  $T_p^*\mathcal{M}$ ,  $\alpha$  or  $\beta$ , is called a *covector* and  $\alpha(\mathbf{u})$  is called the *duality pairing* between the vector  $\mathbf{u}$  and the covector  $\alpha$ .

The cotangent space  $T_p^*\mathcal{M}$  is isomorphic to the tangent space  $T_p\mathcal{M}$ . If  $\{\epsilon_1^p, \epsilon_2^p, \dots, \epsilon_k^p\}$  is a basis of  $T_p^*\mathcal{M}$ , then any covector in  $T_p^*\mathcal{M}$  can be expressed as

$$\alpha = \sum_j \alpha^j \epsilon_j^p. \quad (2.1.10)$$

A good option of  $\{\epsilon_1^p, \epsilon_2^p, \dots, \epsilon_k^p\}$  is the canonical basis  $\{dx_1^p, dx_2^p, \dots, dx_k^p\}$  which satisfies

$$dx_j^p \partial x_p^i = \delta_j^i = \begin{cases} 1 & i = j \\ 0 & i \neq j \end{cases}. \quad (2.1.11)$$

Hence, for any covector  $\alpha$  in  $T_p^*\mathcal{M}$ , we have

$$\alpha(\mathbf{u}) = \sum_{i=1}^k \alpha^i u_i. \quad (2.1.12)$$

Similarly, we can construct cotangent spaces for all points in  $\mathcal{M}$ , the collection of which is then called the *cotangent bundle*, denoted by  $T^*\mathcal{M}$ :

$$T^*\mathcal{M} := \bigcup_{p \in \mathcal{M}} T_p^*\mathcal{M}. \quad (2.1.13)$$

Operators which switch between covector and vector are the *flat operator*  $\flat$  and the *sharp operator*  $\sharp$ . In a Cartesian coordinate system, for a vector  $\mathbf{u}$  given as  $\mathbf{u} = \sum_{i=1}^k u_i \partial x^i$ , the flat operator  $\flat$  converts it into a covector by

$$(\mathbf{u})^\flat = \left( \sum_{i=1}^k u_i \partial x^i \right)^\flat = \sum_{i=1}^k u_i dx_k = \mathbf{v}. \quad (2.1.14)$$

While a sharp operator  $\sharp$  converts the covector  $\mathbf{v}$  back to the vector  $\mathbf{u}$ :

$$(\mathbf{v})^\sharp = \left( \sum_{i=1}^k u_i dx_k \right)^\sharp = \sum_{i=1}^k u_i \partial x^i = \mathbf{u}. \quad (2.1.15)$$

Remember, only in Cartesian coordinate systems, above two equations are correct since the metric tensors,  $g_{ij}$ , of Cartesian coordinate systems are always identity matrices,  $I$ :

$$\partial x^i = g_{i,j} dx^j = I dx^j.$$

In this project, we use the Cartesian coordinate system as our coordinate system. So Eq. (2.1.14) and Eq. (2.1.15) are correct here.

If you apply the above analysis to the normal space  $T_p^\perp \mathcal{M}$ , you eventually get two bundles,  $T^\perp \mathcal{M}$  and  $T^{\perp*} \mathcal{M}$ , which are the tangent bundle and cotangent bundle of the  $(n - k)$ -dimensional manifold embedded in the  $n$ -dimensional space. Recognizing this point contributes to understanding concepts of orientations for manifolds (Section 2.1.3).

### 2.1.3 Orientations

An important concept for manifolds is the concept of orientations [9]. They are generalized from the concept of orientations in vector calculus. In a  $k$ -dimensional vector space, for two arbitrary sets of orthogonal unit basis vectors, for example,  $\{a_1, a_2, \dots, a_k\}$  and  $\{b_1, b_2, \dots, b_k\}$ , we can always find a matrix  $T_{a,b}$  which transforms  $\{a_1, a_2, \dots, a_k\}$  into  $\{b_1, b_2, \dots, b_k\}$ . This transformation implies the idea of the orientation. The transformation can only belong to one of the two equivalence classes according to the sign of the determinant of the transform matrix,  $\det(T_{a,b})$ . In the remaining part of this thesis, two equivalence classes always refer to this concept. By declaring one of the two equivalence classes to be positive, we orient the vector space. For example, if you select the equivalence class represented by transformation matrices of positive determinants to be the positive orientation, the other equivalence class represented by transformation matrices of negative determinants automatically becomes the negative orientation.

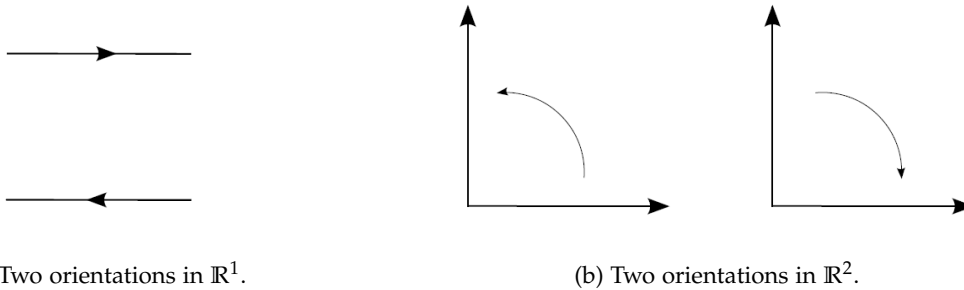


Figure 2.3: Orientations in vector spaces.

In low dimensional spaces, the concept of orientations can be recognized easily. For example [38], in  $\mathbb{R}^1$ , the two possible directions represent the two possible orientations, see Fig. 2.3a. In  $\mathbb{R}^2$ , the clockwise and counterclockwise directions represent the two possible orientations, see Fig. 2.3b.

From Section 2.1.1 and Section 2.1.2, we know  $k$ -dimensional manifolds locally resemble  $\mathbb{R}^k$ . According to this property, the concept of orientations for the vector space can be easily

generalized to manifolds. We can orient a manifold by declaring one of the two equivalence classes of the vector space associated with the manifold to be positive. Remember, a vector space (tangent space  $T_p\mathcal{M}$  or normal space  $T_p^\perp\mathcal{M}$ ) is actually associated with a point in manifolds. For  $1, 2, \dots, n$ -dimensional manifolds, we have infinite numbers of points. Hence we have infinite numbers of vector spaces the collection of which is called bundle. Because of the topological relation within a manifold, the positive orientations according to vector spaces on different points must be compatible with each other. Therefore, we can always define the positive orientation of a  $k$ -dimensional manifold ( $k \geq 1$ ) by declaring one of the equivalence classes of the vector space associated with a point on this manifold to be positive. By projecting this orientation into the manifold  $\mathcal{M}$ , we get the positive orientation of the manifold. The other orientation then becomes negative orientation automatically. For example, see Fig. 2.4 in which the positive orientation of the 2-dimensional vector space  $T_p\mathcal{M}$  is defined as the orientation represented by the red arrowed circle. By projecting the red arrowed circle into the manifold  $\mathcal{M}$ , we get the positive orientation of the manifold  $\mathcal{M}$ .

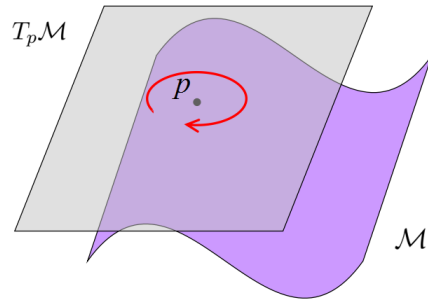


Figure 2.4: The positive orientation of 2-dimensional manifold  $\mathcal{M}$ .

However, there are two different vector spaces, the tangent space  $T_p\mathcal{M}$  and the normal space  $T_p^\perp\mathcal{M}$ , attached on the point  $p$  of a  $k$ -dimensional manifold  $\mathcal{M}$ . We already know that the tangent space  $T_p\mathcal{M}$  can be used to define orientations of a manifold naturally. These orientations are called *inner orientations*. While the normal space  $T_p^\perp\mathcal{M}$  can be used to define the so called *outer orientations*.

**Inner orientations:** *If one of the two equivalence classes of the tangent space  $T_p\mathcal{M}$  at each point of a  $k$ -manifold  $\mathcal{M}$ ,  $k \geq 0$ , is declared to be positive, this manifold is said to be inner oriented. The two equivalence classes, positive one or negative one, are then called the positive and negative inner orientations.*

Now, we know that the orientation in Fig. 2.4 is actually the inner orientation. As we know, the dimension of the tangent space of a manifold only depends on the dimension of the manifold. Therefore, the dimension of the space in which the manifold is embedded does

not affect the inner orientation. For example, see Fig. 2.5, inner orientations, represented by red circles, are same in 2-dimensional and 3-dimensional spaces.

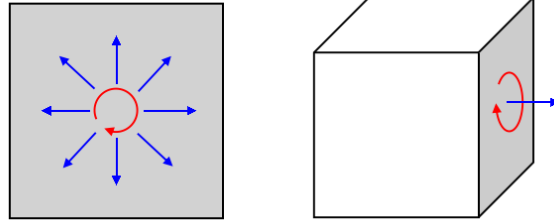


Figure 2.5: Inner (red) and outer (blue) orientations of a 2-manifold in 2-dimensional (left) and 3-dimensional (right) spaces.

**Outer Orientations:** A  $k$ -manifold  $\mathcal{M}$  embedded in  $n$ -dimensional space,  $0 \leq k \leq n$ , is said to be outer oriented if one of the two equivalence classes of the normal space  $T_p^\perp \mathcal{M}$  at each point of the  $k$ -manifold  $\mathcal{M}$  is declared to be positive. The two equivalence classes, positive one and negative one, are then called the positive and negative outer orientations.

As we can see from Section 2.1.2, differing from the tangent space  $T_p \mathcal{M}$ , the normal space  $T_p^\perp \mathcal{M}$  not only depends on the dimension of the manifold  $\mathcal{M}$ , but also depends on the dimension of the space in which the manifold  $\mathcal{M}$  is embedded. Recall that, for a  $k$ -manifold in  $n$ -dimensional space, the dimension of the normal space  $T_p^\perp \mathcal{M}$  is given as  $(n - k)$ . Hence, the outer orientation of a  $k$ -manifold  $\mathcal{M}$  in a  $n$ -dimensional space changes when the dimension of the space,  $n$ , changes. This point is clearly shown in Fig. 2.5 where the outer orientation, represented by blue arrowed lines, of a 2-manifold (a surface) in the 2-dimensional space (left) differs from that of a 2-manifold in the 3-dimensional space (right).

In this thesis, we always stay in the 3-dimensional space. The inner and outer orientations of  $k$ -manifolds ( $k = \{0, 1, 2, 3\}$ ) in a 3-dimensional space are expressed in Fig. 2.6.

More discussions about orientations will be given in Section 2.1.4 where the concept of differential forms is involved.

#### 2.1.4 Differential forms

From Section 2.1.2, we already know that, in an  $n$ -dimensional space, given a  $k$ -manifold  $\mathcal{M}$ , a covector  $\alpha$  in the cotangent space  $T_p^* \mathcal{M}$  maps a vector in the tangent space  $T_p \mathcal{M}$  into  $\mathbb{R}$ :

$$\alpha : T_p \mathcal{M} \rightarrow \mathbb{R} . \quad (2.1.16)$$

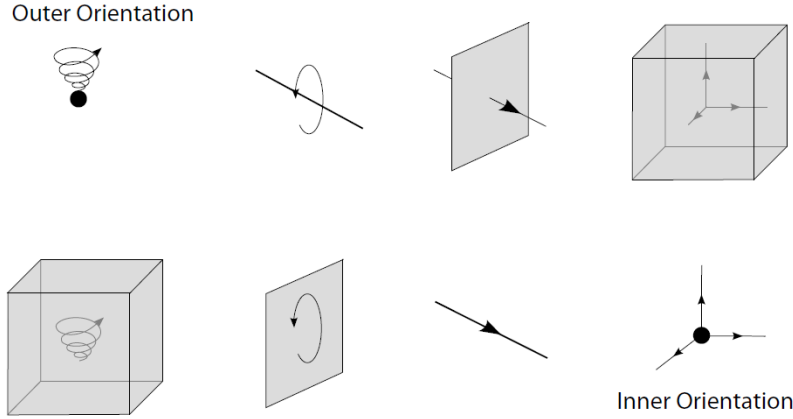


Figure 2.6: Inner and outer orientations of 0, 1, 2, 3-manifolds in  $\mathbb{R}^3$  [28].

This covector  $\alpha$  locally resembles a 1-form. A covector is defined in one point. While a 1-form is defined in the manifold. The formal definition of differential forms (forms in short) is given as

**Differential forms:** [25, 28, 38] For an  $n$ -manifold  $\mathcal{M}$ , a differential  $k$ -form,  $\alpha^{(k)}$ ,  $1 \leq k \leq n$ , is a mapping that

$$\alpha^{(k)} : \underbrace{T_p\mathcal{M} \times T_p\mathcal{M} \times \cdots \times T_p\mathcal{M}}_k \rightarrow \mathbb{R},$$

which is skew symmetric.

$$\alpha^{(k)}(\mathbf{u}_1, \mathbf{u}_2, \cdots, \mathbf{u}_k) = \text{sign} \cdot \alpha^{(k)}(\mathbf{u}_{P(1)}, \mathbf{u}_{P(2)}, \cdots, \mathbf{u}_{P(k)}), \quad (2.1.17)$$

where  $\text{sign} = +$  when  $\{P(1), P(2), \cdots, P(k)\}$  is an even permutation of  $\{1, 2, \cdots, k\}$ ,  $\text{sign} = -$  when  $\{P(1), P(2), \cdots, P(k)\}$  is an odd permutation of  $\{1, 2, \cdots, k\}$ .

A 0-form is simply defined as a scalar valued function, and when  $k < 0$  or  $k > n$ ,  $\alpha^{(k)} = 0$ . The space of  $k$ -forms on the  $n$ -manifold  $\mathcal{M}$  is expressed by  $\Lambda^k(\mathcal{M})$ . Five extremely important operators for differential forms are the *wedge product*  $\wedge$ , *exterior derivative*  $d$ , *Hodge star operator*  $\star$ , *codifferential*  $d^*$  and *Lie derivative*  $\mathcal{L}$ .

**Wedge product  $\wedge$ :** [28] For an  $n$ -manifold  $\mathcal{M}$ , a wedge product  $\wedge$  between two differential forms,  $\alpha^{(k)} \in \Lambda^k(\mathcal{M})$  and  $\beta^{(l)} \in \Lambda^l(\mathcal{M})$  ( $k, l \leq n$ ), is a mapping:

$$\wedge : \Lambda^k(\mathcal{M}) \times \Lambda^l(\mathcal{M}) \rightarrow \Lambda^{k+l}(\mathcal{M}),$$

with following properties satisfied.

- (1) *Distributivity*:

$$\left(\alpha^{(k)} + \beta^{(l)}\right) \wedge \gamma^{(m)} = \alpha^{(k)} \wedge \gamma^{(m)} + \beta^{(l)} \wedge \gamma^{(m)} ; \quad (2.1.18)$$

- (2) *Associativity*:

$$\left(\alpha^{(k)} \wedge \beta^{(l)}\right) \wedge \gamma^{(m)} = \alpha^{(k)} \wedge \left(\beta^{(l)} \wedge \gamma^{(m)}\right) ; \quad (2.1.19)$$

- (3) *Skew symmetry*:

$$\alpha^{(k)} \wedge \beta^{(l)} = (-1)^{kl} \beta^{(l)} \wedge \alpha^{(k)} ; \quad (2.1.20)$$

- (4) *If  $c$  is a scalar, then*

$$c\alpha^{(k)} \wedge \beta^{(l)} = \alpha^{(k)} \wedge c\beta^{(l)} = c \left(\alpha^{(k)} \wedge \beta^{(l)}\right) . \quad (2.1.21)$$

From this definition, we know

$$\alpha^{(k)} \wedge \beta^{(l)} = 0 \quad \text{if } k + l > n , \quad (2.1.22)$$

$$\alpha^{(k)} \wedge \alpha^{(k)} = 0 \quad \text{if } k \text{ is odd or } k > \frac{n}{2} . \quad (2.1.23)$$

If we set up a local coordinate system  $\{x^1, x^2, \dots, x^n\}$  in the  $n$ -manifold  $\mathcal{M}$ , according to Section 2.1.2, we know the basis for 1-forms (covectors) is usually selected as the canonical basis:

$$\{dx^1, dx^2, \dots, dx^n\} .$$

Remember that in Section 2.1.2 we consider an  $k$ -manifold in an  $n$ -dimensional space, while here we consider the  $n$ -manifold. In addition, in Section 2.1.2 we use  $\{dx_1, dx_2, \dots, dx_n\}$  to represent the canonical basis, while here we use  $\{dx^1, dx^2, \dots, dx^n\}$  to represent it. Each element of the basis  $\{dx^1, dx^2, \dots, dx^n\}$  is itself a 1-form. It follows, from the definition of the wedge product, that

$$dx^{i_1} \wedge dx^{i_2} \wedge \dots \wedge dx^{i_k} = \text{sign} \cdot \left(dx^{j_1} \wedge dx^{j_2} \wedge \dots \wedge dx^{j_k}\right) , \quad (2.1.24)$$

where  $1 \leq i_1, i_2, \dots, i_k, j_1, j_2, \dots, j_k \leq n$  and  $\text{sign} = +$  if  $\{j_1, j_2, \dots, j_k\}$  is an even permutation of  $\{i_1, i_2, \dots, i_k\}$ ,  $\text{sign} = -$  if  $\{j_1, j_2, \dots, j_k\}$  is an odd permutation of  $\{i_1, i_2, \dots, i_k\}$ . Meanwhile, we have

$$dx^{i_l} \wedge dx^{i_l} = 0 \quad i_l = 1, 2, \dots, n . \quad (2.1.25)$$

Now, we can set up a basis for general  $k$ -forms ( $1 \leq k \leq n$ ). The basis has  $\frac{n!}{(n-k)!k!}$  linear

independent elements. A typical choice of the basis is given by

$$\left\{ dx^{i_1} \wedge dx^{i_2} \wedge \cdots \wedge dx^{i_k} \mid 1 \leq i_1 < i_2 < \cdots < i_k \leq n \right\}. \quad (2.1.26)$$

Using the basis, some examples of 0-forms, 1-forms, 2-forms and 3-forms in the coordination system  $\{x, y, z\}$  then can be given as

$$\alpha^{(0)} = \alpha(x, y, z); \quad (2.1.27)$$

$$\beta^{(1)} = \beta_1(x, y, z) dx + \beta_2(x, y, z) dy + \beta_3(x, y, z) dz; \quad (2.1.28)$$

$$\gamma^{(2)} = \gamma_1(x, y, z) dy \wedge dz + \gamma_2(x, y, z) dz \wedge dx + \gamma_3(x, y, z) dx \wedge dy; \quad (2.1.29)$$

$$\delta^{(3)} = \delta(x, y, z) dx \wedge dy \wedge dz. \quad (2.1.30)$$

where  $\alpha, \beta, \gamma, \delta$  are scalar functions. The wedge product between  $\beta^{(1)}$  and  $\gamma^{(2)}$  is written as

$$\beta^{(1)} \wedge \gamma^{(2)} = (\beta_1\gamma_1 + \beta_2\gamma_2 + \beta_3\gamma_3) dx \wedge dy \wedge dz. \quad (2.1.31)$$

This form is a 3-form which is also called the *volume form*. Its basis is called the *unit volume form*, denoted by *vol*. In above example,  $vol = dx \wedge dy \wedge dz$ . For an  $n$ -manifold with a local coordinate system  $\{x^1, x^2, \dots, x^n\}$ , a natural choice of the unit volume form is

$$vol = dx^1 \wedge dx^2 \wedge \cdots \wedge dx^n. \quad (2.1.32)$$

**Exterior derivative d:** [28] In an  $n$ -manifold  $\mathcal{M}$ , the exterior derivative  $d$  of a differential  $k$ -form  $\alpha^{(k)}$ ,  $0 \leq k \leq n-1$ , of space  $\Lambda^k(\mathcal{M})$  is a mapping:

$$d : \Lambda^k(\mathcal{M}) \rightarrow \Lambda^{k+1}(\mathcal{M}).$$

If  $\alpha^{(k)}$  is given as  $\alpha^{(k)} = \sum_i \alpha_i dx^{i_1} \wedge dx^{i_2} \wedge \cdots \wedge dx^{i_k}$  where  $i \in \left\{1, 2, \dots, \frac{n!}{(n-k)!k!}\right\}$  and  $dx^{i_1} \wedge dx^{i_2} \wedge \cdots \wedge dx^{i_k}$  is the  $i$ -th element of the basis, see Eq. (2.1.26), then

$$\begin{aligned} d\alpha^{(k)} &= \sum_i d\alpha_i dx^{i_1} \wedge dx^{i_2} \wedge \cdots \wedge dx^{i_k} \\ &= \sum_i \sum_{j=1}^n \frac{\partial \alpha_i}{\partial x_j} dx^j \wedge dx^{i_1} \wedge dx^{i_2} \wedge \cdots \wedge dx^{i_k}. \end{aligned} \quad (2.1.33)$$

- (1) Leibniz rule:

$$d(\alpha^{(k)} \wedge \beta^{(l)}) = d\alpha^{(k)} \wedge \beta^{(l)} + (-1)^k \alpha^{(k)} \wedge d\beta^{(l)}; \quad (2.1.34)$$

- (2) It is a nilpotent:

$$dd\alpha^{(k)} = 0. \quad (2.1.35)$$

For example, in a three-dimensional space with a coordinate system  $\{x, y, z\}$ , the exterior derivatives of the 0-form (Eq. (2.1.27)), 1-form (Eq. (2.1.28)) and 2-form (Eq. (2.1.29)) are

$$d\alpha^{(0)} = \frac{\partial\alpha}{\partial x}dx + \frac{\partial\alpha}{\partial y}dy + \frac{\partial\alpha}{\partial z}dz ; \quad (2.1.36)$$

$$d\beta^{(1)} = \left( \frac{\partial\beta_3}{\partial y} - \frac{\partial\beta_2}{\partial z} \right) dy \wedge dz + \left( \frac{\partial\beta_1}{\partial z} - \frac{\partial\beta_3}{\partial x} \right) dz \wedge dx + \left( \frac{\partial\beta_2}{\partial x} - \frac{\partial\beta_1}{\partial y} \right) dx \wedge dy ; \quad (2.1.37)$$

$$d\gamma^{(2)} = \left( \frac{\partial\gamma_1}{\partial x} + \frac{\partial\gamma_2}{\partial y} + \frac{\partial\gamma_3}{\partial z} \right) dx \wedge dy \wedge dz . \quad (2.1.38)$$

Note that exterior derivatives of a 0-form, a 1-form and a 2-form are analogous to the gradient of a scalar function, the curl of a vector field and the divergence of a vector field in vector calculus.

We say  $k$ -manifolds are associated with  $k$ -forms because of the fact that  $k$ -forms are integrable on  $k$ -manifolds. There is nothing different between this manifold integral and the general integral in an Euclidean space. For example, an integral of a 1-form  $\beta^{(1)}$  given by Eq. (2.1.28) over a 1-manifold  $\mathcal{M}$  which in fact is analogous to a line integral of a vector space. For example, given a line (C) (a 1-manifold  $\mathcal{M}$ ) expressed as

$$\mathbf{r} = \mathbf{r}(t) = (x(t), y(t), z(t)) \quad a \leq t \leq b , \quad (2.1.39)$$

then, we have the integral of a 1-form  $\beta^{(1)} = \beta_1(x, y, z)dx + \beta_2(x, y, z)dy + \beta_3(x, y, z)dz$  over the line is

$$\int_{\mathcal{M}} \beta^{(1)} = \int_{(C)} \beta_1(x, y, z)dx + \beta_2(x, y, z)dy + \beta_3(x, y, z)dz , \quad (2.1.40)$$

where

$$\int_{(C)} \beta_1(x, y, z)dx = \int_a^b \beta_1 [x(t), y(t), z(t)] x'(t)dt ;$$

$$\int_{(C)} \beta_2(x, y, z)dy = \int_a^b \beta_2 [x(t), y(t), z(t)] y'(t)dt ;$$

$$\int_{(C)} \beta_3(x, y, z)dz = \int_a^b \beta_3 [x(t), y(t), z(t)] z'(t)dt .$$

which is exactly the line integral of a vector  $\boldsymbol{\beta} = (\beta^{(1)})^\sharp$  over the line (C).

The integral of a  $k$ -form  $\alpha^{(k)}$  over a  $k$ -manifold  $\mathcal{M}$  can also be expressed as the duality pairing between the  $k$ -form  $\alpha^{(k)}$  and the  $k$ -manifold  $\mathcal{M}$ :

$$\langle \alpha^{(k)}, \mathcal{M} \rangle = \int_{\mathcal{M}} \alpha^{(k)} . \quad (2.1.41)$$

**Generalized Stokes' theorem:** *The integral of a  $(k+1)$ -form,  $d\omega^{(k)}$ , over a  $(k+1)$ -manifold  $\mathcal{M}$  is equal to the integral of the  $k$ -form,  $\omega^{(k)}$ , over the  $k$ -manifold  $\partial\mathcal{M}$*

$$\int_{\mathcal{M}} d\omega^{(k)} = \int_{\partial\mathcal{M}} \omega^{(k)}, \quad (2.1.42)$$

or in duality pairing:

$$\langle d\omega^{(k)}, \mathcal{M} \rangle = \langle \omega^{(k)}, \partial\mathcal{M} \rangle. \quad (2.1.43)$$

If  $n = 1, k = 0$ , it refers to the *Newton-Leibniz integral rule*:

$$\int_a^b f'(x) dx = f(x) \Big|_a^b. \quad (2.1.44)$$

If  $n = 3, k = 1$ , it refers to the *Stokes' theorem*:

$$\int_S (\nabla \times \mathbf{g}) \cdot \mathbf{n} dS = \oint_{\partial S} \mathbf{g} \cdot \mathbf{n} dr. \quad (2.1.45)$$

If  $n = 3, k = 2$ , it then refers to the *Gauss Theorem*:

$$\int_V \nabla \cdot \mathbf{h} dV = \oint_S \mathbf{h} \cdot \mathbf{n} dS. \quad (2.1.46)$$

Ensuring that the generalized Stokes' theorem is satisfied exactly is one of the main features of the mimetic spectral element method we will present in Chapter 3.

### 2.1.5 True forms and pseudo-forms

As we know, every manifold has 2 possible orientations (positive and negative) no matter whether this manifold is outer oriented or inner oriented. Integrals of a  $k$ -forms  $\alpha^{(k)}$  over a  $k$ -manifold  $\mathcal{M}$  from different orientations result in opposite values (If  $\alpha^{(k)}$  does not change when we integrate it from different orientation):

$$\int_{\mathcal{M}^+} \alpha^{(k)} = - \int_{\mathcal{M}^-} \alpha^{(k)}. \quad (2.1.47)$$

For example, in  $\mathbb{R}^1$ , there is a 1-manifold  $\mathcal{M}$  given as  $[a, b]$ , and we define the orientation from  $a$  to  $b$  is the positive orientation. Then in  $\mathcal{M}$ , for an arbitrary 1-form  $\beta^{(1)}$  which is always given as  $\beta^{(1)} = \beta dx$  no matter from which orientation  $\beta^{(1)}$  is integrated, we know

$$\int_{\mathcal{M}^+} \beta^{(1)} = \int_a^b \beta dx = - \int_b^a \beta dx = - \int_{\mathcal{M}^-} \beta^{(1)}. \quad (2.1.48)$$

From now on, when we say the orientation of a manifold  $\mathcal{M}$ , we usually refer to the orientation from which we integrate forms over the manifold  $\mathcal{M}$ . We usually choose the positive orientation as the integral orientation.

If we change the orientation of a manifold  $\mathcal{M}$ , there are some integral values on this manifold  $\mathcal{M}$  change sign while some other integral values do not change sign. For example, the mass  $M$  is the integral of the density 3-form,  $\rho^{(3)}$  over a 3-manifold  $\mathcal{M}$ :

$$M = \int_{\mathcal{M}} \rho^{(3)}. \quad (2.1.49)$$

This value does not depend on the orientation of  $\mathcal{M}$ . It is always positive:

$$M = \int_{\mathcal{M}^+} \rho_+^{(3)} = \int_{\mathcal{M}^-} \rho_-^{(3)} = M. \quad (2.1.50)$$

Through Eq. (2.1.48), we know  $\rho_+^{(3)} = -\rho_-^{(3)}$ . This means when we change the orientation of the manifold, the density 3-form,  $\rho^{(3)}$ , changes sign.

While there are some other values do change sign when the orientation of the manifold changes like the  $\alpha^{(k)}$  in Eq. (2.1.47), the  $\beta^{(1)}$  in Eq. (2.1.47) and the work of a force along a curve. The work of a force (1-form  $f^{(1)}$ ) along a curve from point  $A$  to point  $B$ , denoted by  $W_{AB}$ , is always equal to the work of the force along the curve from point  $B$  to point  $A$ ,  $W_{AB} = -W_{BA}$ , which implies the force, 1-form  $f^{(1)}$ , does not change sign when the orientation of the manifold (curve) changes.

**True forms and pseudo forms:** For a  $k$ -form  $\alpha^{(k)}$  in a  $k$ -manifold  $\mathcal{M}$ , when the orientation of  $\mathcal{M}$  changes, if  $\alpha^{(k)}$  does not change sign and  $\int_{\mathcal{M}} \alpha^{(k)}$  does change sign,  $\alpha^{(k)}$  is said to be a true form, and if  $\alpha^{(k)}$  does change sign and  $\int_{\mathcal{M}} \alpha^{(k)}$  does not change sign,  $\alpha^{(k)}$  is said to be a pseudo form.

According to this definition, we know that the force 1-form  $f^{(1)}$  is a true form while the density 3-form  $\rho^{(3)}$  is a pseudo form. As a matter of fact, true forms are associated with inner oriented manifolds, while pseudo forms are associated with outer oriented manifolds. Therefore, we have

*Remark.* True forms are also called inner forms, pseudo forms are also called outer forms, and usually we use a tilde upon a form or a space to represent an inner one.

For example the force 1-form is expressed as  $\tilde{f}^{(1)}$ . The space of inner  $k$ -forms is expressed as  $\tilde{\Lambda}^k(\mathcal{M})$ . However, mathematically space  $\Lambda^k(\mathcal{M})$  and space  $\tilde{\Lambda}^k(\mathcal{M})$  are in fact the same space. For example, in a three-dimensional manifold  $\mathcal{M}$  with local coordinate system  $\{x, y, z\}$ , if there is an outer 2-form  $\gamma^{(2)}$ :

$$\gamma^{(2)} = \gamma_1(x, y, z) dy \wedge dz + \gamma_2(x, y, z) dz \wedge dx + \gamma_3(x, y, z) dx \wedge dy,$$

in  $\Lambda^2(\mathcal{M})$ , you can always find an inner 2-form  $\tilde{\gamma}^{(2)}$ :

$$\tilde{\gamma}^{(2)} = \gamma_1(x, y, z) \, dy \wedge dz + \gamma_2(x, y, z) \, dz \wedge dx + \gamma_3(x, y, z) \, dx \wedge dy ,$$

in  $\tilde{\Lambda}^2(\mathcal{M})$ . Vice versa. As you can see, mathematically  $\gamma^{(2)} = \tilde{\gamma}^{(2)}$ . While physically  $\gamma^{(2)} \neq \tilde{\gamma}^{(2)}$  if you take the orientation into account.

**Remark.** In a statement, symbols without tildes upon them like  $\alpha^{(k)}$ ,  $\Lambda^k(\mathcal{M})$ ,  $L^2\Lambda^k(\mathcal{M})$  (not appear yet),  $\pi$  (not appear yet), etc. can represent either outer oriented or inner oriented forms, spaces, projections, etc. unless both symbols with tildes and without tildes appear or it is emphasized that the statement is only proper for one specific kind of forms, spaces, etc..

For example, all theorems in previous sections are suitable for both inner oriented and outer oriented forms and spaces. Distinguishing true (inner) forms and pseudo (outer) forms is crucial to fully understand physical phenomena.

### 2.1.6 Hodge star operator and codifferential

We already know that forms can be divided into inner forms and outer forms. If an inner form can be converted into an outer form and vice versa? The answer is yes. The operator which switches between inner forms and outer forms is called the Hodge star operator.

**Hodge star operator  $\star$ :** Provided  $\mathcal{M}$  is an  $n$ -manifold, for a  $k$ -form  $\alpha^{(k)}$  in  $\Lambda^k(\mathcal{M})$ , the Hodge star operator,  $\star$ , is a mapping:

$$\star : \Lambda^k(\mathcal{M}) \rightarrow \Lambda^{n-k}(\mathcal{M}) ,$$

where  $\Lambda^k(\mathcal{M})$  and  $\Lambda^{n-k}(\mathcal{M})$  are differently oriented, which satisfies

$$\alpha^{(k)} \wedge \star\beta^{(k)} = \left( \alpha^{(k)}, \beta^{(k)} \right) \text{vol} , \quad (2.1.51)$$

where  $\left( \alpha^{(k)}, \beta^{(k)} \right)$  is the inner product between  $\alpha^{(k)}$  and  $\beta^{(k)}$ , and  $\text{vol}$  is the unit volume form, see Eq. (2.1.32).

The formal definition of the inner product between two forms [9, 28, 38] is relatively complicated and beyond the range of this project. So it is not given in this thesis. Commonly, for two differential forms  $\alpha^{(k)}$  and  $\beta^{(k)}$ :

$$\alpha^{(k)} = \sum_i \alpha_i \, dx^{i_1} \wedge dx^{i_2} \wedge \dots \wedge dx^{i_k} ,$$

and

$$\beta^{(k)} = \sum_i \beta_i \, dx^{i_1} \wedge dx^{i_2} \wedge \dots \wedge dx^{i_k} ,$$

the inner product between  $\alpha^{(k)}$  and  $\beta^{(k)}$  is

$$\left(\alpha^{(k)}, \beta^{(k)}\right) = \sum_i \alpha_i \beta_i . \quad (2.1.52)$$

This is correct only for Cartesian coordinate systems. The inner product between two forms is metric-dependent. Therefore, the Hodge star operator is a metric-dependent operator. Provided a  $k$ -form  $\alpha^{(k)} = \sum_i \alpha_i dx^{i_1} \wedge dx^{i_2} \wedge \cdots \wedge dx^{i_k}$  in an  $n$ -manifold with the local coordinate system  $\{x^1, x^2, \dots, x^n\}$ . If the unit volume form is given as  $vol = dx^1 \wedge dx^2 \wedge \cdots \wedge dx^n$ , then

$$\star \alpha^{(k)} = \sum_i \alpha_i \star dx^{i_1} \wedge dx^{i_2} \wedge \cdots \wedge dx^{i_k} , \quad (2.1.53)$$

and

$$\star dx^{i_1} \wedge dx^{i_2} \wedge \cdots \wedge dx^{i_k} = \text{sign} \cdot dx^{j_1} \wedge dx^{j_2} \wedge \cdots \wedge dx^{j_{n-k}} , \quad (2.1.54)$$

where  $\{i_1, i_2, \dots, i_k\}$  is a subset of the set  $\{1, 2, \dots, n\}$  with  $\{j_1, j_2, \dots, j_{n-k}\}$  being its complementary set. If  $\{j_1, j_2, \dots, j_{n-k}, i_1, i_2, \dots, i_k\}$  is an even permutation of  $\{1, 2, \dots, n\}$ ,  $\text{sign} = +$ . If  $\{j_1, j_2, \dots, j_{n-k}, i_1, i_2, \dots, i_k\}$  is an odd permutation of  $\{1, 2, \dots, n\}$ ,  $\text{sign} = -$ . Then, we know

$$\star \star \alpha^{(k)} = (-1)^{k(n-k)} \alpha^{(k)} \quad \forall \alpha^{(k)} \in \Lambda^k(\mathcal{M}) . \quad (2.1.55)$$

For example, for a 3-manifold with the local coordinate system  $\{x, y, z\}$  and the unit volume form  $vol = dx \wedge dy \wedge dz$ , we have

$$\begin{aligned} \star 1 &= dx \wedge dy \wedge dz & \star dx \wedge dy \wedge dz &= 1 , \\ \star dx &= dy \wedge dz & \star dy &= dz \wedge dx & \star dz &= dx \wedge dy , \\ \star dy \wedge dz &= dx & \star dz \wedge dx &= dy & \star dx \wedge dy &= dz . \end{aligned}$$

Once we have the Hodge star operator, we can define the Hilbert space  $L^2\Lambda^k(\mathcal{M})$  and the  $L^2$ -inner product,  $(\cdot, \cdot)_{\mathcal{M}}$ , between two forms.

**Hilbert space  $L^2\Lambda^k(\mathcal{M})$  and  $L^2$ -inner product  $(\cdot, \cdot)_{\mathcal{M}}$ :** A Hilbert space  $L^2\Lambda^k(\mathcal{M})$  is a space of  $k$ -forms  $\Lambda^k(\mathcal{M})$  equipped with the  $L^2$ -inner product  $(\cdot, \cdot)_{\mathcal{M}} : L^2\Lambda^k(\mathcal{M}) \times L^2\Lambda^k(\mathcal{M}) \rightarrow \mathbb{R}$  which, for arbitrary two  $k$ -forms  $\alpha^{(k)}$  and  $\beta^{(k)} \in L^2\Lambda^k(\mathcal{M})$ , satisfies

$$\left(\alpha^{(k)}, \beta^{(k)}\right)_{\mathcal{M}} = \int_{\mathcal{M}} \left(\alpha^{(k)}, \beta^{(k)}\right) vol . \quad (2.1.56)$$

From Eq. (2.1.51) and Eq. (2.1.56), we obtain

$$\left(\alpha^{(k)}, \beta^{(k)}\right)_{\mathcal{M}} = \int_{\mathcal{M}} \alpha^{(k)} \wedge \star \beta^{(k)} . \quad (2.1.57)$$

In conventional vector calculus, The natural differential operators, *gradient*, *curl* and *divergence*, have their adjoint operators [19, 20]. As the generalized form of the differential operators, the exterior derivative  $d$  also has its adjoint operator which is called the *codifferential*.

**Codifferential:** *The codifferential operator is the  $L^2$ -adjoint of exterior derivative with respect to the  $L^2$ -inner product, which satisfies*

$$\left( \alpha^{(k)}, d^* \beta^{(k+1)} \right)_{\mathcal{M}} = \left( d\alpha^{(k)}, \beta^{(k+1)} \right)_{\mathcal{M}} - \int_{\partial\mathcal{M}} \alpha^{(k)} \wedge \star \beta^{(k+1)} \quad \forall \alpha^{(k)} \in L^2 \Lambda^k(\mathcal{M}), \quad (2.1.58)$$

where  $0 \leq k \leq (n-1)$ . The Eq. (2.1.58) is called the integration by parts in differential forms.

The exterior derivative and codifferential operators actually refer to the natural differential operators and their adjoint operators mentioned in [19, 20] and the Eq. (2.1.58) in fact is an expression in differential geometry of the supporting integral identities, Eq. (1.1.1) and Eq. (1.1.2), used for the discretizations of adjoint operators in the mimetic finite difference method, see [18, 22, 23].

For a  $k$ -form  $\beta^{(k)}$ , we have

$$\star d^* \beta^{(k)} = (-1)^k d \star \beta^{(k)} \quad \forall \beta^{(k)} \in \Lambda^k(\mathcal{M}). \quad (2.1.59)$$

Together with Eq. (2.1.55), we obtain (if the boundary integral term in Eq. (2.1.58) is zero.)

$$d^* = (-1)^{n(k+1)+1} \star d \star. \quad (2.1.60)$$

The codifferential is also a nilpotent:

$$d^* d^* \beta^{(k)} = 0 \quad \forall \beta^{(k)} \in \Lambda^k(\mathcal{M}). \quad (2.1.61)$$

### 2.1.7 Lie derivative

The convective terms,  $(\mathbf{u} \cdot \nabla) \mathbf{u}$  and  $(\mathbf{u} \cdot \nabla) \boldsymbol{\omega}$ , in Euler equations represent the relative changes of  $\mathbf{u}$  and  $\boldsymbol{\omega}$  because of the motional flow field. The convection of a variable ( $k$ -form  $\alpha^{(k)}$ ) because of vector field  $\mathbf{u}$  is expressed by

$$\mathcal{L}_{\mathbf{u}} \alpha^{(k)} = d \iota_{\mathbf{u}} \alpha^{(k)} + \iota_{\mathbf{u}} d \alpha^{(k)} \quad \forall \alpha^{(k)} \in \Lambda^k(\mathcal{M}), \quad (2.1.62)$$

where  $\mathcal{L}_{\mathbf{u}}$  and  $\iota_{\mathbf{u}}$  are the *Lie derivative* and *interior product* with respect to the vector field  $\mathbf{u}$ .

**Interior product  $\iota_u$ :** In an  $n$ -manifold  $\mathcal{M}$ , if there is a vector field given by  $\mathbf{u}$ , the interior derivation  $\iota_u$  is a mapping

$$\iota_u : \Lambda^k(\mathcal{M}) \rightarrow \Lambda^{k-1}(\mathcal{M}) .$$

If  $\alpha^{(k)} \in \Lambda^k(\mathcal{M})$ ,

$$\iota_u \alpha^{(k)}(\omega_1, \omega_2, \dots, \omega_{k-1}) = \alpha^{(k)}(\mathbf{u}, \omega_1, \omega_2, \dots, \omega_{k-1}) .$$

Hence,  $\iota_u \alpha^{(0)} = 0$ , and given a 1-form  $\alpha^{(1)} = \sum_i \alpha_i dx^i$  and a vector field  $\mathbf{u} = \sum_i u^i \partial x_i$ , we have

$$\iota_u \alpha^{(1)} = \sum_i \alpha_i u^i . \quad (2.1.63)$$

The interior product satisfies the Leibniz rule:  $\forall \alpha^{(k)}, \beta^{(l)} \in \Lambda^k(\mathcal{M}), \Lambda^l(\mathcal{M})$  and  $k + l \leq n$

$$\iota_u (\alpha^{(k)} \wedge \beta^{(l)}) = (\iota_u \alpha^{(k)}) \wedge \beta^{(l)} + (-1)^k \alpha^{(k)} \wedge (\iota_u \beta^{(l)}) . \quad (2.1.64)$$

From above two properties, Eq. (2.1.63) and Eq. (2.1.64), we can generalize the computation of the interior product for 1-forms to those for arbitrary forms.

In  $\mathbb{R}^3$ , a Cartesian coordinate system is given as  $\{x, y, z\}$ . If the vector field is  $\mathbf{u} = u \partial x + v \partial y + w \partial z$ , for a 1-form  $\alpha^{(1)} = a dx + b dy + c dz$ , we have

$$\iota_u \alpha^{(1)} = au + bv + cw . \quad (2.1.65)$$

For a 2-form  $\beta^{(2)} = d dy \wedge dz + e dz \wedge dx + f dx \wedge dy$ , we have

$$\iota_u \beta^{(2)} = (we - vf) dx + (uf - wd) dy + (vd - ue) dz . \quad (2.1.66)$$

The interior product resembles the cross product in conventional vector calculus where  $\mathbf{a} \times \mathbf{b}$  is perpendicular to either  $\mathbf{a}$  or  $\mathbf{b}$ . In differential geometry, given a 3-manifold  $\mathcal{M}$ , it is very easy to see that,  $\forall \alpha^{(1)} \in \Lambda^1(\mathcal{M}), \forall \beta^{(2)} \in \Lambda^2(\mathcal{M})$

$$\int_{\mathcal{M}} \iota_{\alpha} \beta^{(2)} \wedge \beta^{(2)} = \int_{\mathcal{M}} \iota_{\alpha} \beta^{(2)} \wedge \star \alpha^{(1)} = 0 , \quad (2.1.67)$$

where  $\alpha = (\alpha^{(1)})^\sharp$ .

**Proof:** According to definitions given above, we can see that

$$\begin{aligned} & \iota_{\alpha} \beta^{(2)} \wedge \beta^{(2)} \\ &= \left( (ce - bf) dx + (af - cd) dy + (bd - ae) dz \right) \wedge (d dy \wedge dz + e dz \wedge dx + f dx \wedge dy) \\ &= d(ce - bf) dx \wedge dy \wedge dz + e(af - cd) dy \wedge dz \wedge dx + f(bd - ae) dz \wedge dx \wedge dy \\ &= 0 , \end{aligned} \quad (2.1.68)$$

and

$$\begin{aligned}
& \iota_\alpha \beta^{(2)} \wedge \star \alpha^{(1)} \\
&= \left( (ce - bf) dx + (af - cd) dy + (bd - ae) dz \right) \wedge (a dy \wedge dz + b dz \wedge dx + c dx \wedge dy) \\
&= a(ce - bf) dx \wedge dy \wedge dz + b(af - cd) dy \wedge dz \wedge dx + c(bd - ae) dz \wedge dx \wedge dy \\
&= 0.
\end{aligned} \tag{2.1.69}$$

The adjoint operator,  $j$ , of interior product is defined as

$$\star j_u \alpha^{(k)} = (-1)^k \iota_u \star \alpha^{(k)} \quad \forall \alpha^{(k)} \in \Lambda^k(\mathcal{M}), \tag{2.1.70}$$

and the adjoint operator,  $L$ , of the Lie derivative is defined as

$$L_u \star \alpha^{(k)} = -\star \mathcal{L}_u \alpha^{(k)} \quad \forall \alpha^{(k)} \in \Lambda^k(\mathcal{M}). \tag{2.1.71}$$

See [15, 28] for more details.

## 2.2 Algebraic topology

In this section, a basic introduction of algebraic topology will be presented.

### 2.2.1 Cell complex

Numerical schemes can not work with infinite numbers of degrees of freedom. So every scheme needs one or more grids in which variables are discretized. Given an  $n$ -manifold, by setting up a grid within this manifold, we get a series of sub-manifolds. This grid is called the *cell complex*. Within the cell complex, sub-manifolds are of order from 0 to  $n$ . These sub-manifolds are called  $k$ -cells ( $0 \leq k \leq n$ ). A 0-cell is a point (0-manifold), a 1-cell is a line (1-manifold), a 2-cell is a surface (2-manifold) and a 3-cell is a volume (3-manifold). The cell complex, a set of cells, is the grid in which our mimetic scheme will work.

Here in this project, we consider the  $n$ -manifold given as a unit  $n$ -cube. A unit  $n$ -cube denoted by  $I^n$  is a manifold given by  $[-1, 1]^n$ . By setting up a structured grid within the  $n$ -cube, we set up a constructed cell complex. For example, in a 3-cube, by constructing a structured grid, we get a cell complex containing points (0-cells), straight lines (1-cells) and surfaces (2-cells) and cubes (3-cells), see Fig. 2.7.

As a fact of matter, a cell which is a manifold can be inner or outer oriented. Cells in a cell complex can not be differently oriented. That means all of them are either inner oriented

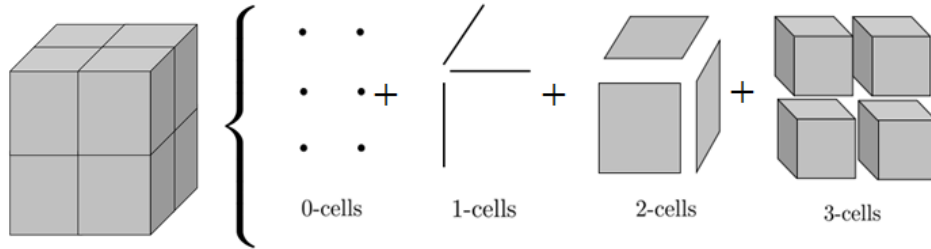


Figure 2.7: Cells of a cell complex in  $\mathbb{R}^3$ .

or outer oriented. More discussions about the orientation of cell complexes can be find in Section 2.2.3. For the time being we use outer oriented cell complexes as example.

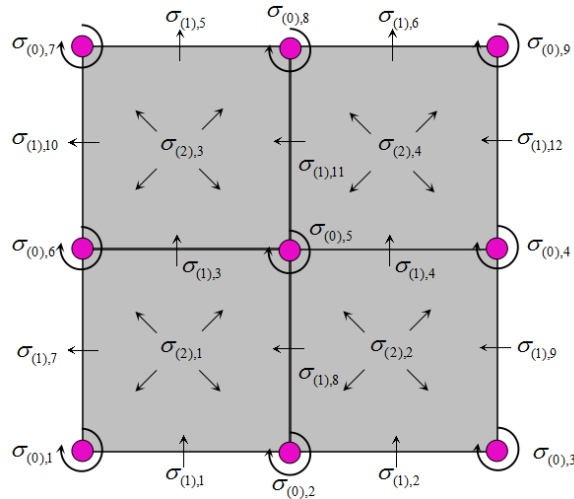


Figure 2.8: A cell complex in  $\mathbb{R}^2$ .

There is an example in Fig. 2.8 where a cell complex in  $\mathbb{R}^2$  containing 9 0-cells, 12 1-cells and 4 2-cells is presented. As we can see in this figure, all cells are outer oriented and their positive orientations are given. Meanwhile we denote  $k$ -cells by  $\sigma_{(k)}$  and number them as  $\sigma_{(k),i}$ . Remember, the way of defining the positive orientation of each cell is non-unique, as well as the method of numbering them. But once you make your choice, you should not change it during the computation.

### 2.2.2 Chain and cochain

In a cell complex,  $D$ , we can associate a weight  $c^i$  to each  $k$ -cell  $\sigma_{(k),i}$  then add all weighted  $k$ -cells together, which results in the so called  $k$ -chain  $c_{(k)}$ :

$$c_{(k)} = \sum_i c^i \sigma_{(k),i} . \tag{2.2.1}$$

The set of all  $c_{(k)}$  then form a vector space denoted as  $C_k(D)$ . One basis of the space  $C_k(D)$  is  $\{\sigma_{(k),1}, \sigma_{(k),2}, \dots, \sigma_{(k),\#k}\}$ , where  $\#k$  is the number of  $k$ -cells in the cell complex. (Different from the  $\#$  operator in differential geometry, see Section 2.1.2.)

We can introduce an operator  $\varphi$  which converts a  $k$ -chain into a vector form by

$$c_k = \varphi(c_{(k)}) = \{c^1, c^2, \dots, c^{\#k}\}^T. \quad (2.2.2)$$

Although a weight  $c^i$ , also called a coefficient, of  $c_{(k)}$  can be any value, in our applications,  $c^i$  commonly belongs to  $\{-1, 0, 1\}$ . For a  $k$ -chain  $c_{(k)}$ , coefficient  $c^i = 1$  means the  $k$ -cell  $\sigma_{(k),i}$  is in the chain and its orientation is same with its positive default orientation. If  $c^i = -1$ ,  $\sigma_{(k),i}$  is in the chain as well but its orientation is opposite with its positive orientation. When  $c^i = 0$ , the corresponding  $k$ -cell  $\sigma_{(k),i}$  is not in the chain.

We can obtain the boundary of a  $k$ -chain  $c_{(k)}$  by applying the *boundary operator*  $\partial$  to it which gives a  $(k-1)$ -chain  $\partial c_{(k)}$ :

$$\partial c_{(k)} = \sum_i c^i \partial \sigma_{(k),i} \quad \forall c_k \in C_k(D). \quad (2.2.3)$$

The boundary of  $\sigma_{(k),i}$ ,  $\partial \sigma_{(k),i}$ , only contains  $(k-1)$ -cells which bound  $\sigma_{(k),i}$ . Take the cell complex in Fig. 2.8 as example,

$$\begin{aligned} \partial \sigma_{(2),1} &= -\sigma_{(1),1} + \sigma_{(1),7} + \sigma_{(1),3} - \sigma_{(1),8}, \\ \partial \sigma_{(2),2} &= -\sigma_{(1),2} + \sigma_{(1),8} + \sigma_{(1),4} - \sigma_{(1),9}, \\ \partial \sigma_{(2),3} &= -\sigma_{(1),3} + \sigma_{(1),10} + \sigma_{(1),5} - \sigma_{(1),11}, \\ \partial \sigma_{(2),4} &= -\sigma_{(1),4} + \sigma_{(1),11} + \sigma_{(1),6} - \sigma_{(1),12}. \end{aligned}$$

Express this in matrix form

$$\begin{pmatrix} \partial \sigma_{(2),1} \\ \partial \sigma_{(2),2} \\ \partial \sigma_{(2),3} \\ \partial \sigma_{(2),4} \end{pmatrix} = \begin{pmatrix} -1 & 0 & 1 & 0 & 0 & 0 & 1 & -1 & 0 & 0 & 0 & 0 \\ 0 & -1 & 0 & 1 & 0 & 0 & 0 & 1 & -1 & 0 & 0 & 0 \\ 0 & 0 & -1 & 0 & 1 & 0 & 0 & 0 & 0 & 1 & -1 & 0 \\ 0 & 0 & 0 & -1 & 0 & 1 & 0 & 0 & 0 & 0 & 1 & -1 \end{pmatrix} \begin{pmatrix} \sigma_{(1),1} \\ \sigma_{(1),2} \\ \vdots \\ \sigma_{(1),12} \end{pmatrix}. \quad (2.2.4)$$

The matrix on the right side is usually denoted by  $\mathbb{E}_{(2,1)}$ . Given a cell complex in a  $n$ -manifold, if all cells are labeled and oriented, we can set up matrices  $\mathbb{E}_{(k,k-1)}$  ( $k = 1, 2, \dots, n$ ) easily. Given a  $k$ -chain  $c_k = \varphi(c_{(k)}) = \{c^1, c^2, \dots, c^{\#k}\}^T$ , we know

$$\varphi(\partial c_{(k)}) = \mathbb{E}_{(k-1,k)} c_k \quad \forall c_{(k)} \in C_k(D), \quad (2.2.5)$$

where  $\mathbb{E}_{(k-1,k)}$ , the discrete form of the boundary operator, is called *incidence matrix* which is the transpose of  $\mathbb{E}_{(k,k-1)}$ :

$$\mathbb{E}_{(k-1,k)} = \mathbb{E}_{(k,k-1)}^T. \quad (2.2.6)$$

The boundary of the boundary is empty,  $\partial\partial\mathbf{c}_{(k)} = \emptyset, \forall \mathbf{c}_{(k)} \in C_k(D)$ . Therefore, we have

$$\mathbb{E}_{(k-1,k)}\mathbb{E}_{(k,k+1)} = \mathbf{0}. \quad (2.2.7)$$

With the vector space  $C_k(D)$ , we can associate a linear function space, a dual space, denoted by  $C^k(D)$ , see Eq. (2.1.6). A basis of  $C^k(D)$  is written as  $\{\sigma^{(k),1}, \sigma^{(k),2}, \dots, \sigma^{(k),\#k}\}$  such that

$$\sigma^{(k),i}(\sigma_{(k),j}) = \delta_j^i, \quad (2.2.8)$$

where  $\delta_j^i$  is the Kronecker delta. The element of  $C^k(D)$  is called the  $k$ -cochain, denoted by  $\mathbf{c}^{(k)}$ :

$$\mathbf{c}^{(k)} = \sum_i c_i \sigma^{(k),i}, \quad (2.2.9)$$

which can be converted into vector as  $\mathbf{c}^k = \varphi(\mathbf{c}^{(k)}) = \{c_1, c_2, \dots, c_{\#k}\}^T$ . (Suppose that operator  $\varphi$  can also work on a cochain.) The *duality pairing* between a chain and a cochain is expressed as

$$\langle \mathbf{c}^{(k)}, \mathbf{c}_{(k)} \rangle = \mathbf{c}^{(k)}(\mathbf{c}_{(k)}) = \sum_i c_i c^i. \quad (2.2.10)$$

**Coboundary:** Given a cell complex  $D$ , a coboundary operator  $\delta$  is a mapping:

$$\delta : C^k(D) \rightarrow C^{k+1}(D),$$

such that,  $\forall \mathbf{c}^{(k)} \in C^k(D)$  and  $\forall \mathbf{c}_{(k+1)} \in C_{k+1}(D)$ ,

$$\langle \delta \mathbf{c}^{(k)}, \mathbf{c}_{(k+1)} \rangle = \langle \mathbf{c}^{(k)}, \partial \mathbf{c}_{(k+1)} \rangle. \quad (2.2.11)$$

Given a cell complex  $D$  and a  $k$ -cochain  $\mathbf{c}^{(k)} \in C^k(D)$ ,  $\mathbf{c}^{(k)} = \{c_1, c_2, \dots, c_{\#k}\}^T$ , the duality pairing between  $\mathbf{c}^{(k)}$  and each  $k$ -cell,  $\langle \mathbf{c}^{(k)}, \sigma_{(k),i} \rangle = c_i$ , resembles that the  $k$ -cochain associates a value  $c_i$  to the  $k$ -cell. Therefore, a  $k$ -cochain can be considered as a set of a series of values associated with  $k$ -cells, and the coboundary  $\delta$  takes these values then projects them into values associated with  $(k+1)$ -cells according to the boundaries ( $k$ -chains) of the  $(k+1)$ -cells, for example, see Fig. 2.9. In Fig. 2.9a, a 0-cochain is given as  $\mathbf{c}^{(0)} = \sigma^{(0),1} + 7\sigma^{(0),2} - 4\sigma^{(0),3}$ , and the two boundaries of the two 1-cells are  $\partial\sigma_{(1),1} = \sigma_{(0),1} - \sigma_{(0),2}$  and  $\partial\sigma_{(1),2} = \sigma_{(0),2} - \sigma_{(0),3}$ . Then we have

$$\langle \delta \mathbf{c}^{(0)}, \mathbf{c}_{(1),1} \rangle = \langle \mathbf{c}^{(0)}, \partial \mathbf{c}_{(1),1} \rangle = \sigma^{(0),1}(\sigma_{(0),1}) - 7\sigma^{(0),2}(\sigma_{(0),2}) = -6,$$

$$\langle \delta \mathbf{c}^{(0)}, \mathbf{c}_{(1),2} \rangle = \langle \mathbf{c}^{(0)}, \partial \mathbf{c}_{(1),2} \rangle = 7\sigma^{(0),1}(\sigma_{(0),2}) + 4\sigma^{(0),3}(\sigma_{(0),2}) = 11.$$

In Fig. 2.9b, a 1-cochain is given as  $\mathbf{c}^{(1)} = 4\sigma^{(1),1} + 3\sigma^{(1),2} - 5\sigma^{(1),3} + 9\sigma^{(1),4}$ , and the boundary of the 2-cell is  $\partial\sigma_{(2),1} = -\sigma_{(1),1} - \sigma_{(1),2} + \sigma_{(1),3} + \sigma_{(1),4}$ . Then we have

$$\langle \delta\mathbf{c}^{(1)}, \mathbf{c}_{(2),1} \rangle = \langle \mathbf{c}^{(1)}, \partial\mathbf{c}_{(2),1} \rangle = -4 - 3 - 5 + 9 = -3.$$

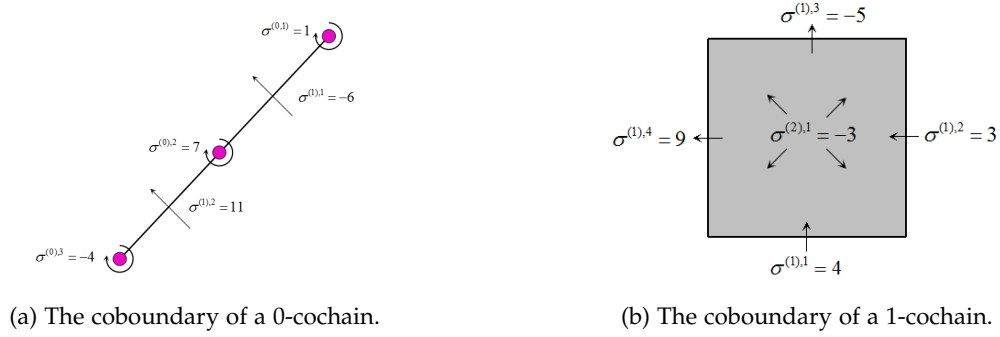


Figure 2.9: Coboundaries of cochains.

Given a cell complex  $D$  and a  $k$ -cochain  $\mathbf{c}^{(k)}$  of  $C^k(D)$ ,  $\mathbf{c}^k = \varphi(\mathbf{c}^{(k)}) = \{c_1, c_2, \dots, c_{\#k}\}^T$ , then we have

$$\varphi(\delta\mathbf{c}^{(k)}) = \mathbb{E}^{(k+1,k)} \mathbf{c}^k, \quad (2.2.12)$$

where  $\mathbb{E}^{(k+1,k)} = \mathbb{E}_{(k,k+1)}^T = \mathbb{E}_{(k+1,k)}$  is the *incidence matrix* for coboundary. The coboundary of the coboundary is empty,  $\delta\delta\mathbf{c}^{(k)} = \emptyset, \forall \mathbf{c}^{(k)} \in C^k(D)$ , which indicates

$$\mathbb{E}^{(k+1,k)} \mathbb{E}^{(k,k-1)} = \mathbf{0}. \quad (2.2.13)$$

For example, if you assign an arbitrary 0-cochain to the cell complex in Fig. 2.9b, then take the coboundary twice, you will find  $\sigma^{(2),1} = 0$ . A simple proof of Eq. (2.2.13) can be done by applying the transpose operator to Eq. (2.2.7).

Note the strong analogy between the generalized Stokes' theorem, Eq. (2.1.43), and the coboundary relation Eq. (2.2.11). This analogy is the key factor to set up the mimetic spectral element method that satisfies the generalized Stokes' theorem exactly. The analogy can also be clearly seen, for example, in Fig. 2.9b where the computation of the coboundary resembles an integral of a 2-form  $d\alpha^{(1)}$  over a 2-manifold given by  $\sigma_{(2),1}$  which is the generalized form of the Stokes' theorem, Eq. (2.1.45).

### 2.2.3 Dual complex

As we said, a cell complex is in fact a grid in which we are going to set up our mimetic discretization. Since our variables (forms) are either inner oriented (true forms) or outer

oriented (pseudo forms), if both of these two kinds of forms appear in the scheme, we have introduced two cell complexes to discretize them. We usually call the one with outer oriented geometries (manifolds) the *primal grid* which is used for the discretization of outer forms and call the other one with inner oriented geometries (manifolds) the *dual grid* (*dual complex*), like the examples in Section 2.2.2, which is used to discretize inner forms. An example of the dual complex, an inner oriented cell complex, can be seen in the following figure, Fig. 2.10.

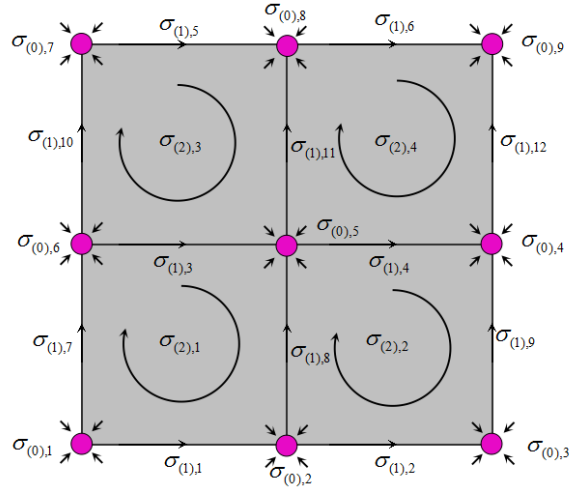


Figure 2.10: A dual complex.

We use the tilde upon a symbol to represent inner oriented one in Chapter 2. Similarly, here the tilde upon a symbol means this symbol is related to the dual grid (inner oriented, associated to true forms). For example, we use

$$\tilde{D}, \tilde{c}_{(k)}, \tilde{c}^{(k)}, C_k(\tilde{D}), C^k(\tilde{D}), \tilde{\mathbb{E}},$$

to represent a dual complex and a  $k$ -chain, a  $k$ -cochain, the  $k$ -chain space, the  $k$ -cochain space and an incidence matrix of the dual complex. While we use

$$D, c_{(k)}, c^{(k)}, C_k(D), C^k(D), \mathbb{E},$$

to represent a cell complex and a  $k$ -chain, a  $k$ -cochain, the  $k$ -chain space, the  $k$ -cochain space and an incidence matrix of the cell complex.

The kind of orientations of a grid does not mathematically affect the computation on the grid. That means the boundary operator  $\partial$  and coboundary operator  $\delta$  work on a complex in the same way no matter it is inner oriented or outer oriented.

## Mimetic spectral element method

Differential geometry, algebraic topology and the strong analogy between them have been presented. Now, with them, we introduce the way of setting up our mimetic framework—the mimetic spectral element method.

Provided a domain denoted by  $\Omega$  which in fact is a  $n$ -manifold, we can split the domain  $\Omega$  into several sub-domains  $\Omega_i$ . Through a *map operator*, we can then map the sub-domain  $\Omega_i$  into a unit  $n$ -cube  $I^n = [-1, 1]^n$ . The map operator together with its adjoint operator, *pullback*, which pull forms on  $I^n$  back to  $\Omega_i$  provide tools to deal with problems in arbitrary domains. The method of how to discretize the map operator and the pullback operator in the mimetic spectral element method is already well developed, see [17, 25, 26, 38], and once our scheme is constructed in  $I^3$ , that method can be used to our scheme, which will make our scheme applicable to arbitrary domains. However, because our main objective of this project is to find a spatially mass-, kinetic energy- and helicity-preserving scheme for three-dimensional flows, we will just use the simplest domain  $I^3$  as our flow domain. Therefore, there is no necessity for us to take the map operator and the pullback operator into account in this project.

**Remark.** From now on, we always use symbol  $\Omega$  to represent our unit flow domain, unit 3-cube  $I^3 = [-1, 1]^3$ .

In  $\Omega$ , given a  $k$ -form  $\alpha^{(k)} \in \Lambda^k(\Omega)$ , to make it solvable in a mimetic scheme, we first set up a grid (cell complex)  $D$  (primal or dual, depends on the type of  $\alpha^{(k)}$ ), then project  $\alpha^{(k)}$  into a discrete  $k$ -form  $\alpha_h^{(k)} \in \Lambda_h^k(\Omega; C_k)$  by the *projection operator*  $\pi$ . The space  $\Lambda_h^k(\Omega; C_k)$  represents a subspace, associated with the  $k$ -chain space  $C_k(D)$ , of  $\Lambda^k(\Omega)$ :

$$\Lambda_h^k(\Omega; C_k) \subset \Lambda^k(\Omega) .$$

The projection operator  $\pi$  is a direct application of differential geometry, algebraic topology and the analogy between them.

In this chapter, the projection operator together with another two important kinds of ingredients of the mimetic spectral element method, discrete operators and basis functions, will be introduced.

### 3.1 Projections

In the mimetic framework, the projection  $\pi$  is given as  $\pi = \mathcal{I} \circ \mathcal{R}$  where  $\mathcal{R}$  is the *reduction operator* and  $\mathcal{I}$  is the *reconstruction operator*, see Fig. 3.1.

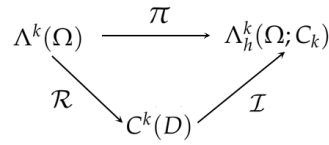


Figure 3.1: Projection  $\pi$ , reduction  $\mathcal{R}$  and reconstruction  $\mathcal{I}$ .

**Reduction:** Given a domain  $\Omega$  and a grid  $D$  in  $\Omega$ , the reduction operator  $\mathcal{R}$  is a mapping that maps differential forms to cochains:

$$\mathcal{R} : \Lambda^k(\Omega) \rightarrow C^k(D) ,$$

which satisfies,  $\forall \alpha^{(k)} \in \Lambda^k(\Omega), \forall \sigma_{(k)} \in D$ ,

$$\langle \mathcal{R}\alpha^{(k)}, \sigma_{(k)} \rangle = \int_{\sigma_{(k)}} \alpha^{(k)} = \langle \alpha^{(k)}, \sigma_{(k)} \rangle , \quad (3.1.1)$$

where the duality pairing on the left side is the duality pairing between a  $k$ -cochain and a  $k$ -chain, see Eq. (2.2.10), while the one on the right side is the duality pairing between a  $k$ -form and a  $k$ -manifold (recall that a  $k$ -cell in fact is a  $k$ -manifold), see Eq. (2.1.41).

The reduction of a 0-form  $\alpha^{(0)}$  from the domain  $\Omega$  to the cell complex  $D$  is just a 0-cochain with values of the scalar valued function  $\alpha^{(0)}$  at all 0-cells of  $D$  being its coefficients:

$$\mathcal{R}\alpha^{(0)} = \sum_{i=1}^{\#0} \alpha^{(0)}(\sigma_{(0),i}) \sigma^{(0),i} . \quad (3.1.2)$$

While the reduction of a 1-form  $\beta^{(1)}$  is a 1-cochain with integral values of  $\beta^{(1)}$  over all 1-cells as its coefficients:

$$\mathcal{R}\beta^{(1)} = \sum_{i=1}^{\#1} \int_{\sigma_{(1),i}} \beta^{(1)} \sigma^{(1),i} . \quad (3.1.3)$$

A very important property of the reduction operator is its commutativity with respect to the exterior derivative  $d$  and the coboundary  $\delta$ :

$$\mathcal{R}d = \delta\mathcal{R} . \quad (3.1.4)$$

To prove this, we start with the duality pairing between a  $(k+1)$ -cochain  $\mathcal{R}d\alpha^{(k)}$  and a  $(k+1)$ -chain  $c_{(k+1)}$ :

$$\begin{aligned} \langle \mathcal{R}d\alpha^{(k)}, c_{(k+1)} \rangle &\stackrel{(3.1.1)}{=} \int_{c_{(k+1)}} d\alpha^{(k)} \\ &\stackrel{(2.1.43)}{=} \int_{\partial c_{(k+1)}} \alpha^{(k)} \\ &\stackrel{(3.1.1)}{=} \langle \mathcal{R}\alpha^{(k)}, \partial c_{(k+1)} \rangle \\ &\stackrel{(2.2.11)}{=} \langle \delta\mathcal{R}\alpha^{(k)}, c_{(k+1)} \rangle . \end{aligned} \quad (3.1.5)$$

**Reconstruction:** Given a domain  $\Omega$  and a grid  $D$  in  $\Omega$ , the reconstruction operator  $\mathcal{I}$  is a mapping that maps cochains back to differential forms:

$$\mathcal{I} : C^k(D) \rightarrow \Lambda_h^k(\Omega; C_k) .$$

The reconstruction operator should satisfy many properties. We only mention those do matter in this project.

- (1) The reduction of the reconstruction must be identity:

$$\mathcal{R} \circ \mathcal{I} = Id ; \quad (3.1.6)$$

- (2) The reconstruction is commutative with respect to the exterior derivative  $d$  and the coboundary  $\delta$ :

$$d\mathcal{I} = \mathcal{I}\delta . \quad (3.1.7)$$

Note that the projection  $\pi = \mathcal{I} \circ \mathcal{R}$  is not an identity:

$$\alpha^{(k)} = \pi(\alpha^{(k)}) + \mathcal{O}(h^p) , \quad (3.1.8)$$

where  $\mathcal{O}(h^p)$  is the discretization error in terms of the grid size  $h$  and the polynomial order  $p$ , which is unavoidable when we project a variable of infinite degrees of freedom to a domain with finite degrees of freedom.

Because the Hodge star operator is an isomorphism, so if we have a outer form space  $\Lambda^k(\Omega)$  and a projection  $\pi : \Lambda^k(\Omega) \rightarrow \Lambda_h^k(\Omega; C_k)$ , we can also find a inner form space  $\tilde{\Lambda}^k(D)$  and a projection  $\tilde{\pi} : \tilde{\Lambda}^k(\Omega) \rightarrow \tilde{\Lambda}_h^k(\Omega; \tilde{C}_k)$ . In general, we have

$$\star \pi \neq \tilde{\pi} \star \quad \text{and} \quad \star \tilde{\pi} \neq \pi \star . \quad (3.1.9)$$

## 3.2 Discrete operators

With the projection operator, we project the space  $\Lambda^k(\Omega)$  of infinite degrees of freedom into the space  $\Lambda_h^k(\Omega; C_k)$  of finite degrees of freedom. In this section, we will present how does the projection operator perform when it is applied to differential operators (exterior derivative  $d$ , wedge product  $\wedge$ ,  $L^2$ -inner product  $(\cdot, \cdot)_\Omega$ , interior product  $\iota$  and Hodge star operator  $\star$ ).

**Discrete exterior derivative  $d_h$**  : From previous sections, we already see that the exterior derivative commutes with the projection operator:

$$d\mathcal{I}\mathcal{R} = \mathcal{I}\delta\mathcal{R} = \mathcal{I}\mathcal{R}d . \quad (3.2.1)$$

So we know the discrete exterior derivative  $d_h$  performs in the same way on discrete forms of  $\Lambda_h^k(\Omega; C_k)$  as how the exterior derivative  $d$  performs on forms of  $\Lambda^k(\Omega)$ :

$$d_h\alpha_h^{(k)} = d\alpha_h^{(k)} = \mathcal{I}\delta\mathcal{R}\alpha_h^{(k)} \quad \forall \alpha_h^{(k)} \in \Lambda_h^k(\Omega; C_k) , \quad (3.2.2)$$

where  $\delta$  is the coboundary operator. If we apply the  $\varphi$  operator to above equation, we get

$$\varphi(\delta\mathcal{R}\alpha_h^{(k)}) = \mathbb{E}^{(k+1,k)}\varphi(\mathcal{R}\alpha_h^{(k)}) , \quad (3.2.3)$$

where  $\mathbb{E}^{(k+1,k)}$  is the metric-free incidence matrix.

**Discrete wedge product  $\wedge_h$** : Given a domain  $\Omega$ , a cell complex  $D$  in  $\Omega$  and a projection  $\pi : \Lambda^k(\Omega) \rightarrow \Lambda_h^k(\Omega; C_k)$ , we can introduce a discrete wedge product  $\wedge_h : \Lambda_h^k(\Omega; C_k) \times \Lambda_h^l(\Omega; C_l) \rightarrow \Lambda_h^{k+l}(\Omega; C_{k+l})$  by defining

$$\alpha_h^{(k)} \wedge_h \beta_h^{(l)} = \pi \left( \alpha_h^{(k)} \wedge \beta_h^{(l)} \right) , \quad (3.2.4)$$

$$\forall \alpha_h^{(k)} \in \Lambda_h^k(\Omega; C_k), \forall \beta_h^{(l)} \in \Lambda_h^l(\Omega; C_l).$$

Note that  $\wedge$  does not commute with projection  $\pi$ , so  $\alpha_h^{(k)} \wedge_h \beta_h^{(l)}$  is not equal to  $\alpha_h^{(k)} \wedge \beta_h^{(l)}$ . In fact [25]

$$\alpha_h^{(k)} \wedge_h \beta_h^{(l)} = \alpha_h^{(k)} \wedge \beta_h^{(l)} + \mathcal{O}(h^p) . \quad (3.2.5)$$

While in application, we always use  $\alpha_h^{(k)} \wedge_h \beta_h^{(l)} = \alpha_h^{(k)} \wedge \beta_h^{(l)}$ . Hence we introduce some error.

The same happens to the **discrete interior product  $\iota^h$** . We commonly use  $\iota_{u_h}^h \alpha_h^{(k)} = \iota_{u_h} \alpha_h^{(k)}$  while in fact

$$\iota_{u_h}^h \alpha_h^{(k)} = \iota_{u_h} \alpha_h^{(k)} + \mathcal{O}(h^p) . \quad (3.2.6)$$

**Discrete inner product**  $(\cdot, \cdot)_{\Omega, h}$  : Given a domain  $\Omega$ , a cell complex  $D$  of  $\Omega$  and a projection  $\pi : \Lambda^k(\Omega) \rightarrow \Lambda_h^k(\Omega; C_k)$ , we define the discrete inner product as:

$$\left( \alpha_h^{(k)}, \beta_h^{(k)} \right)_h = \pi \left( \alpha_h^{(k)}, \beta_h^{(k)} \right) \text{vol} \quad \forall \alpha_h^{(k)}, \beta_h^{(k)} \in \Lambda_h^k(\Omega; C_k), \quad (3.2.7)$$

where  $\text{vol}$  is the unit volume form. With this definition and the fact that

$$\int_{\Omega} \pi \alpha^{(n)} = \int_{\Omega} \alpha^{(n)},$$

where  $\alpha^{(n)}$  is a volume form in  $\Lambda^n(\Omega)$ , we can easily get the discrete inner product  $(\cdot, \cdot)_{\Omega}$ :

$$\left( \alpha_h^{(k)}, \beta_h^{(k)} \right)_{\Omega, h} = \int_{\Omega} \pi \left( \alpha_h^{(k)}, \beta_h^{(k)} \right) \text{vol} = \left( \alpha_h^{(k)}, \beta_h^{(k)} \right)_{\Omega}, \quad (3.2.8)$$

$$\forall \alpha_h^{(k)}, \beta_h^{(k)} \in \Lambda_h^k(\Omega; C_k).$$

**Discrete Hodge star operator**  $\star_h$  : The projection  $\pi$  and projection  $\tilde{\pi}$  naturally give us a discrete Hodge star operator  $\star_h$  defined as

$$\star_h \pi = \tilde{\pi} \star \quad \text{and} \quad \star_h \tilde{\pi} = \pi \star. \quad (3.2.9)$$

Comparing Eq. (3.1.9) and Eq. (3.2.9), we can easily find the differences between the Hodge star operator  $\star$  and this discrete Hodge star operator  $\star_h$ . This discrete Hodge star operator will not be calculated through the method that we use in Section 2.1.6 anymore.

**Codifferential operator**  $d^*$  : In terms of the codifferential operator  $d^*$ , for a term containing the codifferential operator, we can always use the integration by parts, see Eq. (2.1.58), to transfer that term into a new term containing the exterior derivative which already has its discrete counterpart, see Eq. 3.2.2.

### 3.3 Basic functions and reconstructions of discrete forms

The philosophy of how to constitute the mimetic framework has been given in previous sections. The reduction has been shown with examples in Section 3.1. Meanwhile, how differential operators perform at the discrete level is presented in Section 3.2. However, for the reconstruction operator  $\mathcal{I}$ , only its definition is already given. The process of reconstructing discrete differential forms is not presented in this thesis yet. In this section, the basis functions which are basic elements of reconstructions and the method of how to reconstruct discrete differential forms with these basis functions will be introduced.

**Basis functions:** [25, 28, 38] Given a line segment  $[-1, 1]$ ,  $(N + 1)$  nodes (including two end points) split this line segment into  $N$  intervals. We express these  $(N + 1)$  nodes as

$$x_0, x_1, x_2, \dots, x_N,$$

where  $-1 = x_0 < x_1 < \dots < x_N = 1$ . The  $N$  line intervals are expressed by

$$h_1, h_2, \dots, h_N,$$

where  $h_i = [x_{i-1}, x_i]$  ( $1 \leq i \leq N$ ). If there are a series of functions  $\phi_i^0(x)$  ( $0 \leq i \leq N$ ) and a series of functions  $\phi_i^1(x)$  ( $1 \leq i \leq N$ ) such that

- (1) For  $x_j \in \{x_0, x_1, x_2, \dots, x_N\}$ ,

$$\phi_i^0(x_j) = \delta_j^i; \quad (3.3.1)$$

- (2) For  $h_j \in \{h_1, h_2, \dots, h_N\}$ ,

$$\int_{h_j} \phi_i^1(x) dx = \int_{x_{j-1}}^{x_j} \phi_i^1(x) dx = \delta_j^i; \quad (3.3.2)$$

- (3) For an arbitrary linear combination of  $\psi_i^0(x)$  ( $0 \leq i \leq N$ ),  $\sum_{i=0}^N \alpha_i \psi_i^0(x)$ ,  $\alpha_i \in \mathbb{R}$ ,

$$d \sum_{i=0}^N \alpha_i \phi_i^0(x) = \sum_{i=1}^N (\alpha_i - \alpha_{i-1}) \phi_i^1(x) dx. \quad (3.3.3)$$

Then function sets  $\left\{ \phi_i^0(x) \mid 0 \leq i \leq N \right\}$  and  $\left\{ \phi_i^1(x) \mid 1 \leq i \leq N \right\}$  can be used to reconstruct discrete differential forms. The elements of these two sets are called basis functions and  $x_0, x_1, x_2, \dots, x_N$  are the nodes of these basis functions. Examples of basis functions  $\phi_i^0(x)$  and basis functions  $\phi_i^1(x)$  can be found in sub-figures (a), (c), (e) and (b), (d), (f) of Fig. 3.3 respectively.

In  $\mathbb{R}^1$ , given a domain  $\Omega = [-1, 1]$  and a cell complex in this domain, the 0-cells of the cell complex are the nodes of basis functions. For a 0-form  $\alpha^{(0)} \in \Lambda^0(\Omega)$ , we first reduce  $\alpha^{(0)}$  onto the 0-cells and get a 0-cochain  $\mathcal{R}\alpha^{(0)}$ ,  $\varphi(\mathcal{R}\alpha^{(0)}) = \{\alpha_0, \alpha_1, \alpha_2, \dots, \alpha_N\}^T$ . Then with basis functions  $\phi_i^0(x)$  ( $0 \leq i \leq N$ ), we reconstruct  $\alpha_0$  according to the 0-cochain  $\mathcal{R}\alpha^{(0)}$  as

$$\alpha_h^{(0)} = \mathcal{I}\mathcal{R}\alpha^{(0)} = \sum_{i=0}^N \alpha_i \phi_i^0(x) \quad \alpha_h^{(0)} \in \Lambda_h^0(\Omega; C_0). \quad (3.3.4)$$

In terms of a 1-form  $\beta^{(1)} \in \Lambda^1(\Omega)$ , we can obtain its discrete form  $\beta_h^{(1)}$  through the same approach, reducing the form to 1-cells then reconstructing the 1-cochain with basis functions

$\phi_i^1(x)$  ( $1 \leq i \leq N$ ):

$$\beta_h^{(1)} = \sum_{i=1}^N \beta_i \phi_i^1(x) dx \quad \beta_h^{(1)} \in \Lambda_h^1(\Omega; C_1). \quad (3.3.5)$$

Furthermore, if  $\beta^{(1)} = d\alpha^{(0)}$ , then we have

$$\beta_h^{(1)} = \mathcal{I}\mathcal{R}\beta^{(1)} = \mathcal{I}\mathcal{R}d\alpha^{(0)} = d\mathcal{I}\mathcal{R}\alpha^{(0)} = \mathcal{I}\delta\mathcal{R}\alpha^{(0)}. \quad (3.3.6)$$

Suppose that the  $\varphi$  operator can also work on discrete forms as  $\varphi(\alpha_h^{(k)}) = \varphi(\mathcal{R}\alpha_h^{(k)})$  (get coefficients and form a vector). Apply  $\varphi$  operator to both sides of above equation, yielding

$$\{\beta_1, \beta_2, \dots, \beta_N\}^T = \mathbb{E}^{(1,0)} \{\alpha_0, \alpha_1, \alpha_2, \dots, \alpha_N\}^T. \quad (3.3.7)$$

where  $\mathbb{E}^{(1,0)}$  is the incidence matrix of the cell complex  $D$ .

For example, when  $\alpha^{(0)} = \sin(\pi x) + \cos(0.5\pi x)$ ,  $\beta^{(1)} = d\alpha^{(0)} = \pi \cos(\pi x) - 0.5\pi \sin(0.5\pi x)$ , their projections using Gauss-Lobatto-Legendre polynomials at  $N = 4$  as basis functions are given in Fig. 3.2. Gauss-Lobatto-Legendre polynomials are the basis functions used in this project. More details about these basis functions can be found later in this section.

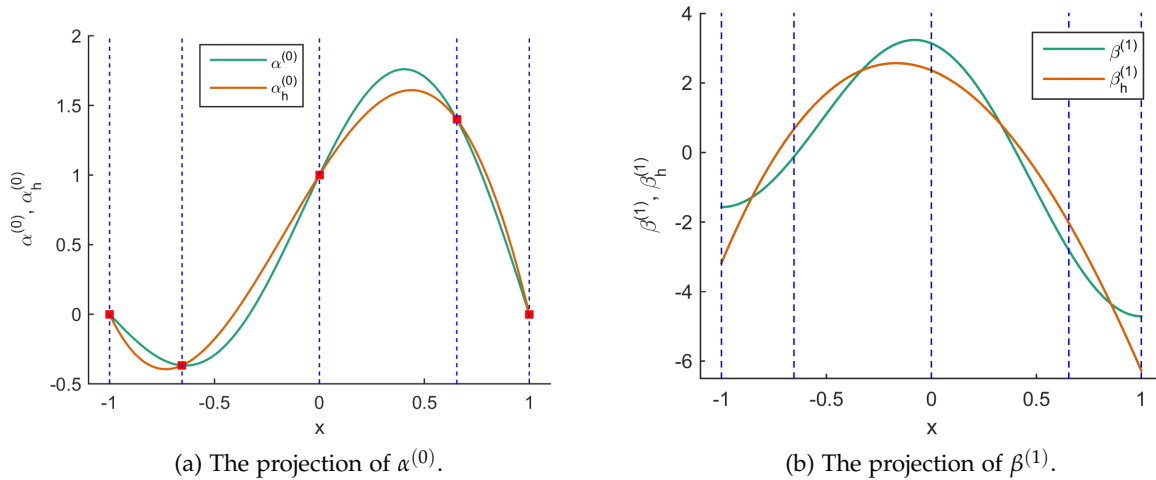


Figure 3.2: Projections using Gauss-Lobatto-Legendre polynomials at  $N = 4$ .

These basis functions can also be used to reconstruct forms in  $\mathbb{R}^n$  ( $n > 1$ ). For example, in a domain  $\Omega = [-1, 1]^3$  with orthogonal coordinate system  $\{x, y, z\}$ , if  $[-1, 1]$  is divided into  $N$  intervals by the  $(N + 1)$  nodes along each coordinate, we can construct a cell complex containing  $(N + 1)^3$  0-cells (points),  $3N(N + 1)^2$  1-cells (lines),  $3N^2(N + 1)$  2-cells (faces) and  $N^3$  volumes. Then forms can be reduced onto corresponding cells and sequentially be reconstructed as [38]:

- Discrete 0-forms (associated with points):

$$\alpha_h^{(0)} = \sum_{i=0}^N \sum_{j=0}^N \sum_{k=0}^N \alpha_{i,j,k} \phi_i^0(x) \phi_j^0(y) \phi_k^0(z) ; \quad (3.3.8)$$

- Discrete 1-forms (associated with lines):

$$\begin{aligned} \beta_h^{(1)} &= \sum_{i=1}^N \sum_{j=0}^N \sum_{k=0}^N \beta_{i,j,k}^x \phi_i^1(x) \phi_j^0(y) \phi_k^0(z) \, dx \\ &+ \sum_{i=0}^N \sum_{j=1}^N \sum_{k=0}^N \beta_{i,j,k}^y \phi_i^0(x) \phi_j^1(y) \phi_k^0(z) \, dy \\ &+ \sum_{i=0}^N \sum_{j=0}^N \sum_{k=1}^N \beta_{i,j,k}^z \phi_i^0(x) \phi_j^0(y) \phi_k^1(z) \, dz ; \end{aligned} \quad (3.3.9)$$

- Discrete 2-forms (associated with faces):

$$\begin{aligned} \gamma_h^{(2)} &= \sum_{i=0}^N \sum_{j=1}^N \sum_{k=1}^N \gamma_{i,j,k}^x \phi_i^0(x) \phi_j^1(y) \phi_k^1(z) \, dy \wedge dz \\ &+ \sum_{i=1}^N \sum_{j=0}^N \sum_{k=1}^N \gamma_{i,j,k}^y \phi_i^1(x) \phi_j^0(y) \phi_k^1(z) \, dz \wedge dx \\ &+ \sum_{i=1}^N \sum_{j=1}^N \sum_{k=0}^N \gamma_{i,j,k}^z \phi_i^1(x) \phi_j^1(y) \phi_k^0(z) \, dx \wedge dy ; \end{aligned} \quad (3.3.10)$$

- Discrete 3-forms (associated with volumes):

$$\delta_h^{(3)} = \sum_{i=1}^N \sum_{j=1}^N \sum_{k=1}^N \delta_{i,j,k} \phi_i^1(x) \phi_j^1(y) \phi_k^1(z) \, dx \wedge dy \wedge dz . \quad (3.3.11)$$

Once we number the cells of the cell complex and the coefficients of discrete differential forms in the same way, we have

$$\beta_h^{(k+1)} = d\alpha_h^{(k)} \iff \boldsymbol{\beta}^{k+1} = \mathbb{E}^{(k+1,k)} \boldsymbol{\alpha}^k , \quad (3.3.12)$$

where  $\boldsymbol{\beta}_h^{k+1}$  and  $\boldsymbol{\alpha}^k$  are the vector proxy of forms  $\beta_h^{(k+1)}$  and  $\alpha_h^{(k)}$ ,  $\boldsymbol{\beta}_h^{k+1} = \varphi(\beta_h^{(k+1)})$  and  $\boldsymbol{\alpha}^k = \varphi(\alpha_h^{(k)})$ .

By now, several kinds of spaces of basis functions have been developed, for example, the space of polynomials [5, 10, 28, 33, 38], the space of B-splines[25], the space of interpolator and histopolator functions [45]. The one we are going to use is the space of polynomials. Polynomials have been widely used in the numerical integration. With polynomials as basis functions, integrals of basis functions on  $[-1, 1]$  can be computed easily and exactly [33, 25].

The basic polynomials are Gauss-Lobatto-Legendre polynomials, an application of these polynomials is already shown in Fig 3.2. In addition, there are Gauss-Legendre polynomials and extended Gauss-Legendre polynomials. Different from the  $N$ th order Gauss-Lobatto-Legendre polynomials which need a grid of  $N$  line intervals and  $(N + 1)$  nodes on  $[-1, 1]$ , the  $N$ th order extended Gauss-Legendre polynomials require a grid of  $(N + 2)$  line intervals and  $(N + 1)$  nodes and the  $N$ th order Gauss-Legendre polynomials require a grid of  $N$  line intervals and  $(N - 1)$  nodes (excluding the two end points of extended Gauss-Legendre grid), for example, see Figure 4.1. The scheme, using staggered grids, a Gauss-Lobatto-Legendre grid and an extended Gauss-Legendre grid, in which we can construct an exact duality for the Hodge star operator has been developed, for example, see [3, 42]. With this duality, the Hodge star operator is exactly satisfied at the discrete level, which means we can project a discrete  $k$ -form on the Gauss-Lobatto-Legendre grid onto the extended Gauss-Legendre grid as a discrete  $(n - k)$ -form directly. Keeping this property in discrete systems is good. However, this kind of staggered grids does not help in our scheme. The reason of this will be given in Section 4.2.

Here in this project, the  $N$ th order Gauss-Lobatto-Legendre polynomials are used. The nodes of the corresponding grid, the Gauss-Lobatto-Legendre grid [5], are zeros of the function:

$$f(x) = (1 - x^2)L'_N(x), \quad (3.3.13)$$

where  $L'_N(x)$  is the derivative of the Legendre polynomials.

$$L_p(x) = \frac{(-1)^p}{2^p p!} \frac{d^p}{dx^p} (1 - x^2)^p \quad p \in \mathbb{N}, \quad (3.3.14)$$

$$L'_p(x) = \frac{1}{2}(p + 1)\phi_{p-1}^{1,1}(x) \quad p \in \mathbb{N}, \quad (3.3.15)$$

where  $\phi_{i-1}^{1,1}(x)$  is the Jacobi polynomial. For  $p \in \mathbb{N} \cup \{0\}$  and  $a, b > -1$ ,

$$\phi_p^{a,b}(x) = \frac{(-1)^p}{2^p p!} (1 - x)^{-a} (1 + x)^{-b} \frac{d^p}{dx^p} \left[ (1 - x)^{a+p} (1 + x)^{b+p} \right]. \quad (3.3.16)$$

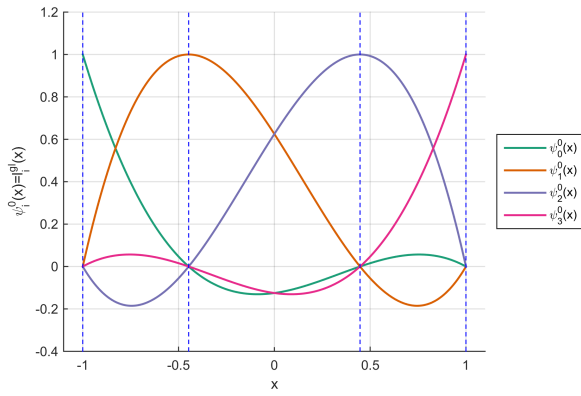
On a Gauss-Lobatto-Legendre grid of  $N$  line intervals, the corresponding Gauss-Lobatto-Legendre polynomials are written as

$$l_i^{gl}(x) = -\frac{(1 - x^2)L'_N(x)}{N(N + 1)L_N(x_i)(x - x_i)} \quad i = 0, 1, 2, \dots, N. \quad (3.3.17)$$

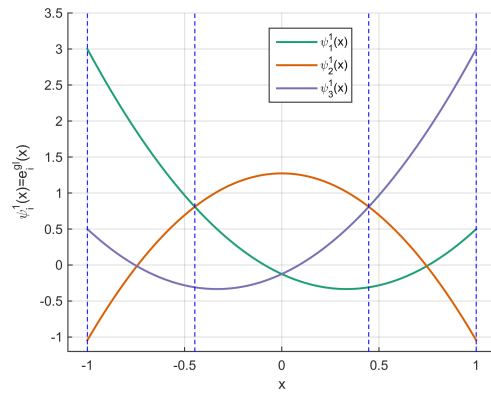
which are used as the basis functions  $\psi_i^0(x) = l_i^{gl}(x)$ . The so called *edge polynomials* [10] of Gauss-Lobatto-Legendre polynomials are

$$e_i^{gl}(x) = -\sum_{k=0}^{i-1} dl_k^{gl}(x) = -\sum_{k=0}^{i-1} l_k^{gl}(x) dx \quad i = 1, 2, \dots, N. \quad (3.3.18)$$

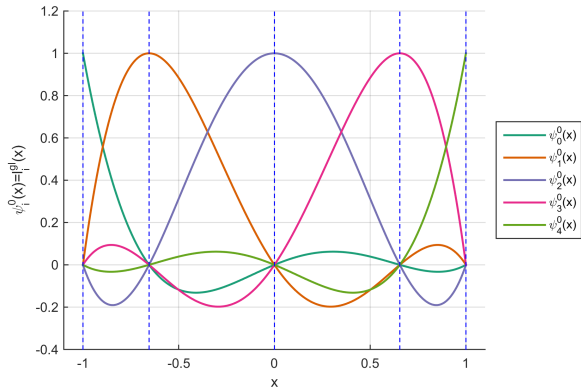
They are used as the basis functions  $\psi_i^1(x) = e_i^{gl}(x)$ . The Gauss-Lobatto-Legendre polynomials and its edge polynomials for  $N = 3, 4, 5$  are given in Fig. 3.3 where the blue dash lines represent the nodes of grids.



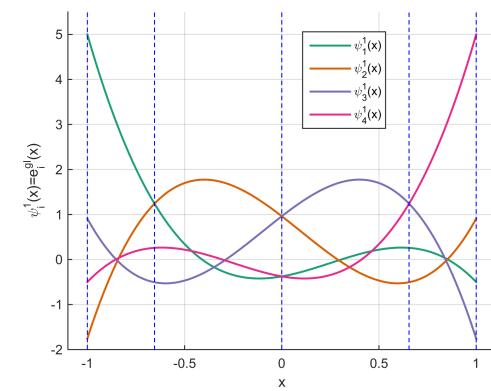
(a) Gauss-Lobatto-Legendre polynomials at  $N = 3$ .



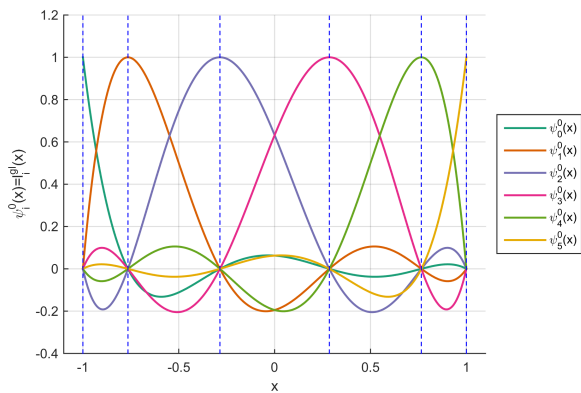
(b) Edge polynomials at  $N = 3$ .



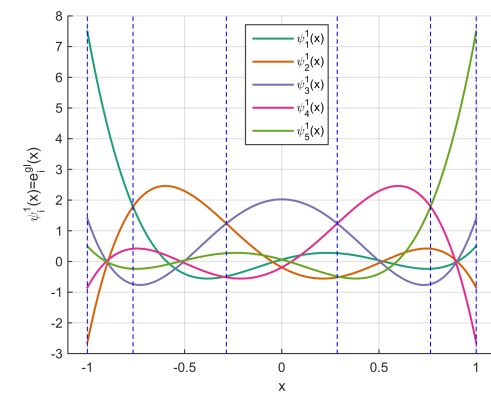
(c) Gauss-Lobatto-Legendre polynomials at  $N = 4$ .



(d) Edge polynomials at  $N = 4$ .



(e) Gauss-Lobatto-Legendre polynomials at  $N = 5$ .



(f) Edge polynomials at  $N = 5$ .

Figure 3.3: Gauss-Lobatto-Legendre polynomials and their edge polynomials for  $N = 3, 4, 5$ .

## Numerical modeling

By now, all tools we are going to use have been presented. In this chapter, we first apply ideas of differential geometry given in Section 2.1 to Euler equations [25] and analyze the conservation laws in terms of the mimetic framework. Then we set up two weak forms of Euler equations. By applying discrete operators given in Section 3.2 to weak forms of Euler equations, we get two spatially discrete systems. To preserve mass, kinetic energy and helicity simultaneously, some interactions between the two semi-discrete systems are constructed. Finally, with discretizations of the time derivative terms in weak Euler equations, a fully discretized system which conserves the discrete mass, kinetic energy and helicity is obtained.

### 4.1 Conservation laws in mimetic framework

We start from the periodic three-dimensional incompressible Euler equations in the mimetic framework where the pressure can be expressed as either inner 0-form  $\tilde{p}^{(0)}$  (*inner oriented pressure or inner pressure*) or outer 3-form  $p^{(3)}$  (*outer oriented pressure or outer pressure*), the velocity can be expressed as either inner 1-form  $\tilde{u}^{(1)}$  (*inner oriented velocity or inner velocity*) or outer 2-form  $u^{(2)}$  (*outer oriented velocity or outer velocity*) and the vorticity can be expressed as either inner 2-form  $\tilde{\omega}^{(2)}$  (*inner oriented vorticity or inner vorticity*) or outer 1-form  $\omega^{(1)}$  (*outer oriented vorticity or outer vorticity*).

Relations between  $\tilde{u}^{(1)}$ ,  $\tilde{\omega}^{(2)}$ ,  $\omega^{(1)}$  and  $u^{(2)}$  are

$$\begin{array}{ccc} \omega^{(1)} & \xleftarrow{d^*} & u^{(2)} \\ \downarrow \star & & \downarrow \star \\ \tilde{\omega}^{(2)} & \xleftarrow{d} & \tilde{u}^{(1)} \end{array} \quad (4.1.1)$$

### 4.1.1 Inner Euler

**Inner oriented Euler equations:** For Euler flows in a domain  $\Omega$ , the inner oriented incompressible Euler equations (inner Euler for short) are given as [25]

$$\left\{ \begin{array}{l} \frac{\partial \tilde{u}^{(1)}}{\partial t} + \iota_{\mathbf{u}} \tilde{\omega}^{(2)} + \mathbf{d} \tilde{p}_0^{(0)} = 0 \quad (\text{a}) \\ \frac{\partial \tilde{\omega}^{(2)}}{\partial t} + \mathbf{d} \iota_{\mathbf{u}} \tilde{\omega}^{(2)} = 0 \quad (\text{b}) \\ \mathbf{d}^* \tilde{u}^{(1)} = 0 \quad (\text{c}) \end{array} \right. \quad (4.1.2)$$

where  $\tilde{u}^{(1)} \in L^2 \tilde{\Lambda}^1(\Omega)$ ,  $\tilde{\omega}^{(2)} \in L^2 \tilde{\Lambda}^2(\Omega)$ ,  $\tilde{p}_0^{(0)} = \tilde{p}^{(0)} + \frac{1}{2} \iota_{\mathbf{u}} \tilde{u}^{(1)}$  with  $\tilde{p}^{(0)} \in L^2 \tilde{\Lambda}^0(\Omega)$  is the generalized inner pressure and  $\mathbf{u} = (\tilde{u}^{(1)})^\sharp$  is the vector field. Equation (a) and equation (b) in fact imply that  $\tilde{\omega}^{(2)} = \mathbf{d} \tilde{u}^{(1)}$ .

**Mass conservation** For the inner Euler, the mass conservation law is very easy to get. For the incompressible flow, the mass flux through the boundary is the boundary integral of outer oriented velocity  $\star \tilde{u}^{(1)}$

$$\int_{\partial \Omega} \star \tilde{u}^{(1)} = \int_{\Omega} \mathbf{d} \star \tilde{u}^{(1)} \stackrel{(2.1.59)}{=} - \int_{\Omega} \star \mathbf{d}^* \tilde{u}^{(1)} \stackrel{(4.1.2c)}{=} 0. \quad (4.1.3)$$

The overall mass flux through the boundary is always zero. Meanwhile the flow is incompressible. Therefore, the mass must be conserved. In fact, since we have  $\mathbf{d}^* \tilde{u}^{(1)} = 0$  everywhere, Eq. (4.1.3) is satisfied for any volume of the domain  $\Omega$ .

**Kinetic energy conservation** For the inner Euler, the kinetic energy is given as

$$\tilde{K} = \frac{1}{2} \int_{\Omega} \tilde{u}^{(1)} \wedge \star \tilde{u}^{(1)} = \frac{1}{2} \left( \tilde{u}^{(1)}, \tilde{u}^{(1)} \right)_{\Omega}. \quad (4.1.4)$$

In order to get the conservation law of kinetic energy, we take the wedge product between the momentum equation of the inner Euler, Eq. (4.1.2a), and  $\star \tilde{u}^{(1)}$ , then integrate the equation over the domain  $\Omega$ . We get

$$\int_{\Omega} \frac{\partial \tilde{u}^{(1)}}{\partial t} \wedge \star \tilde{u}^{(1)} + \int_{\Omega} \iota_{\mathbf{u}} \tilde{\omega}^{(2)} \wedge \star \tilde{u}^{(1)} + \int_{\Omega} \mathbf{d} \tilde{p}_0^{(0)} \wedge \star \tilde{u}^{(1)} = 0, \quad (4.1.5)$$

where from Eq. (2.1.67), we know

$$\int_{\Omega} \iota_{\mathbf{u}} \tilde{\omega}^{(2)} \wedge \star \tilde{u}^{(1)} \stackrel{(2.1.67)}{=} 0, \quad (4.1.6)$$

and for the third term

$$\int_{\Omega} \mathbf{d}\tilde{p}_0^{(0)} \wedge \star \tilde{u}^{(1)} \stackrel{(2.1.34)}{=} \int_{\Omega} \mathbf{d} \left( \tilde{p}_0^{(0)} \wedge \star \tilde{u}^{(1)} \right) - \int_{\Omega} \tilde{p}_0^{(0)} \wedge \mathbf{d} \star \tilde{u}^{(1)}, \quad (4.1.7)$$

where the second term on the right side is

$$\int_{\Omega} \tilde{p}_0^{(0)} \wedge \mathbf{d} \star \tilde{u}^{(1)} \stackrel{(2.1.57)}{=} \left( \tilde{p}^{(0)}, \star \mathbf{d} \star \tilde{u}^{(1)} \right)_{\Omega} \stackrel{(2.1.60)}{=} \left( \tilde{p}^{(0)}, \mathbf{d}^* \tilde{u}^{(1)} \right)_{\Omega} \stackrel{(4.1.2c)}{=} 0, \quad (4.1.8)$$

and in terms of the first term on the right side, from the generalized Stokes' theorem and the periodic boundary condition, it is zero as well. Therefore, we obtain

$$\frac{\mathbf{d}\tilde{K}}{\mathbf{d}t} = \left( \frac{\partial \tilde{u}^{(1)}}{\partial t}, \tilde{u}^{(1)} \right)_{\Omega} = \int_{\Omega} \frac{\partial \tilde{u}^{(1)}}{\partial t} \wedge \star \tilde{u}^{(1)} = 0. \quad (4.1.9)$$

The kinetic energy is conserved.

**Helicity conservation** For the inner Euler, the helicity is written as

$$\tilde{H} = \int_{\Omega} \tilde{u}^{(1)} \wedge \tilde{\omega}^{(2)} = \left( \tilde{u}^{(1)}, \star \tilde{\omega}^{(2)} \right)_{\Omega} = \left( \tilde{\omega}^{(2)}, \star \tilde{u}^{(1)} \right)_{\Omega}. \quad (4.1.10)$$

We first take the left wedge product of the vorticity equation of inner Euler, Eq. (4.1.2b), with the inner oriented velocity  $\tilde{u}^{(1)}$ , then integrate the equation over the domain, which gives

$$\int_{\Omega} \tilde{u}^{(1)} \wedge \frac{\partial \tilde{\omega}^{(2)}}{\partial t} + \int_{\Omega} \tilde{u}^{(1)} \wedge \mathbf{d} \iota_{\mathbf{u}} \tilde{\omega}^{(2)} = 0. \quad (4.1.11)$$

where according to the Leibniz rule Eq. (2.1.34)

$$\int_{\Omega} \tilde{u}^{(1)} \wedge \mathbf{d} \iota_{\mathbf{u}} \tilde{\omega}^{(2)} = \int_{\Omega} \tilde{\omega}^{(2)} \wedge \iota_{\mathbf{u}} \tilde{\omega}^{(2)} - \int_{\Omega} \mathbf{d} \left( \tilde{u}^{(1)} \wedge \iota_{\mathbf{u}} \tilde{\omega}^{(2)} \right). \quad (4.1.12)$$

which is zero because the fact that

$$\int_{\Omega} \tilde{\omega}^{(2)} \wedge \iota_{\mathbf{u}} \tilde{\omega}^{(2)} \stackrel{(2.1.67)}{=} 0,$$

and

$$\int_{\Omega} \mathbf{d} \left( \tilde{u}^{(1)} \wedge \iota_{\mathbf{u}} \tilde{\omega}^{(2)} \right) = \int_{\partial\Omega} \tilde{u}^{(1)} \wedge \iota_{\mathbf{u}} \tilde{\omega}^{(2)} = 0,$$

according to the generalized Stokes' theorem and the periodic boundary condition. Therefore

$$\int_{\Omega} \tilde{u}^{(1)} \wedge \frac{\partial \tilde{\omega}^{(2)}}{\partial t} = 0. \quad (4.1.13)$$

If we take the right wedge product of the momentum equation of inner Euler, Eq. (4.1.2a), with the inner oriented vorticity  $\tilde{\omega}^{(2)}$ , then integrate the equation over the domain, we get

$$\int_{\Omega} \frac{\partial \tilde{u}^{(1)}}{\partial t} \wedge \tilde{\omega}^{(2)} + \int_{\Omega} \iota_{\mathbf{u}} \tilde{\omega}^{(2)} \wedge \tilde{\omega}^{(2)} + \int_{\Omega} \mathbf{d}\tilde{p}_0^{(0)} \wedge \tilde{\omega}^{(2)} = 0. \quad (4.1.14)$$

With the Leibniz rule, the fact  $\tilde{\omega}^{(2)} = d\tilde{u}^{(1)}$  and the periodic boundary condition, we know

$$\int_{\Omega} d\tilde{p}_0^{(0)} \wedge \tilde{\omega}^{(2)} \stackrel{(2.1.34)}{=} \int_{\Omega} d(\tilde{p}_0^{(0)} \wedge \tilde{\omega}^{(2)}) - \int_{\Omega} \tilde{p}_0^{(0)} \wedge d\tilde{\omega}^{(2)} = 0, \quad (4.1.15)$$

and

$$\int_{\Omega} \tilde{\omega}^{(2)} \wedge \iota_{\mathbf{u}} \tilde{\omega}^{(2)} \stackrel{(2.1.67)}{=} 0, \quad (4.1.16)$$

So

$$\int_{\Omega} \frac{\partial \tilde{u}^{(1)}}{\partial t} \wedge \tilde{\omega}^{(2)} = 0. \quad (4.1.17)$$

Adding Eq.(4.1.13) and Eq.(4.1.17), we obtain

$$\frac{d\tilde{H}}{dt} = \int_{\Omega} \tilde{u}^{(1)} \wedge \frac{\partial \tilde{\omega}^{(2)}}{\partial t} + \int_{\Omega} \frac{\partial \tilde{u}^{(1)}}{\partial t} \wedge \tilde{\omega}^{(2)} = 0. \quad (4.1.18)$$

The helicity is conserved.

The kinetic energy and helicity expressed with inner forms are called the *inner kinetic energy* and *inner helicity*.

### 4.1.2 Outer Euler

If we apply the Hodge-star operator,  $\star$ , to the inner Euler, we can get outer oriented Euler equations.

**Outer oriented Euler equations:** For Euler flows in domain  $\Omega$ , the outer oriented incompressible Euler equations (outer Euler for short) are given as [25]

$$\left\{ \begin{array}{l} \frac{\partial u^{(2)}}{\partial t} + j_{\mathbf{u}} \omega^{(1)} + d^* p_0^{(3)} = 0 \quad (a) \\ \frac{\partial \omega^{(1)}}{\partial t} + d^* j_{\mathbf{u}} \omega^{(1)} = 0 \quad (b) \\ du^{(2)} = 0 \quad (c) \end{array} \right. \quad (4.1.19)$$

where  $u^{(2)} \in L^2 \Lambda^2(\Omega)$ ,  $\omega^{(1)} \in L^2 \Lambda^1(\Omega)$ ,  $p_0^{(3)} = p^{(3)} + \frac{1}{2} j_{\mathbf{u}} u^{(2)}$  with  $p^{(3)} \in L^2 \Lambda^3(\Omega)$  and  $\mathbf{u} = (\star u^{(2)})^{\sharp}$  represents the velocity field given by  $u^{(2)}$ . The operator  $j$  is the adjoint operator of interior product  $\iota$ , see Eq. (2.1.70). Equation (a) and Equation (b) imply that  $\omega^{(1)} = d^* u^{(2)}$ .

The time derivative here in the outer Euler actually is the adjoint operator of the time derivative in the inner Euler. The time derivative and its adjoint have the relation as follow [25]

$$\star \left( \frac{\partial}{\partial t} \right) = - \frac{\partial}{\partial t} \star. \quad (4.1.20)$$

This relation is in fact included in the two differently oriented Euler. To proof that, for example, we can apply the Hodge star operator,  $\star$ , to Eq. (4.1.19a), we get

$$\star \frac{\partial u^{(2)}}{\partial t} + \star j_u \omega^{(1)} + \star d^* p_0^{(3)} = 0, \quad (4.1.21)$$

with

$$\star \frac{\partial u^{(2)}}{\partial t} \stackrel{(4.1.20)}{=} -\frac{\partial \tilde{u}^{(1)}}{\partial t}, \quad \star j_u \omega^{(1)} \stackrel{(2.1.70)}{=} -\iota_u \tilde{\omega}^{(2)} \quad \text{and} \quad \star d^* p_0^{(3)} \stackrel{(2.1.59)}{=} -d\tilde{p}_0^{(0)}. \quad (4.1.22)$$

So we obtain

$$-\frac{\partial \tilde{u}^{(1)}}{\partial t} - \iota_u \tilde{\omega}^{(2)} - d\tilde{p}_0^{(0)} = 0, \quad (4.1.23)$$

which is actually identical with Eq. (4.1.2a). If we apply one more Hodge star operator,  $\star$ , to above equation, we again get Eq. (4.1.19a) because of the relation given in Eq. (2.1.55).

The time derivative and its adjoint operator are also convection operators which represent the change of a variable due to the change of time along two orientation. However, different from spacial dimensions which naturally have two orientations, the dimension time only have one physically reasonable orientation. This is the reason why we consider a three-dimension space  $\{x, y, z\}$  instead of a four-dimension space  $\{x, y, z, t\}$  in this project.

**Mass conservation** Obviously, mass conservation is automatically satisfied because of Eq. (4.1.19c).

**Kinetic energy conservation** For the outer Euler, the kinetic energy is given as

$$K = \frac{1}{2} \left( u^{(2)}, u^{(2)} \right)_{\Omega} = \frac{1}{2} \int_{\Omega} u^{(2)} \wedge \star u^{(2)}. \quad (4.1.24)$$

If we take the inner product of Eq. (4.1.19a) with the outer oriented velocity  $u^{(2)}$ , we get

$$\left( \frac{\partial u^{(2)}}{\partial t}, u^{(2)} \right)_{\Omega} + \left( u^{(2)}, j_u \omega^{(1)} \right)_{\Omega} + \left( u^{(2)}, d^* p_0^{(3)} \right)_{\Omega} = 0. \quad (4.1.25)$$

With the integration by parts, it becomes

$$\left( \frac{\partial u^{(2)}}{\partial t}, u^{(2)} \right)_{\Omega} + \int_{\Omega} u^{(2)} \wedge \star j_u \omega^{(1)} + \left( du^{(2)}, p_0^{(3)} \right)_{\Omega} - \int_{\partial\Omega} u^{(2)} \wedge \star p_0^{(3)} = 0, \quad (4.1.26)$$

where

$$\int_{\Omega} u^{(2)} \wedge \star j_u \omega^{(1)} = - \int_{\Omega} u^{(2)} \wedge \iota_u \star \omega^{(1)} \stackrel{(2.1.67)}{=} 0. \quad (4.1.27)$$

Meanwhile, because of the divergence free flow condition, Eq. (4.1.19c), and the periodic boundary condition, the third and fourth terms of Eq. (4.1.26) are zero. So

$$\frac{dK}{dt} = \left( \frac{\partial u^{(2)}}{\partial t}, u^{(2)} \right)_{\Omega} = 0. \quad (4.1.28)$$

The kinetic energy is conserved.

**Helicity conservation** For the outer Euler, the helicity is expressed as

$$H = \int_{\Omega} u^{(2)} \wedge \omega^{(1)} = \left( \star u^{(2)}, \omega^{(1)} \right)_{\Omega} = \left( u^{(2)}, \star \omega^{(1)} \right)_{\Omega}. \quad (4.1.29)$$

Take the inner product between the vorticity equation of the outer Euler, Eq. (4.1.19b), and  $\star u^{(2)}$ , we obtain

$$\left( \star u^{(2)}, \frac{\partial \omega^{(1)}}{\partial t} \right)_{\Omega} + \left( \star u^{(2)}, d^* j_u \omega^{(1)} \right)_{\Omega} = 0. \quad (4.1.30)$$

With integration by parts, the equation becomes

$$\left( \star u^{(2)}, \frac{\partial \omega^{(1)}}{\partial t} \right)_{\Omega} + \left( d \star u^{(2)}, j_u \omega^{(1)} \right)_{\Omega} - \int_{\partial \Omega} \star u^{(2)} \wedge \star j_u \omega^{(1)} = 0, \quad (4.1.31)$$

$$\left( \star u^{(2)}, \frac{\partial \omega^{(1)}}{\partial t} \right)_{\Omega} - \int_{\Omega} d \star u^{(2)} \wedge \iota_u \star \omega^{(1)} + \int_{\partial \Omega} \star u^{(2)} \wedge \iota_u \star \omega^{(1)} = 0. \quad (4.1.32)$$

Since  $d \star u^{(2)} \stackrel{(2.1.59)}{=} \star d^* u^{(2)} \stackrel{(4.1.1)}{=} \star \omega^{(1)}$ , we have

$$\int_{\Omega} d \star u^{(2)} \wedge \iota_u \star \omega^{(1)} \stackrel{(2.1.67)}{=} 0. \quad (4.1.33)$$

In addition, because of the periodic boundary condition, the boundary integral term drops out. So we have

$$\left( \star u^{(2)}, \frac{\partial \omega^{(1)}}{\partial t} \right)_{\Omega} = 0. \quad (4.1.34)$$

If we take the inner product between  $\star \omega^{(1)}$  and momentum equation of outer oriented Euler equation, Eq. (4.1.19a), we get

$$\left( \frac{\partial u^{(2)}}{\partial t}, \star \omega^{(1)} \right)_{\Omega} + \left( \star \omega^{(1)}, j_u \omega^{(1)} \right)_{\Omega} + \left( \star \omega^{(1)}, d^* p_0^{(3)} \right)_{\Omega} = 0. \quad (4.1.35)$$

Again, with the integral by parts, we have

$$\left( \frac{\partial u^{(2)}}{\partial t}, \star \omega^{(1)} \right)_{\Omega} + \int_{\Omega} \star \omega^{(1)} \wedge \star j_u \omega^{(1)} + \left( d \star \omega^{(1)}, p_0^{(3)} \right)_{\Omega} - \int_{\partial \Omega} \star \omega^{(1)} \wedge \star p_0^{(3)} = 0. \quad (4.1.36)$$

The second term is zero because

$$\int_{\Omega} \star \omega^{(1)} \wedge \star j_u \omega^{(1)} = - \int_{\Omega} \star \omega^{(1)} \wedge \iota_u \star \omega^{(1)} \stackrel{(2.1.67)}{=} 0. \quad (4.1.37)$$

The third term is zero as well because

$$d \star \omega^{(1)} \stackrel{(2.1.59)}{=} - \star d^* \omega^{(1)} \stackrel{(4.1.1)}{=} - \star d^* d^* u^{(2)} \stackrel{(2.1.61)}{=} 0. \quad (4.1.38)$$

The fourth term is also zero because of the periodic boundary condition. Therefore,

$$\left( \frac{\partial u^{(2)}}{\partial t}, \star \omega^{(1)} \right)_{\Omega} = 0. \quad (4.1.39)$$

Adding Eq. (4.1.34) and Eq. (4.1.39) yields

$$\frac{dH}{dt} = 0. \quad (4.1.40)$$

The helicity is conserved.

The kinetic energy and helicity expressed with outer forms are usually called the *outer kinetic energy* and *outer helicity*. Note that the inner product used here actually is the  $L^2$ -inner product. Because we are only going to use  $L^2$ -inner product, from now on, we always use the inner product to represent the  $L^2$ -inner product.

## 4.2 Weak forms and spatial discretizations

As we can see in Section 4.1, the kinetic energy and helicity, no matter inner or outer, can be expressed in terms of either wedge product or inner product, as well as the weak forms of Euler equations, Eq. (4.2.16) and Eq. (4.2.22). In Section 4.1, the proofs of conservation laws in the inner Euler make use of expressions of the kinetic energy and helicity with respect to the wedge product. While those in the outer Euler make use of expressions with respect to the inner product. In fact, because at the continuous level, we have

$$\tilde{\alpha}^{(n-k)} = \star \alpha^{(k)} \quad \text{and} \quad \alpha^{(k)} = \star \tilde{\alpha}^{(n-k)} \quad \alpha^{(k)} = \omega^{(1)}, u^{(2)}, p^{(3)}, \quad (4.2.1)$$

and

$$\left( \alpha^{(k)}, \beta^{(k)} \right)_{\Omega} = \int_{\Omega} \alpha^{(k)} \wedge \star \beta^{(k)} \quad \forall \alpha^{(k)}, \beta^{(k)} \in L^2 \Lambda^k(\Omega), \quad (4.2.2)$$

these two kinds of proofs can convert into each other exactly. In addition, although we distinguish the inner kinetic energy (helicity) and outer kinetic energy (helicity), they are identical with each other at the continuous level because of the same reasons.

**Remark.** *No matter what kind of definitions of the kinetic energy and helicity, with respect to wedge product or inner product, we use, if we want to get expressions for time derivatives of kinetic energy and helicity, both inner and outer oriented velocity and vorticity are needed and we always need to take the wedge product or inner product of the Euler equations with inner oriented form and outer oriented form respectively.*

Now, we take the outer Euler as example. in outer Euler, to get the time derivative of the inner kinetic energy, we take the inner product of the momentum equation with the outer oriented velocity  $u^{(2)}$ , see Eq. (4.1.25). Meanwhile, to get the time derivative of the

inner helicity, we take the inner product of the momentum equation with the inner oriented vorticity  $\star\omega^{(1)}$ , see Eq. (4.1.35). This does not introduce any problems at the continuous level because

$$u^{(2)} \in L^2\Lambda^2(\Omega) \quad \text{and} \quad \tilde{\omega}^{(2)} = \star\omega^{(1)} \in L^2\tilde{\Lambda}^2(\Omega), \quad (4.2.3)$$

and mathematically  $\Lambda^2(\Omega) = \tilde{\Lambda}^2(\Omega)$  (see Section 2.1.5) and the calculation of Hodge star operator is natural. However at the discrete level, the calculation of the discrete Hodge star operator is not natural. It requires the existence of both primal grid and dual grid. Moreover, at the discrete level,

$$u_h^{(2)} \in L^2\Lambda_h^2(\Omega; C_2) \quad \text{and} \quad \tilde{w}_h^{(2)} = \star_h w_h^{(1)} \in L^2\tilde{\Lambda}_h^2(\Omega; \tilde{C}_2), \quad (4.2.4)$$

where  $L^2\Lambda_h^2(\Omega; C_2)$  does not necessarily equal to  $L^2\tilde{\Lambda}_h^2(\Omega; \tilde{C}_2)$ . In order to make them to be equal, we have to make sure that  $C_2 = \tilde{C}_2$  (in fact  $C_2(D) = \tilde{C}_2(\tilde{D})$ ). *In other words, we need to use only one grid as both primal grid and dual grid.* Once  $D = \tilde{D}$ ,  $L^2\Lambda_h^1(\Omega; C_1) = L^2\tilde{\Lambda}_h^1(\Omega; \tilde{C}_1)$  is satisfied as well. As we said in Section 3.3, the Gauss-Lobatto-Legendre grid will be used for both primal grid and dual grid in this project.

Seemingly, we only use a single grid. To be exact, we should consider that we use dual grids but these two dual grids coincide with each other. This duality is obviously different from the duality used by Palha et al. in [42] and Bouman et al. in [3] where a Gauss-Lobatto-Legendre primal grid is associated with an extended Gauss-Legendre dual grid, see Fig. 4.1. Under this kind of duality, we have

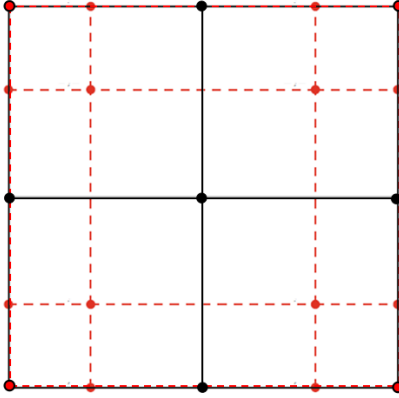


Figure 4.1: The Gauss-Lobatto-Legendre primal grid (black) and the extended Gauss-Legendre dual grid (red) for  $N = 2$ .

$$L^2\Lambda^k(\Omega; C_k) \subseteq L^2\tilde{\Lambda}^{n-k}(\Omega; \tilde{C}_{n-k}) \quad k = 0, 1, \dots, n. \quad (4.2.5)$$

Therefore, we can set up Hodge matrices representing the Hodge star operator according to the relation given in Eq. (2.1.57). However, in this project, the duality does not satisfy Eq. (4.2.5) anymore. Hence, we can not obtain direct discrete counterparts, the Hodge matrices,

for the Hodge star operator. That means at any time step, even if we already have solutions of outer oriented variables, we can not calculate the inner oriented variables by applying the Hodge matrices to vector forms of the outer oriented variables. Therefore, we know

**Remark.** To obtain both inner and outer oriented variables, the computation of both inner Euler and outer Euler must be preformed simultaneously on the primal grid and dual grid.

In this case, connections between inner oriented variables and outer oriented variables are represented by the discrete Hodge star operator given in Eq. (3.2.9). In fact, because of the relation in Eq. (3.1.9), this discretization is more accurate than the discretization (Hodge matrices) in [3, 42] for the Hodge star operator.

For mimetic spectral schemes, degrees of freedom of are defined not only on points, but also on lines, faces, volumes etc. in the cell complex. Sometimes we can not find suitable degrees of freedom to define the boundary condition. For example, in this project, we solve a periodic flow in a unit 3-cube. The inner velocity, 1-form  $\tilde{u}^{(1)}$ , is expanded onto the 1-cells of the dual grid. These 1-cells are actually representing the degrees of freedom. However, 1-cells in the boundary can only used to expand the tangential components of velocity. So, we have no degrees of freedom which can be used to expand normal component of velocity on the boundary. Therefore, it seems that we lose control of the normal velocity component on the boundary. Similarly, for the outer oriented velocity, 2-form  $u^{(2)}$ , it seem that we only control the normal velocity component on the boundary. The same happens to the vorticity and pressure. For the components that have no degrees of freedom on the boundary, to impose boundary conditions to them, *weak boundary conditions* are employed. While for those that have degrees of freedom on the boundary, the boundary conditions applied to them are then called *strong boundary conditions*.

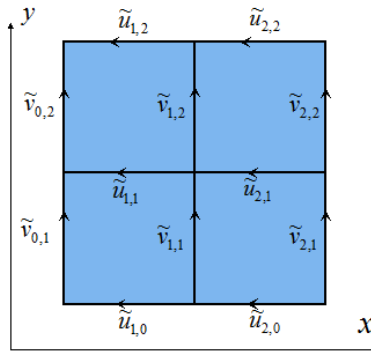


Figure 4.2: A discrete inner velocity on a Gauss-Lobatto-Legendre grid at  $N = 2$ .

For example, in a periodic unit 2-cube  $([-1, 1]^2)$  equipped with a Gauss-Lobatto-Legendre

grid at  $N = 2$ , see Fig. 4.2, the discrete inner velocity 1-form  $\tilde{u}^{(1)}$  is given as

$$\tilde{u}^{(1)} = \sum_{i=1}^2 \sum_{j=0}^2 \tilde{u}_{i,j} dx + \sum_{i=0}^2 \sum_{j=1}^2 \tilde{v}_{i,j} dy . \quad (4.2.6)$$

Because the flow is periodic, we can set  $\tilde{u}_{i,0} = \tilde{u}_{i,2}, i = 1, 2$  for the top and bottom boundaries, which is the strong boundary condition. However, the normal component of the velocity on top and bottom boundaries where we have no degrees of freedom for it is also periodic and we need to apply boundary condition for it. In this case, we have to introduce the weak boundary condition.

In our project, weak boundary conditions are imposed to the system by making use of either the integration by parts, Eq. (2.1.58), or the Leibniz rule of wedge product, Eq. (2.1.34). For a differential  $k$ -form  $\alpha^{(k)}$  which is the target to impose the weak boundary condition, when there is a term  $d^* \alpha^{(k)}$  in the control equation, we can test the equation with test functions  $\zeta^{(k-1)}$  by taking the inner product between the control equation and the test functions, which results in a series of terms:

$$\left( d^* \alpha^{(k)}, \zeta^{(k-1)} \right)_{\Omega} \stackrel{(2.1.58)}{=} \left( \alpha^{(k)}, d \zeta^{(k-1)} \right)_{\Omega} - \int_{\partial \Omega} \zeta^{(k-1)} \wedge \star \alpha^{(k)} . \quad (4.2.7)$$

Once the test functions  $\zeta^{(k-1)}$  are periodic, by making the boundary integral terms to be zero:

$$\int_{\partial \Omega} \zeta^{(k-1)} \wedge \star \alpha^{(k)} := 0 ,$$

we weakly apply a periodic boundary condition to  $\alpha^{(k)}$  since if only  $\alpha^{(k)}$  is periodic, the boundary integral terms can be zero.

If there is a term  $d\beta^{(k)}$  in the control equation, we can test the equation by taking the wedge product of the equation with test functions  $\sigma^{(n-k)}$  then integral the equation over the domain, which gives rise to a series of terms:

$$\begin{aligned} \int_{\Omega} d\beta^{(k)} \wedge \sigma^{(n-k-1)} &\stackrel{(2.1.34)}{=} \int_{\Omega} d \left( \beta^{(k)} \wedge \sigma^{(n-k-1)} \right) - (-1)^k \int_{\Omega} \beta^{(k)} \wedge d\sigma^{(n-k-1)} \\ &\stackrel{(2.1.43)}{=} \int_{\partial \Omega} \beta^{(k)} \wedge \sigma^{(n-k)} - (-1)^k \int_{\Omega} \beta^{(k)} \wedge d\sigma^{(n-k-1)} . \end{aligned} \quad (4.2.8)$$

Once the test functions are periodic, by making the boundary integral term to be zero,

$$\int_{\partial \Omega} \beta^{(k)} \wedge \sigma^{(n-k)} := 0 ,$$

we weakly impose a periodic boundary condition to  $\beta^{(k)}$  because if only  $\beta^{(k)}$  is also periodic, the boundary integral term can be zero. Note that here we do not use the inner product between  $d\beta^{(k)}$  and test functions  $\tau^{(k+1)}$ . This is because if we do that, to avoid the appearance of the metric-dependent operator codifferential (So we can not use the integration by parts.),

we have to first use the relation given in Eq. (2.1.57) and then use the Leibniz rule,

$$\begin{aligned}
\left( d\beta^{(k)}, \tau^{(k+1)} \right)_\Omega &\stackrel{(2.1.57)}{=} \int_\Omega d\beta^{(k)} \wedge \star \tau^{(k+1)} \\
&\stackrel{(2.1.34)}{=} \int_\Omega d \left( \beta^{(k)} \wedge \star \tau^{(k+1)} \right) - (-1)^k \int_\Omega \beta^{(k)} \wedge d \star \tau^{(k+1)} \\
&\stackrel{(2.1.43)}{=} \int_{\partial\Omega} \beta^{(k)} \wedge \star \tau^{(k+1)} - (-1)^k \int_\Omega \beta^{(k)} \wedge d \star \tau^{(k+1)}.
\end{aligned} \tag{4.2.9}$$

Similarly, we can make the boundary integral term to be zero to weakly impose the periodic boundary condition to  $\beta^{(k)}$ . However, this will leave a term including  $d \star \tau^{(k+1)}$  which is actually equal to  $(-1)^{(k+1)} \star d \star \tau^{(k+1)}$  in the equation. As we said, the metric-dependent operator codifferential  $d^*$  is what we want to avoid. Therefore, for the equation containing  $d\beta^{(k)}$ , we normally do not use inner production as a tool to impose the weak boundary condition to  $\beta^{(k)}$ .

Because of above analysis, we finally choose the weak form in wedge product for inner Euler and the weak form in inner product for outer Euler. Overall, the general information for our discrete system is

- **The domain:** The domain  $\Omega$  is a unit 3-cube  $I^3 = [-1, 1]^3$ .
- **Boundary conditions:** Periodic boundary conditions
- **Grids:** The same Gauss-Lobatto-Legendre grid for both primal and dual grids.
- **Discrete Euler:** Discrete weak form in wedge product for inner Euler, discrete weak form in inner product for outer Euler.

### 4.2.1 Inner Euler

We start from the weak form of the inner Euler at the continuous level Eq. (4.2.10).

**Weak inner Euler:** Find

$$\left\{ \tilde{p}^{(0)}, \tilde{u}^{(1)}, \tilde{\omega}^{(2)} \right\} \in \left\{ L^2\Lambda^{(0)}(\Omega), L^2\Lambda^{(1)}(\Omega), L^2\Lambda^{(2)}(\Omega) \right\},$$

such that

$$\forall \left\{ \sigma^{(2)}, \varsigma^{(1)}, \phi^{(0)} \right\} \in \left\{ L^2\Lambda^{(2)}(\Omega), L^2\Lambda^{(1)}(\Omega), L^2\Lambda^{(0)}(\Omega) \right\},$$

we have

$$\left\{ \begin{array}{l} \int_\Omega \frac{\partial \tilde{u}^{(1)}}{\partial t} \wedge \sigma^{(2)} + \int_\Omega \iota_u \tilde{\omega}^{(2)} \wedge \sigma^{(2)} + \int_\Omega d\tilde{p}_0^{(0)} \wedge \sigma^{(2)} = 0 \\ \int_\Omega \frac{\partial \tilde{\omega}^{(2)}}{\partial t} \wedge \sigma^{(2)} + \int_\Omega d\iota_u \tilde{\omega}^{(2)} \wedge \sigma^{(2)} = 0 \\ \left( d^* \tilde{u}^{(1)}, \phi^{(0)} \right)_\Omega = 0 \end{array} \right. \tag{4.2.10}$$

With the Leibniz rule and the generalized Stokes' theorem, Eq. (4.2.10) becomes

$$\left\{ \begin{array}{l} \int_{\Omega} \frac{\partial \tilde{u}^{(1)}}{\partial t} \wedge \sigma^{(2)} + \int_{\Omega} \iota_{\mathbf{u}} \tilde{\omega}^{(2)} \wedge \sigma^{(2)} + \int_{\partial\Omega} \tilde{p}_0^{(0)} \wedge \sigma^{(2)} - \int_{\Omega} \tilde{p}_0^{(0)} \wedge d\sigma^{(2)} = 0 \\ \int_{\Omega} \frac{\partial \tilde{\omega}^{(2)}}{\partial t} \wedge \zeta^{(1)} + \int_{\partial\Omega} \iota_{\mathbf{u}} \tilde{\omega}^{(2)} \wedge \zeta^{(1)} + \int_{\Omega} \iota_{\mathbf{u}} \tilde{\omega}^{(2)} \wedge d\zeta^{(1)} = 0 \\ \left( \tilde{u}^{(1)}, d\phi^{(0)} \right)_{\Omega} - \int_{\partial\Omega} \phi^{(0)} \wedge \star \tilde{u}^{(1)} = 0 \end{array} \right. \quad (4.2.11)$$

We first discretize these equations with the mimetic discretization constructed in Chapter 3 and then apply the weak boundary conditions by setting the boundary integral terms to be zero:

$$\int_{\partial\Omega} \tilde{p}_{0,h}^{(0)} \wedge_h \sigma_h^{(2)} = 0, \quad (4.2.12)$$

$$\int_{\partial\Omega} \iota_{\mathbf{u}_h}^h \tilde{\omega}_h^{(2)} \wedge_h \zeta_h^{(1)} = 0. \quad (4.2.13)$$

The discrete test functions  $\sigma_h^{(2)}$  and  $\zeta_h^{(1)}$  are in fact known. By setting up a set of linear independent periodic test functions using the basis functions and making  $\sigma_h^{(2)}$  or  $\zeta_h^{(1)}$  to be each element of the corresponding test functions set, we get a series of linear independent equations. If there are as many equations as the degrees of freedom, the system is solvable. This is as same as the general philosophy of the conventional finite element method or spectral method.

In terms of the periodic test functions, the simplest choice is using all internal basis function and the combinations each of which contains two basis functions associated with two periodic boundary cells. For example, in Fig. 4.2, a set of periodic test functions is given as

$$\{ \phi_{1,1}, \phi_{2,1}, \phi_{1,0} + \phi_{1,2}, \phi_{2,0} + \phi_{2,2}, \psi_{1,1}, \psi_{1,2}, \psi_{0,1} + \psi_{2,1}, \psi_{0,2} + \psi_{2,2} \}, \quad (4.2.14)$$

where  $\phi_{i,j}$  is the basis function related to the cell on which  $\tilde{u}_{i,j}$  are defined and  $\psi_{i,j}$  is the basis function related to the cell on which  $\tilde{v}_{i,j}$  are defined. Note that at the discrete level, the periodic test functions are actually not fully periodic. Only the normal component or tangential components are periodic. But through simple analysis, we can easily find that this point does not affect the weak periodic boundary conditions because the boundary integral being zero only requires that the boundary integral of the normal component is zero.

We eventually get

$$\left\{ \begin{array}{l} \int_{\Omega} \frac{\partial \tilde{u}_h^{(1)}}{\partial t} \wedge_h \sigma_h^{(2)} + \int_{\Omega} \iota_{\mathbf{u}_h}^h \tilde{\omega}_h^{(2)} \wedge_h \sigma_h^{(2)} - \int_{\Omega} \tilde{p}_{0,h}^{(0)} \wedge_h d_h \sigma_h^{(2)} = 0 \\ \int_{\Omega} \frac{\partial \tilde{\omega}_h^{(2)}}{\partial t} \wedge_h \zeta_h^{(1)} + \int_{\Omega} \iota_{\mathbf{u}_h}^h \tilde{\omega}_h^{(2)} \wedge_h d_h \zeta_h^{(1)} = 0 \\ \left( \tilde{u}_h^{(1)}, d_h \phi_h^{(0)} \right)_{\Omega,h} = 0 \end{array} \right. \quad (4.2.15)$$

To make it clear, we omit the sub-script and super-script  $h$ . Eventually, we get a discrete weak inner Euler as

**Discrete weak inner Euler:** *Find*

$$\left\{ \tilde{p}^{(0)}, \tilde{u}^{(1)}, \tilde{\omega}^{(2)} \right\} \in \left\{ L^2 \Lambda_h^{(0)}(\Omega; C_0; P), L^2 \Lambda_h^{(1)}(\Omega; C_1; P), L^2 \Lambda_h^{(2)}(\Omega; C_2; P) \right\},$$

such that

$$\forall \left\{ \sigma^{(2)}, \zeta^{(1)}, \phi^{(0)} \right\} \in \left\{ L^2 \Lambda_h^{(2)}(\Omega; C_2; P), L^2 \Lambda_h^{(1)}(\Omega; C_1; P), L^2 \Lambda_h^{(0)}(\Omega; C_0; P) \right\},$$

we have

$$\left\{ \begin{array}{l} \int_{\Omega} \frac{\partial \tilde{u}^{(1)}}{\partial t} \wedge \sigma^{(2)} + \int_{\Omega} \iota_u \tilde{\omega}^{(2)} \wedge \sigma^{(2)} - \int_{\Omega} \tilde{p}_0^{(0)} \wedge d\sigma^{(2)} = 0 \\ \int_{\Omega} \frac{\partial \tilde{\omega}^{(2)}}{\partial t} \wedge \zeta^{(1)} + \int_{\Omega} \iota_u \tilde{\omega}^{(2)} \wedge d\zeta^{(1)} = 0, \\ \left( \tilde{u}^{(1)}, d\phi^{(0)} \right)_{\Omega} = 0 \end{array} \right. \quad (4.2.16)$$

where  $P$  means the space is periodic.

## 4.2.2 Outer Euler

The weak form of the outer Euler at the continuous level is given as

**Weak outer Euler:** *Find*

$$\left\{ p^{(3)}, u^{(2)}, \omega^{(1)} \right\} \in \left\{ L^2 \Lambda^{(3)}(\Omega), L^2 \Lambda^{(2)}(\Omega), L^2 \Lambda^{(1)}(\Omega) \right\},$$

such that

$$\forall \left\{ \zeta^{(1)}, \sigma^{(2)}, \tau^{(3)} \right\} \in \left\{ L^2 \Lambda^{(1)}(\Omega), L^2 \Lambda^{(2)}(\Omega), L^2 \Lambda^{(3)}(\Omega) \right\},$$

we have

$$\left\{ \begin{array}{l} \left( \frac{\partial u^{(2)}}{\partial t}, \sigma^{(2)} \right)_{\Omega} + \left( j_u \omega^{(1)}, \sigma^{(2)} \right)_{\Omega} + \left( d^* p_0^{(3)}, \sigma^{(2)} \right)_{\Omega} = 0 \\ \left( \frac{\partial \omega^{(1)}}{\partial t}, \zeta^{(1)} \right)_{\Omega} + \left( d^* j_u \omega^{(1)}, \zeta^{(1)} \right)_{\Omega} = 0, \\ \left( du^{(2)}, \tau^{(3)} \right)_{\Omega} = 0 \end{array} \right. \quad (4.2.17)$$

Eq. (4.2.17) can be expressed as

$$\left\{ \begin{array}{l} \left( \frac{\partial u^{(2)}}{\partial t}, \sigma^{(2)} \right)_{\Omega} - \int_{\Omega} \psi^{(2)} \wedge \iota_u \star \omega^{(1)} + (p_0^{(3)}, d\psi^{(2)})_{\Omega} - \int_{\partial\Omega} \psi^{(2)} \wedge \star p_0^{(3)} = 0 \\ \left( \frac{\partial \omega^{(1)}}{\partial t}, \zeta^{(1)} \right)_{\Omega} - \int_{\Omega} d\varphi^{(1)} \wedge \iota_u \star \omega^{(1)} + \int_{\partial\Omega} \varphi^{(1)} \wedge \iota_u \star \omega^{(1)} = 0 \\ (du^{(2)}, \tau^{(3)})_{\Omega} = 0 \end{array} \right. \quad (4.2.18)$$

Again, we discretize above system and define weak boundary conditions by setting all boundary integral terms to be zero,

$$\int_{\partial\Omega} \psi_h^{(2)} \wedge_h \star_h p_{0,h}^{(3)} = 0, \quad (4.2.19)$$

$$\int_{\partial\Omega} \varphi_h^{(1)} \wedge_h \iota_{u_h}^h \star_h \omega_h^{(1)} = 0. \quad (4.2.20)$$

Finally, we get

$$\left\{ \begin{array}{l} \left( \frac{\partial u_h^{(2)}}{\partial t}, \sigma_h^{(2)} \right)_{\Omega,h} - \int_{\Omega} \psi_h^{(2)} \wedge_h \iota_{u_h}^h \star_h \omega_h^{(1)} + (p_{0,h}^{(3)}, d_h \psi_h^{(2)})_{\Omega,h} = 0 \\ \left( \frac{\partial \omega_h^{(1)}}{\partial t}, \zeta_h^{(1)} \right)_{\Omega,h} - \int_{\Omega} d_h \varphi_h^{(1)} \wedge_h \iota_{u_h}^h \star_h \omega_h^{(1)} = 0 \\ (d_h u_h^{(2)}, \tau_h^{(3)})_{\Omega,h} = 0 \end{array} \right. \quad (4.2.21)$$

We again omit the sub-script and super-script  $h$ . Finally the discrete weak outer Euler is expressed as

**Discrete weak outer Euler:** Find

$$\{p^{(3)}, u^{(2)}, \omega^{(1)}\} \in \{L^2\Lambda^{(3)}(\Omega; C_3; P), L^2\Lambda^{(2)}(\Omega; C_2; P), L^2\Lambda^{(1)}(\Omega; C_1; P)\},$$

such that

$$\forall \{\zeta^{(1)}, \sigma^{(2)}, \tau^{(3)}\} \in \{L^2\Lambda^{(1)}(\Omega; C_1; P), L^2\Lambda^{(2)}(\Omega; C_2; P), L^2\Lambda^{(3)}(\Omega; C_3; P)\},$$

we have

$$\left\{ \begin{array}{l} \left( \frac{\partial u^{(2)}}{\partial t}, \sigma^{(2)} \right)_{\Omega} - \int_{\Omega} \sigma^{(2)} \wedge \iota_u \star \omega^{(1)} + (p_0^{(3)}, d\sigma^{(2)})_{\Omega} = 0 \\ \left( \frac{\partial \zeta^{(1)}}{\partial t}, \varphi^{(1)} \right)_{\Omega} - \int_{\Omega} d\zeta^{(1)} \wedge \iota_u \star \omega^{(1)} = 0 \\ (du^{(2)}, \tau^{(3)})_{\Omega} = 0 \end{array} \right. \quad (4.2.22)$$

### 4.3 Conservation laws at the discrete level

Once spatial discretizations for two weak forms are constructed, we need to set up interactions between them to keep the kinetic energy and helicity preserved. The interactions between the discrete inner Euler and outer Euler are strongly related to the discrete Hodge star operator we construct in Section 3.2.

From now on, variables and operators without sub-script or super-script  $h$  represent discrete variables and operators unless it is specifically mentioned that they do not or both discrete and non-discrete variables or operators appear.

#### 4.3.1 Inner Euler

In the discrete inner Euler, we take use of the discrete Hodge star operator between the inner oriented velocity  $\tilde{u}^{(1)}$  and outer oriented velocity  $u^{(2)}$ :

$$u^{(2)} = \star \tilde{u}^{(1)} . \quad (4.3.1)$$

The discrete weak inner Euler is given as

$$\left\{ \begin{array}{l} \int_{\Omega} \frac{\partial \tilde{u}^{(1)}}{\partial t} \wedge \sigma^{(2)} + \int_{\Omega} \iota_{\mathbf{u}} \tilde{\omega}^{(2)} \wedge \sigma^{(2)} - \int_{\Omega} \tilde{p}_0^{(0)} \wedge d\sigma^{(2)} = 0 \\ \int_{\Omega} \frac{\partial \tilde{\omega}^{(2)}}{\partial t} \wedge \zeta^{(1)} + \int_{\Omega} \iota_{\mathbf{u}} \tilde{\omega}^{(2)} \wedge d\zeta^{(1)} = 0 \cdot \\ \left( \tilde{u}^{(1)}, d\tilde{\phi}^{(0)} \right)_{\Omega} = 0 \end{array} \right. \quad (4.3.2)$$

We borrow  $u^{(2)}$  from the discrete outer Euler and use  $\star u^{(2)}$  and  $\mathbf{u} = \left( \star u^{(2)} \right)^{\sharp}$  to replace  $\tilde{u}^{(1)}$  and  $\mathbf{u}$  in the discrete inner Euler except the  $\tilde{u}^{(1)}$  in the time derivative term. We obtain

$$\left\{ \begin{array}{l} \int_{\Omega} \frac{\partial \tilde{u}^{(1)}}{\partial t} \wedge \sigma^{(2)} + \int_{\Omega} \iota_{\mathbf{u}} \tilde{\omega}^{(2)} \wedge \sigma^{(2)} - \int_{\Omega} \tilde{p}_0^{(0)} \wedge d\sigma^{(2)} = 0 \\ \int_{\Omega} \frac{\partial \tilde{\omega}^{(2)}}{\partial t} \wedge \zeta^{(1)} + \int_{\Omega} \iota_{\mathbf{u}} \tilde{\omega}^{(2)} \wedge d\zeta^{(1)} = 0 \cdot \\ \left( \tilde{u}^{(1)}, d\tilde{\phi}^{(0)} \right)_{\Omega} = 0 \end{array} \right. \quad (4.3.3)$$

Here we in fact use  $\mathbf{u}_h = \left( \star \star_h \tilde{u}_h^{(1)} \right)^{\sharp}$ , which means we make use of the vector field given by the outer Euler to solve the inner Euler. Note that  $\star \star_h \neq Id$  from Eq. (3.1.9) and Eq. (3.2.9). The generalized inner pressure  $\tilde{p}_0^{(0)}$  is then expressed as

$$\tilde{p}_0^{(0)} = \tilde{p}^{(0)} + \frac{1}{2} \iota_{\mathbf{u}} \star u^{(2)} . \quad (4.3.4)$$

The red Hodge star operator  $\star$  represents the non-discrete Hodge star operator.

**Kinetic energy conservation** For the kinetic energy conservation, we have

$$\frac{d\tilde{K}}{dt} = \left( \frac{\partial \tilde{u}^{(1)}}{\partial t}, \tilde{u}^{(1)} \right)_{\Omega} = \int_{\Omega} \frac{\partial \tilde{u}^{(1)}}{\partial t} \wedge \star \tilde{u}^{(1)} = \int_{\Omega} \frac{\partial \tilde{u}^{(1)}}{\partial t} \wedge \mathbf{u}^{(2)}. \quad (4.3.5)$$

Because in our discrete system, both  $\mathbf{u}^{(2)}$  and  $\sigma^{(2)}$  belong to the space  $L^2\Lambda^2(\Omega; C_2)$ . We replace  $\sigma^{(2)}$  by  $\mathbf{u}^{(2)}$  for the first equation of Eq. (4.3.3). We obtain

$$\int_{\Omega} \frac{\partial \tilde{u}^{(1)}}{\partial t} \wedge \mathbf{u}^{(2)} + \int_{\Omega} \iota_{\mathbf{u}} \tilde{\omega}^{(2)} \wedge \mathbf{u}^{(2)} - \int_{\Omega} \tilde{p}_0^{(0)} \wedge d\mathbf{u}^{(2)} = 0, \quad (4.3.6)$$

where

$$\int_{\Omega} \tilde{p}_0^{(0)} \wedge d\mathbf{u}^{(2)} = 0, \quad (4.3.7)$$

because we borrow  $\mathbf{u}^{(2)}$  from the outer Euler in which  $d\mathbf{u}^{(2)} = 0$  is satisfied strictly. In addition,

$$\int_{\Omega} \iota_{\mathbf{u}} \tilde{\omega}^{(2)} \wedge \mathbf{u}^{(2)} = \left( \iota_{\mathbf{u}} \tilde{\omega}^{(2)}, \star \mathbf{u}^{(2)} \right)_{\Omega} \stackrel{(2.1.67)}{=} 0. \quad (4.3.8)$$

Therefore

$$\frac{d\tilde{K}}{dt} = \int_{\Omega} \frac{\partial \tilde{u}^{(1)}}{\partial t} \wedge \mathbf{u}^{(2)} = \int_{\Omega} \tilde{p}_0^{(0)} \wedge d\mathbf{u}^{(2)} - \int_{\Omega} \iota_{\mathbf{u}} \tilde{\omega}^{(2)} \wedge \mathbf{u}^{(2)} = 0. \quad (4.3.9)$$

The discrete inner kinetic energy is conserved.

**Helicity conservation** For the helicity conservation, because  $\sigma^2, \tilde{\omega}^{(2)} \in L^2\Lambda^2(\Omega; C_2)$  and  $\zeta^{(1)}, \tilde{u}^{(1)} \in L^2\Lambda^1(\Omega; C_1)$ , we can replace  $\sigma^2$  and  $\zeta^{(1)}$  in the first and second equations of Eq. (4.3.3) by  $\tilde{\omega}^{(2)}$  and  $\tilde{u}^{(1)}$  respectively, which results in

$$\int_{\Omega} \frac{\partial \tilde{u}^{(1)}}{\partial t} \wedge \tilde{\omega}^{(2)} + \int_{\Omega} \iota_{\mathbf{u}} \tilde{\omega}^{(2)} \wedge \tilde{\omega}^{(2)} - \int_{\Omega} \tilde{p}_0^{(0)} \wedge d\tilde{\omega}^{(2)} = 0, \quad (4.3.10)$$

$$\int_{\Omega} \frac{\partial \tilde{\omega}^{(2)}}{\partial t} \wedge \tilde{u}^{(1)} + \int_{\Omega} \iota_{\mathbf{u}} \tilde{\omega}^{(2)} \wedge d\tilde{u}^{(1)} = 0. \quad (4.3.11)$$

Because in the inner Euler, relation  $d\tilde{u}^{(1)} = \tilde{\omega}^{(2)}$  is satisfied, we have

$$\int_{\Omega} \iota_{\mathbf{u}} \tilde{\omega}^{(2)} \wedge d\tilde{u}^{(1)} = \int_{\Omega} \iota_{\mathbf{u}} \tilde{\omega}^{(2)} \wedge \tilde{\omega}^{(2)} \stackrel{(2.1.67)}{=} 0. \quad (4.3.12)$$

And since the exterior derivative  $d$  is a nilpotent (See Eq. (2.1.35)),  $d\tilde{\omega}^{(2)} = dd\tilde{u}^{(1)} = 0$ , we have

$$\int_{\Omega} \tilde{p}_0^{(0)} \wedge d\tilde{\omega}^{(2)} = 0. \quad (4.3.13)$$

Therefore, we get

$$\int_{\Omega} \frac{\partial \tilde{u}^{(1)}}{\partial t} \wedge \tilde{\omega}^{(2)} = \int_{\Omega} \tilde{p}_0^{(0)} \wedge d\tilde{\omega}^{(2)} - \int_{\Omega} \iota_{\mathbf{u}} \tilde{\omega}^{(2)} \wedge \tilde{\omega}^{(2)} = 0, \quad (4.3.14)$$

$$\int_{\Omega} \frac{\partial \tilde{\omega}^{(2)}}{\partial t} \wedge \tilde{u}^{(1)} = - \int_{\Omega} \iota_{\mathbf{u}} \tilde{\omega}^{(2)} \wedge d\tilde{u}^{(1)} = 0. \quad (4.3.15)$$

With above two equations, we eventually obtain

$$\frac{d\tilde{H}}{dt} = \int_{\Omega} \frac{\partial \tilde{u}^{(1)}}{\partial t} \wedge \tilde{\omega}^{(2)} + \int_{\Omega} \frac{\partial \tilde{\omega}^{(2)}}{\partial t} \wedge \tilde{u}^{(1)} = 0. \quad (4.3.16)$$

The discrete inner helicity is conserved.

### 4.3.2 Outer Euler

In outer Euler, we make use of the discrete Hodge star relation between the inner oriented vorticity  $\tilde{\omega}^{(2)}$  and outer oriented vorticity  $\omega^{(1)}$ :

$$\tilde{\omega}^{(2)} = \star \omega^{(1)}. \quad (4.3.17)$$

The weak form of the outer Euler is given as

$$\left\{ \begin{array}{l} \left( \frac{\partial u^{(2)}}{\partial t}, \psi^{(2)} \right)_{\Omega} - \int_{\Omega} \psi^{(2)} \wedge \iota_u \star \omega^{(1)} + \left( p_0^{(3)}, d\psi^{(2)} \right)_{\Omega} = 0 \\ \left( \frac{\partial \omega^{(1)}}{\partial t}, \varphi^{(1)} \right)_{\Omega} - \int_{\Omega} d\varphi^{(1)} \wedge \iota_u \star \omega^{(1)} = 0 \\ \left( du^{(2)}, \tau^{(3)} \right)_{\Omega} = 0 \end{array} \right. \quad (4.3.18)$$

We borrow  $\tilde{\omega}^{(2)}$  from the inner Euler to replace  $\star \omega^{(1)}$ . This is natural because of our definition of the discrete Hodge star, see Eq. (3.2.9).

$$\left\{ \begin{array}{l} \left( \frac{\partial u^{(2)}}{\partial t}, \sigma^{(2)} \right)_{\Omega} - \int_{\Omega} \sigma^{(2)} \wedge \iota_u \tilde{\omega}^{(2)} + \left( p_0^{(3)}, d\sigma^{(2)} \right)_{\Omega} = 0 \\ \left( \frac{\partial \omega^{(1)}}{\partial t}, \varsigma^{(1)} \right)_{\Omega} - \int_{\Omega} d\varsigma \wedge \iota_u \tilde{\omega}^{(2)} = 0 \\ \left( du^{(2)}, \tau^{(3)} \right)_{\Omega} = 0 \end{array} \right. \quad (4.3.19)$$

where  $\tilde{\omega}^{(2)}$  is borrowed from the inner Euler in which  $d\tilde{\omega}^{(2)} = 0$  is satisfied and  $du^{(2)} = 0$  in the outer Euler.

**Kinetic energy conservation** For the kinetic energy conservation, we can replace  $\sigma^{(2)}$  in the first equation of Eq. (4.3.19) by  $u^{(2)}$  because both  $\sigma^{(2)}$  and  $u^{(2)}$  belong to  $\Lambda^2(\Omega; C_2)$ . Hence, we obtain

$$\left( \frac{\partial u^{(2)}}{\partial t}, u^{(2)} \right)_{\Omega} - \int_{\Omega} u^{(2)} \wedge \iota_u \tilde{\omega}^{(2)} + \left( p_0^{(3)}, du^{(2)} \right)_{\Omega} = 0, \quad (4.3.20)$$

where

$$\int_{\Omega} u^{(2)} \wedge \iota_u \tilde{\omega}^{(2)} \stackrel{(2.1.67)}{=} 0, \quad (4.3.21)$$

$$\left( p_0^{(3)}, du^{(2)} \right)_{\Omega} = 0. \quad (4.3.22)$$

Sequentially,

$$\frac{dK}{dt} = \left( \frac{\partial u^{(2)}}{\partial t}, u^{(2)} \right)_{\Omega} = 0. \quad (4.3.23)$$

The discrete outer kinetic energy is conserved.

**Helicity conservation** For the helicity conservation, because of the fact that  $\tilde{\omega}^{(2)}, \sigma^{(2)} \in L^2 \Lambda^2(\Omega; C_2)$  and  $\tilde{u}^{(1)}, \zeta^{(1)} \in L^2 \Lambda^1(\Omega; C_1)$ , we can replace the  $\sigma^{(2)}$  and  $\zeta^{(1)}$  in the first and second equations of Eq. (4.3.19) by  $\tilde{\omega}^{(2)}$  and  $\tilde{u}^{(1)}$ , which leads to

$$\left( \frac{\partial u^{(2)}}{\partial t}, \tilde{\omega}^{(2)} \right)_{\Omega} - \int_{\Omega} \tilde{\omega}^{(2)} \wedge \iota_u \tilde{\omega}^{(2)} + \left( p_0^{(3)}, d\tilde{\omega}^{(2)} \right)_{\Omega} = 0, \quad (4.3.24)$$

$$\left( \frac{\partial \omega^{(1)}}{\partial t}, \tilde{u}^{(1)} \right)_{\Omega} - \int_{\Omega} d\tilde{u}^{(1)} \wedge \iota_u \tilde{\omega}^{(2)} = 0, \quad (4.3.25)$$

where

$$\int_{\Omega} \tilde{\omega}^{(2)} \wedge \iota_u \tilde{\omega}^{(2)} \stackrel{(2.1.67)}{=} 0, \quad (4.3.26)$$

and both  $\tilde{\omega}^{(2)}$  and  $\tilde{u}^{(1)}$  come from inner Euler where  $\tilde{\omega}^{(2)} = d\tilde{u}^{(1)}$ , so

$$\left( p_0^{(3)}, d\tilde{\omega}^{(2)} \right)_{\Omega} = 0, \quad (4.3.27)$$

$$\int_{\Omega} d\tilde{u}^{(1)} \wedge \iota_u \tilde{\omega}^{(2)} \stackrel{(2.1.67)}{=} 0. \quad (4.3.28)$$

Eventually we get

$$\frac{dH}{dt} = \left( \frac{\partial u^{(2)}}{\partial t}, \tilde{\omega}^{(2)} \right)_{\Omega} + \left( \frac{\partial \omega^{(1)}}{\partial t}, \tilde{u}^{(1)} \right)_{\Omega} = 0. \quad (4.3.29)$$

The discrete outer helicity is conserved.

## 4.4 Temporal discretizations

Although we have constructed two spatial discretization systems which preserve mass, kinetic energy and helicity, the temporal terms are not discretized yet. To verify the discrete

conservation laws given in Section 4.3, we use the simplest temporal discretization, the forward Euler. The forward Euler in fact destroys the conservation laws. For example, the kinetic energy conservation in the discrete outer Euler is given as, Eq. (4.3.23),

$$\frac{dK}{dt} = \left( \frac{\partial u^{(2)}}{\partial t}, u^{(2)} \right)_{\Omega} = 0. \quad (4.4.1)$$

With the forward Euler, the fully discretized form of this equation is

$$\left( \frac{u_{n+1}^{(2)} - u_n^{(2)}}{\Delta t}, u_n^{(2)} \right)_{\Omega} = 0, \quad (4.4.2)$$

where the sub-script means the time step. Therefore,

$$\frac{1}{\Delta t} \left( u_{n+1}^{(2)}, u_n^{(2)} \right)_{\Omega} = \frac{1}{\Delta t} \left( u_n^{(2)}, u_n^{(2)} \right)_{\Omega}, \quad (4.4.3)$$

which means

$$K_{n+1} = \left( u_{n+1}^{(2)}, u_{n+1}^{(2)} \right)_{\Omega} \neq \left( u_n^{(2)}, u_n^{(2)} \right)_{\Omega} = K_n. \quad (4.4.4)$$

To eliminate this inaccuracy, higher order temporal discretization is needed. However, in this project, our main objective is verifying the discrete conservation laws given by Eq. (4.3.9), Eq. (4.3.29), Eq. (4.3.23) and Eq. (4.3.29). Hence, we will just use the forward Euler for the temporal discretization.

#### 4.4.1 Inner Euler

If we apply the the forward Euler to the discrete inner Euler, Eq. (4.3.3), we get a fully discretized system given as

$$\left\{ \begin{array}{l} \frac{1}{\Delta t} \int_{\Omega} \tilde{u}_{n+1}^{(1)} \wedge \sigma^{(2)} - \frac{1}{\Delta t} \int_{\Omega} \tilde{u}_n^{(1)} \wedge \sigma^{(2)} + \int_{\Omega} \iota_u \tilde{\omega}_n^{(2)} \wedge \sigma^{(2)} - \int_{\Omega} \tilde{p}_{0,n}^{(0)} \wedge d\sigma^{(2)} = 0 \\ \frac{1}{\Delta t} \int_{\Omega} \tilde{\omega}_{n+1}^{(2)} \wedge \zeta^{(1)} - \frac{1}{\Delta t} \int_{\Omega} \tilde{\omega}_n^{(2)} \wedge \zeta^{(1)} + \int_{\Omega} \iota_u \tilde{\omega}_n^{(2)} \wedge d\zeta^{(1)} = 0, \\ \left( \tilde{u}_{n+1}^{(1)}, d\phi^{(0)} \right)_{\Omega} = 0 \end{array} \right. \quad (4.4.5)$$

where  $\Delta t$  is the time interval between two time steps. Recall that the generalized inner pressure  $\tilde{p}_{0,n}^{(0)} = \tilde{p}_n^{(0)} + \frac{1}{2} \iota_u \star u_n^{(2)}$ . Although we use the forward Euler, the inner velocity and vorticity at time step  $n$ ,  $\tilde{u}_n^{(1)}$  and  $\tilde{\omega}_n^{(2)}$ , are known, the inner pressure  $\tilde{p}_n^{(0)}$  in fact is considered to be unknown. Make  $\sigma^{(2)}, \zeta^{(1)}, \phi^{(0)}$  to be each corresponding periodic test function respectively. This results in a series equations. Actually, by doing that, the first and second equations of Eq. (4.4.5) provide as many equations as the degrees of freedom of the inner velocity and inner vorticity at time step  $n + 1$ ,  $\tilde{u}_{n+1}^{(1)}$  and  $\tilde{\omega}_{n+1}^{(2)}$ . Meanwhile, the third equation

of Eq. (4.4.5) provides as many equations as the degrees of freedom of the inner pressure at time step  $n$ ,  $\tilde{p}_n^{(0)}$ .

Eventually, by expressing this series of equations in matrix form, we get a system expressed as

$$\begin{pmatrix} \frac{1}{\Delta t} \hat{\mathbb{M}}^{(1)} & \emptyset & \mathbb{E}^{(2,3)} \hat{\mathbb{M}}^{(0)} \\ \emptyset & \frac{1}{\Delta t} \hat{\mathbb{M}}^{(2)} & \emptyset \\ \mathbb{M}^{(1)} \mathbb{E}^{(1,0)} & \emptyset & \emptyset \end{pmatrix} \begin{pmatrix} \tilde{\mathbf{u}}_{n+1}^{(1)} \\ \tilde{\boldsymbol{\omega}}_{n+1}^{(2)} \\ \tilde{\mathbf{p}}_n^{(0)} \end{pmatrix} = \begin{pmatrix} \frac{1}{\Delta t} \hat{\mathbb{M}}^{(1)} \tilde{\mathbf{u}}_n^{(1)} - \mathbb{A} + \frac{1}{2} \mathbb{B} \\ \frac{1}{\Delta t} \hat{\mathbb{M}}^{(2)} \tilde{\boldsymbol{\omega}}_n^{(2)} - \mathbb{E}^{(1,2)} \mathbb{A} \\ \mathbf{0} \end{pmatrix}, \quad (4.4.6)$$

where  $\tilde{\mathbf{u}}^{(1)}$ ,  $\tilde{\boldsymbol{\omega}}^{(2)}$ ,  $\tilde{\mathbf{p}}^{(0)}$  are vector proxies, see Appendix A, of inner oriented differential forms  $\tilde{u}^{(1)}$ ,  $\tilde{\omega}^{(2)}$ ,  $\tilde{p}^{(0)}$  and their sub-scripts means the time step, matrices  $\mathbb{E}$  are the metric-free incidence matrices of the grid, matrices  $\hat{\mathbb{M}}$  are the mass matrices and matrices  $\mathbb{A}$ ,  $\mathbb{B}$  come from terms

$$\int_{\Omega} \iota_{\mathbf{u}} \tilde{\boldsymbol{\omega}}_n^{(2)} \wedge \sigma^{(2)}, \quad \int_{\Omega} \iota_{\mathbf{u}} \tilde{u}_n^{(1)} \wedge d\sigma^{(2)},$$

respectively. For more details about this fully discretized system, see Appendix A.1 where derivations of matrices for all terms is given.

#### 4.4.2 Outer Euler

In terms of the outer Euler Eq. (4.3.19), the forward Euler leads to a fully discretized system expressed as

$$\left\{ \begin{array}{l} -\frac{1}{\Delta t} \left( u_{n+1}^{(2)}, \sigma^{(2)} \right)_{\Omega} + \frac{1}{\Delta t} \left( u_n^{(2)}, \sigma^{(2)} \right)_{\Omega} - \int_{\Omega} \sigma^{(2)} \wedge \iota_{\mathbf{u}} \tilde{\boldsymbol{\omega}}_n^{(2)} + \left( p_{0,n}^{(3)}, d\sigma^{(2)} \right)_{\Omega} = 0 \\ -\frac{1}{\Delta t} \left( \tilde{\boldsymbol{\omega}}_{n+1}^{(2)}, \zeta^{(1)} \right)_{\Omega} + \frac{1}{\Delta t} \left( \tilde{\boldsymbol{\omega}}_n^{(2)}, \zeta^{(1)} \right)_{\Omega} - \int_{\Omega} d\zeta \wedge \iota_{\mathbf{u}} \tilde{\boldsymbol{\omega}}_n^{(2)} = 0, \\ \left( du_{n+1}^{(2)}, \tau^{(3)} \right)_{\Omega} = 0 \end{array} \right. \quad (4.4.7)$$

where  $\Delta t$  is the time interval between two time steps and  $p_{0,n}^{(3)} = p_n^{(3)} + \frac{1}{2} j_{\mathbf{u}} u_n^{(2)}$ . In fully discretized outer Euler,  $u_{n+1}^{(2)}$ ,  $\omega_{n+1}^{(1)}$  and  $p_n^{(3)}$  are unknowns. Note that we in fact use

$$\left( \frac{\partial u^{(2)}}{\partial t}, \sigma^{(2)} \right)_{\Omega} = -\frac{\left( u_{n+1}^{(2)}, \sigma^{(2)} \right)_{\Omega} - \left( u_n^{(2)}, \sigma^{(2)} \right)_{\Omega}}{\Delta t}, \quad (4.4.8)$$

$$\left( \frac{\partial \omega^{(1)}}{\partial t}, \zeta^{(1)} \right)_{\Omega} = -\frac{\left( \omega_{n+1}^{(1)}, \zeta^{(1)} \right)_{\Omega} - \left( \omega_n^{(1)}, \zeta^{(1)} \right)_{\Omega}}{\Delta t}, \quad (4.4.9)$$

here. The minus signs are because of we implicitly apply a Hodge star operator,  $\star$ , to the outer Euler by making use of the relation Eq. (2.1.56). According to relation Eq. (4.1.20), if

we use the normal forward Euler, it actually means we are backtracking the flow instead of developing the flow.

By making  $\sigma^{(2)}$  to be the each 2-form test function, we get as many equations as the degrees of freedom of  $u_{n+1}^{(2)}$  from the first equation of Eq. (4.4.7). Meanwhile, by making  $\zeta^{(1)}$  to be the each 1-form periodic test function, we get as many equations as the degrees of freedom of  $\omega_{n+1}^{(1)}$  from the second equation. Furthermore, By making  $\tau^{(3)}$  to be the each 3-form test function, we get as many equations as the degrees of freedom of  $p_n^{(3)}$  from the third equation. Expressing this series of equations in matrix form, we get

$$\begin{pmatrix} \frac{1}{\Delta t} \mathbf{M}^{(1)} & \emptyset & \mathbf{E}^{(2,3)} \mathbf{M}^{(3)} \\ \emptyset & \frac{1}{\Delta t} \mathbf{M}^{(2)} & \emptyset \\ \mathbf{M}^{(3)} \mathbf{E}^{(3,2)} & \emptyset & \emptyset \end{pmatrix} \begin{pmatrix} u_{n+1}^{(2)} \\ \omega_{n+1}^{(1)} \\ p_n^{(3)} \end{pmatrix} = \begin{pmatrix} \frac{1}{\Delta t} \mathbf{M}^{(1)} u_n^{(2)} - \mathbf{A} + \frac{1}{2} \mathbf{B} \\ \frac{1}{\Delta t} \mathbf{M}^{(2)} \omega_n^{(1)} - \mathbf{E}^{(1,2)} \mathbf{A} \\ \mathbf{0} \end{pmatrix}, \quad (4.4.10)$$

where  $u^{(2)}, \omega^{(1)}, p^{(3)}$  are vector proxies, see Appendix A, of outer oriented differential forms  $u^{(2)}, \omega^{(1)}, p^{(3)}$  and their sub-scripts means the time steps, matrices  $\mathbf{E}$  are the metric-free incidence matrices of the grid, matrices  $\mathbf{M}$  are the mass matrices and matrices  $\mathbf{A}, \mathbf{B}$  come from terms

$$\int_{\Omega} \sigma^{(2)} \wedge \iota_u \tilde{\omega}_n^{(2)}, \quad \left( j_u u_n^{(2)}, d\sigma^{(2)} \right)_{\Omega},$$

respectively which are actually identical with the matrices  $\mathbf{A}$  and  $\mathbf{B}$  in Eq. (4.4.6). More details about this fully discretized system is given in Appendix A.2 where the derivation of the matrix expression for each term is given.

Because of the interactions, above two fully discretized systems basically can be considered as one. Eventually, we get a scheme shown in Fig. 4.3.

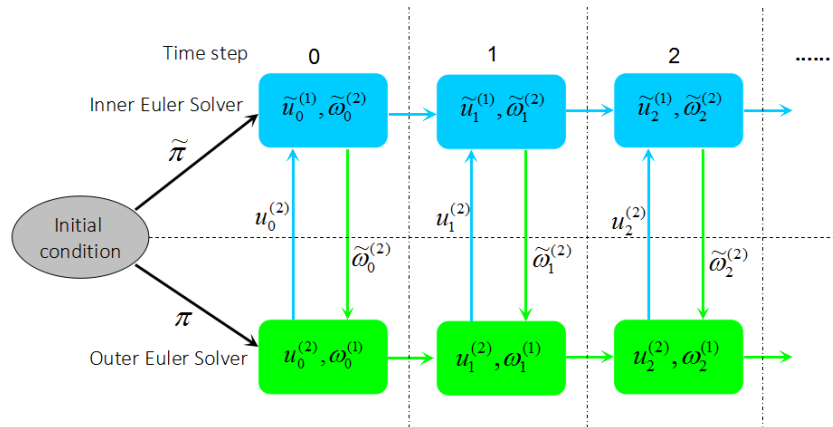


Figure 4.3: Spatially mass-, kinetic energy- and helicity-preserving numerical scheme.



## Test case and results

We test our scheme with the initial condition given as

$$\mathbf{u} = (\cos(\pi x), \sin(\pi x), \sin(\pi x))^T. \quad (5.0.1)$$

The vorticity is obtained by taking the curl of  $\mathbf{u}$

$$\boldsymbol{\omega} = (-\pi \cos(\pi x), -\pi \sin(\pi x) - \pi \cos(\pi x), 0)^T. \quad (5.0.2)$$

As we said in Section. 3.3, we use Gauss-Lobatto-Legendre polynomials to reconstruct our forms. Here we will use Gauss-Lobatto-Legendre polynomials at  $N = 3, 5, 7$  for our test cases. The projections of functions,  $\cos(\pi x)$  and  $\sin(\pi x)$ , are shown in Fig. 5.1 and Fig. 5.2. The square points in 5.1a and 5.2a and the dash lines in 5.1b and 5.2b represent the nodes

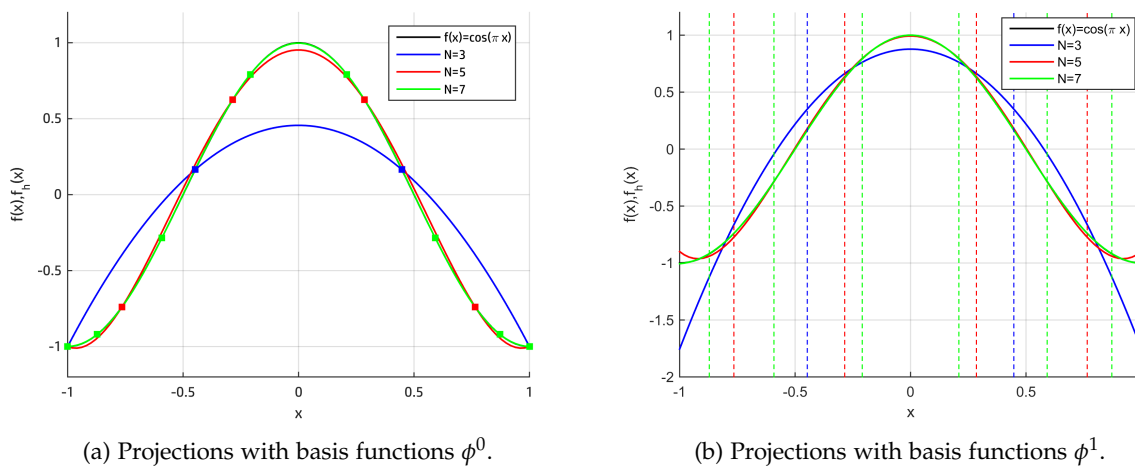


Figure 5.1: Projections of  $\cos(\pi x)$  on Gauss-Lobatto-Legendre grids for  $N = 3, 5, 7$ .

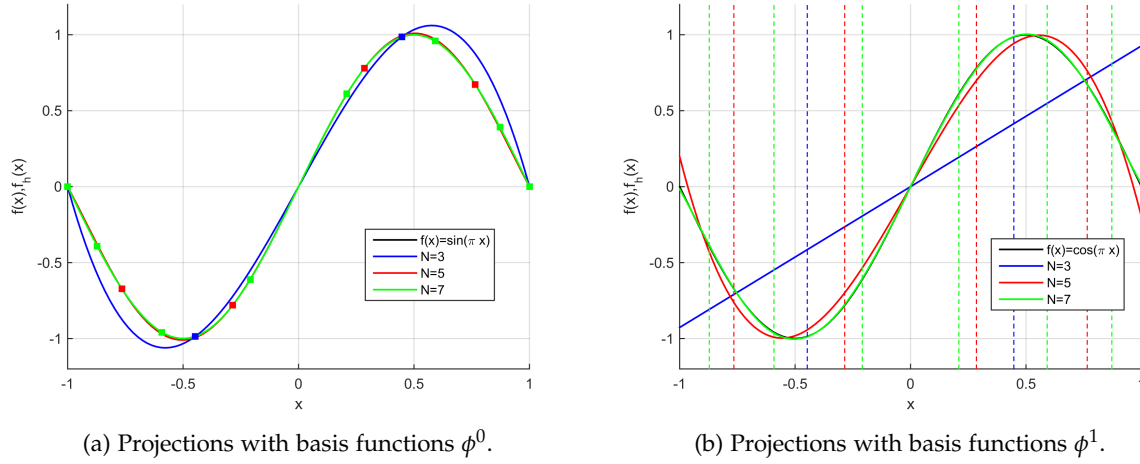


Figure 5.2: Projections of  $\sin(\pi x)$  on Gauss-Lobatto-Legendre grids for  $N = 3, 5, 7$ .

of the Gauss-Lobatto-Legendre grid at  $N = 3, 5, 7$ .

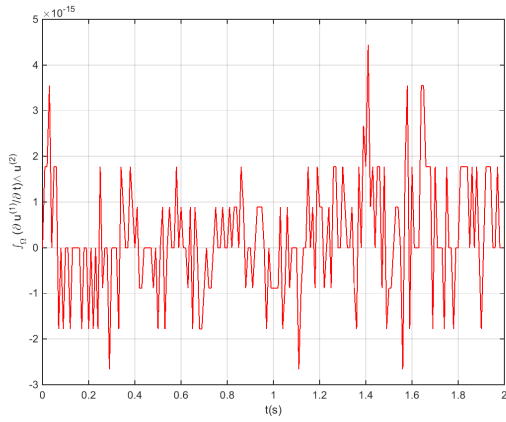
From Fig. 5.1 and Fig. 5.2, we can clearly see that the projection at  $N = 3$  (blue) deviates from the original functions significantly. Especially, the projection with basis functions  $\phi^1$  projects function  $\sin(\pi x)$  into a straight line, see Fig 5.2b. This is because the reduction of the function  $\sin(\pi x)$  at  $N = 3$  results in an arithmetic progression  $\{-a, 0, a\}$  where  $a$  is a positive real number. Meanwhile, for function  $\cos(\pi x)$ , the projection with basis functions  $\phi^1$  in fact projects it into a parabola, see Fig 5.1b. When  $N = 5$ , we get much better approximations (red) although the deviations are still visible. In terms of  $N = 7$ , we get considerable acceptable approximations (green). The projections almost coincide with the original functions represented by black curves, see Fig. 5.1 and Fig. 5.2.

The results using time interval  $\Delta t = 0.0001$ ,  $N = 3, 5, 7$  and computing to  $t = 2s$  are given in Fig. 5.3, Fig. 5.4 and Fig. 5.5. The first four sub-figures of these figures indicate the time derivatives of discrete inner kinetic energy, outer kinetic energy, inner helicity and outer helicity. From these sub-figures we can see that their time derivatives are always kept at relatively low level ( $< 10^{-13}$ ) even on the extremely coarse grid  $N = 3$ . This indicates that our discretization does conserve kinetic energy and helicity spatially. These results also show the great influence of the structure-preserving ability of the mimetic spectral discretization. Keep in mind that, for most conventional numerical schemes, they probably diverge after just a few of steps on a grid of  $N = 3$  unless the time interval is extremely short. Note that we only apply the mimetic spectral discretization to the spatial terms of Euler equations, not to the temporal terms for which we just use the simplest explicit forward Euler, and the interactions keeping the kinetic energy and helicity conserved are constructed based on the spatially discretized systems. As a result, the discrete kinetic energy and the discrete helicity are just conserved spatially, not temporally. So if we plot the discrete kinetic energy and the

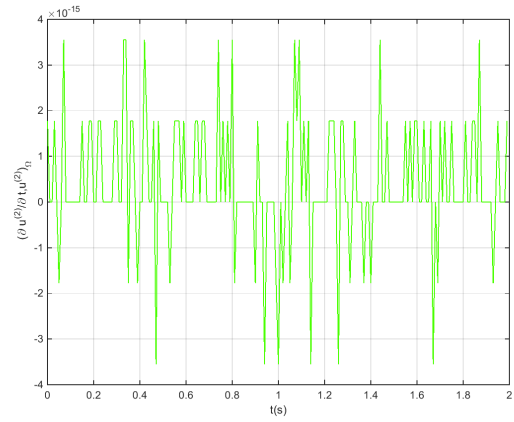
discrete helicity instead of time derivatives of them, we will find they are not conserved. For more details, see Section 4.4. More discussions about this will be given in Section 6.2.

From the  $L^2$ -norm of  $du^{(2)}$ , we can know that if the mass conservation law is satisfied. For our test case, the data of  $L^2$ -norm of  $du^{(2)}$  are shown in sub-figures (e). From these sub-figures, we can see that the value of  $\|du^{(2)}\|_{L^2}$  is always lower than  $10^{-13}$  which proves that the mass conservation law is well satisfied in our scheme. Meanwhile, since we consider the  $L^2$ -norm, we can know that the value of  $du^{(2)}$  at each cell is lower than  $10^{-13}$  as well. Therefore, we can conclude that we obtain a velocity divergence free solution. The last sub-figures (f) show how the  $L^2$ -norm of  $(\tilde{\omega}^{(2)} - d\tilde{u}^{(1)})$  changes over time. The value of  $\|\tilde{\omega}^{(2)} - d\tilde{u}^{(1)}\|_{L^2}$  indicates that how well the relation  $\tilde{\omega}^{(2)} = d\tilde{u}^{(1)}$  is satisfied. In these sub-figures, the value of  $\|\tilde{\omega}^{(2)} - d\tilde{u}^{(1)}\|_{L^2}$  slightly increases over time. But overall, it is constrained at considerably low level.

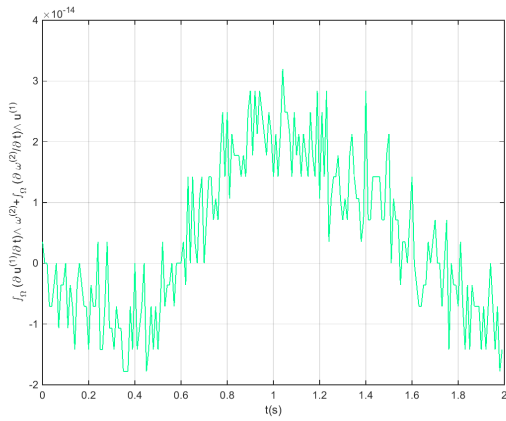
In addition, the long time stability are tested with the same initial condition at  $\Delta t = 0.0001$ ,  $N = 5$  and  $t = 20s$ . The results are presented in Fig. 5.6. In this figure, we can find that the scheme still conserve mass, kinetic energy and helicity after a long time computation. However, the fluctuation of the time derivative of helicity increases over time which is probably because of the accumulation of error that comes from the coarse temporal discretization.



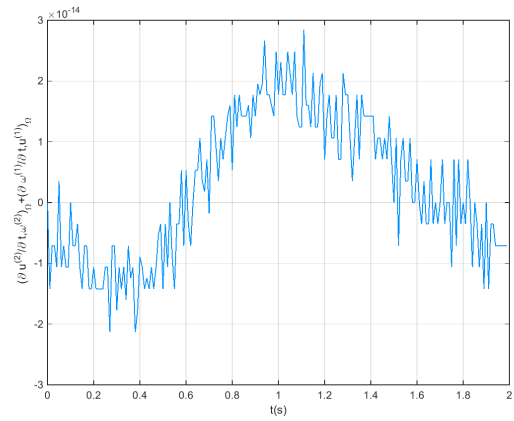
(a) Time derivative of inner kinetic energy.



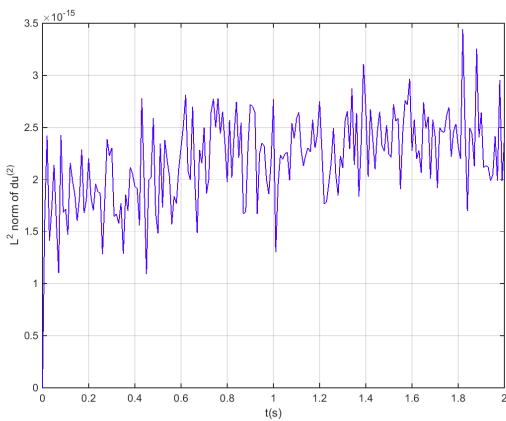
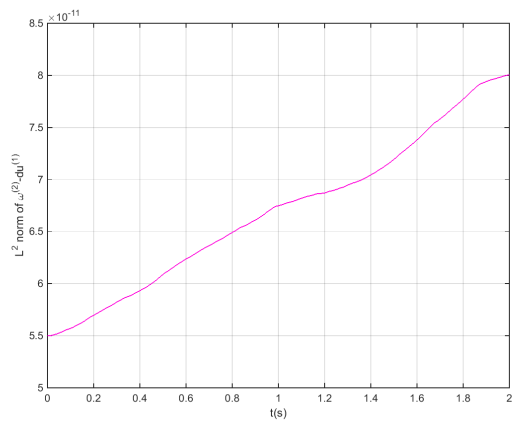
(b) Time derivative of outer kinetic energy.

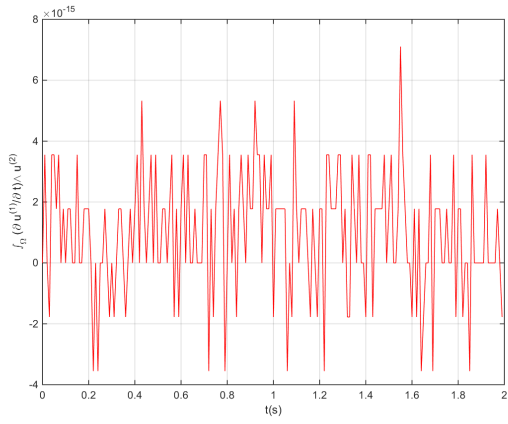


(c) Time derivative of inner helicity.

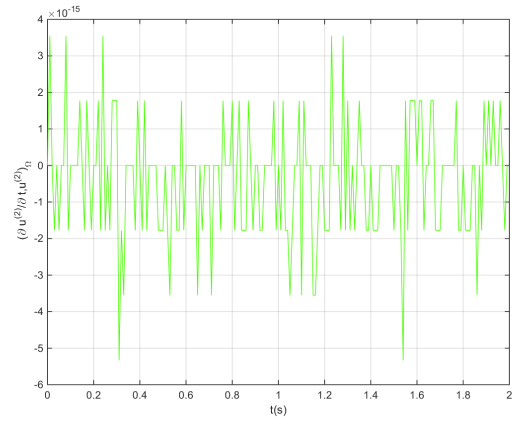


(d) Time derivative of outer helicity.

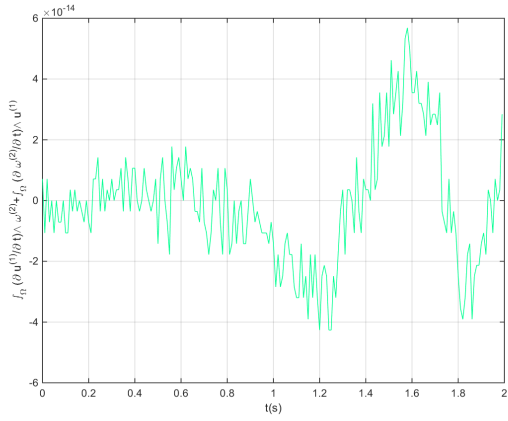
(e)  $L^2$ -norm of  $du^{(2)}$ .(f)  $L^2$ -norm of  $(\tilde{\omega}^{(2)} - d\tilde{u}^{(1)})$ .Figure 5.3: Results at  $N = 3$ ,  $\Delta t = 0.0001$ ,  $t = 2s$ .



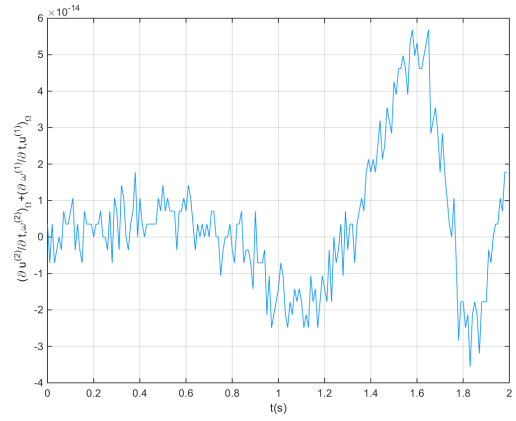
(a) Time derivative of inner kinetic energy.



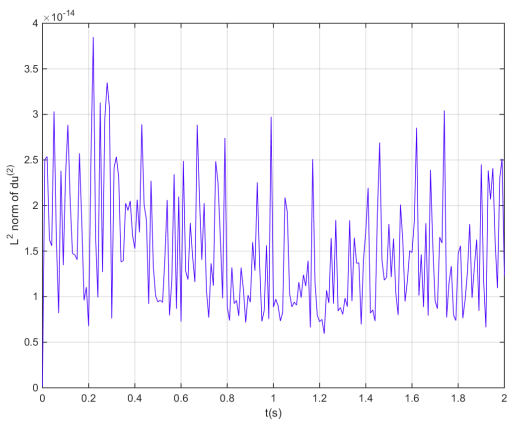
(b) Time derivative of outer kinetic energy.



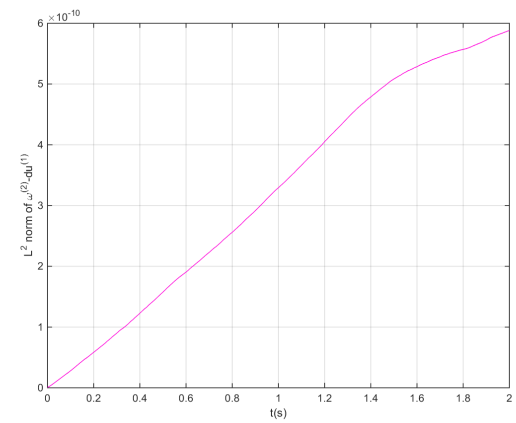
(c) Time derivative of inner helicity.



(d) Time derivative of outer helicity.

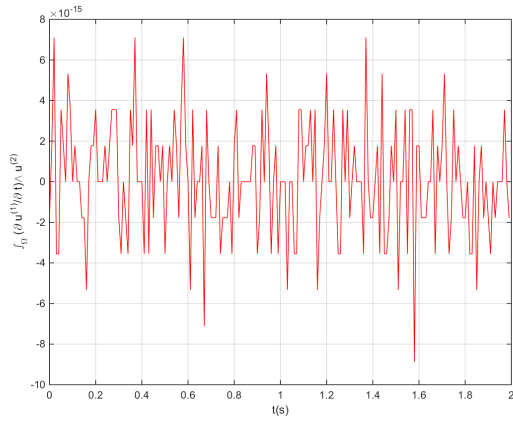


(e)  $L^2$ -norm of  $du^{(2)}$ .

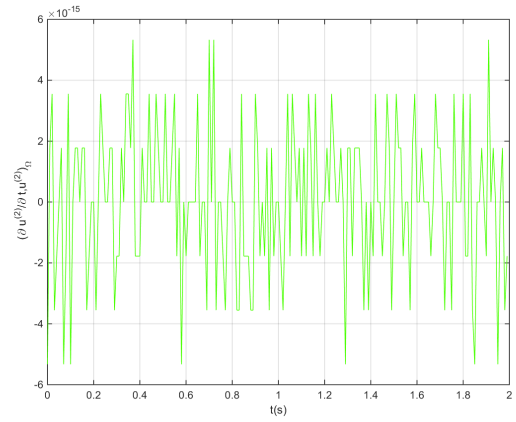


(f)  $L^2$ -norm of  $(\tilde{\omega}^{(2)} - d\tilde{u}^{(1)})$ .

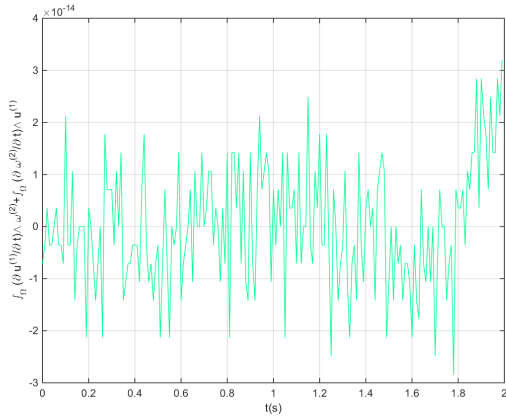
Figure 5.4: Results at  $N = 5$ ,  $\Delta t = 0.0001$ ,  $t = 2s$ .



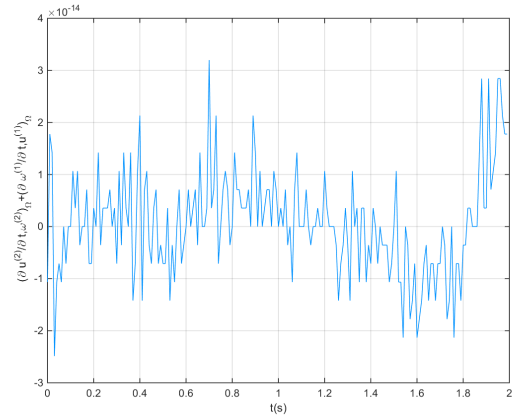
(a) Time derivative of inner kinetic energy.



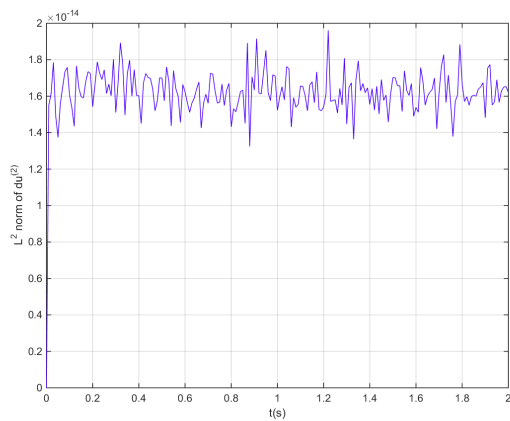
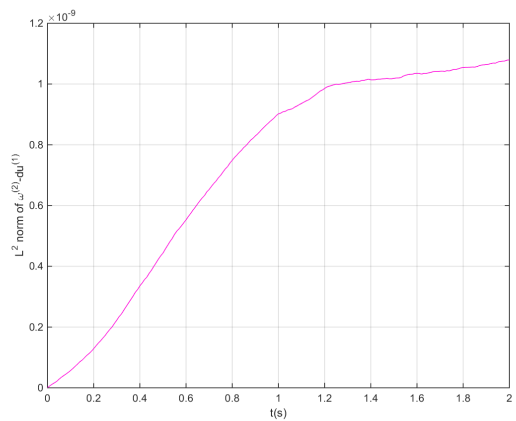
(b) Time derivative of outer kinetic energy.

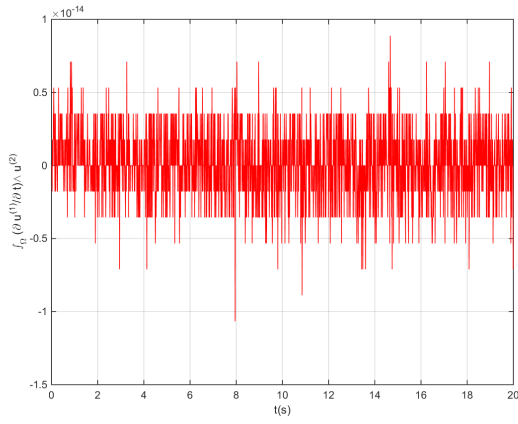


(c) Time derivative of inner helicity.

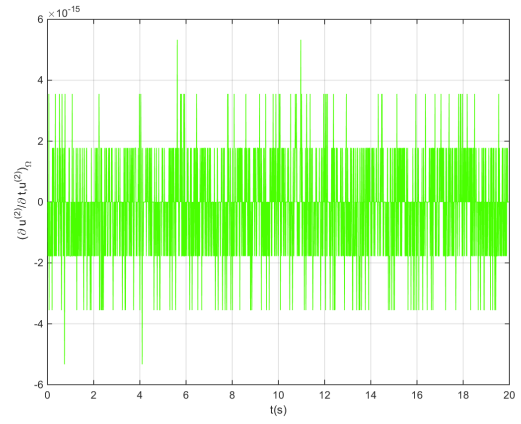


(d) Time derivative of outer helicity.

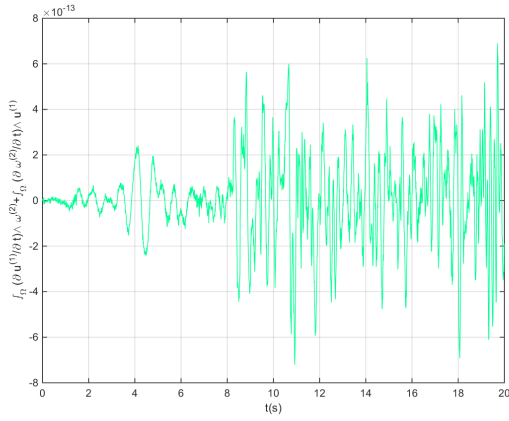
(e)  $L^2$ -norm of  $du^{(2)}$ .(f)  $L^2$ -norm of  $(\tilde{\omega}^{(2)} - d\tilde{u}^{(1)})$ .Figure 5.5: Results at  $N = 7$ ,  $\Delta t = 0.0001$ ,  $t = 2s$ .



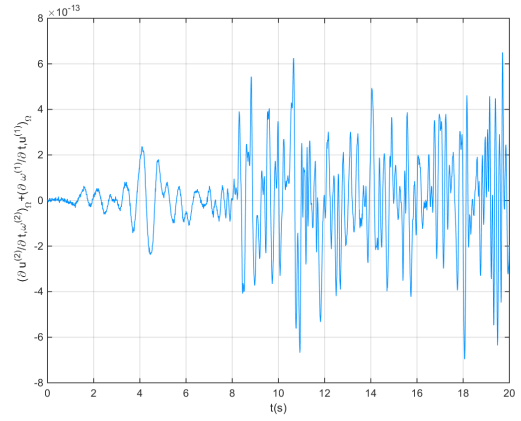
(a) Time derivative of inner kinetic energy.



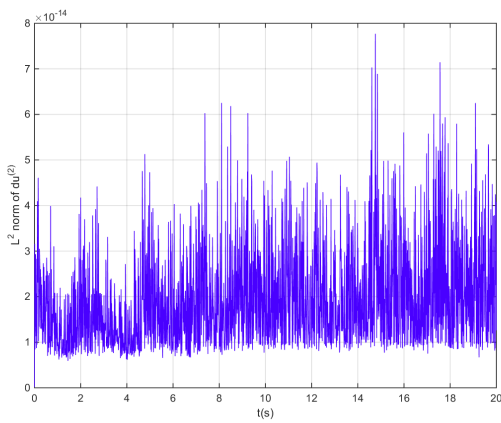
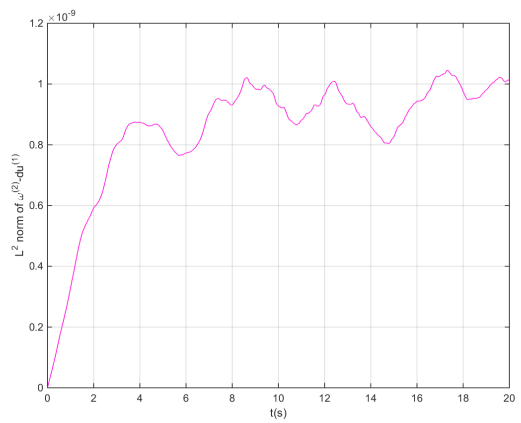
(b) Time derivative of outer kinetic energy.



(c) Time derivative of inner helicity.



(d) Time derivative of outer helicity.

(e)  $L^2$ -norm of  $du^{(2)}$ .(f)  $L^2$ -norm of  $(\tilde{\omega}^{(2)} - d\tilde{u}^{(1)})$ .Figure 5.6: Results at  $N = 5$ ,  $\Delta t = 0.0001$ ,  $t = 20s$ .



## Conclusions and recommendations

In this project, we start from differential geometry and algebraic topology. With these ingredients, we can understand physical variables and differential operators in a more physical and reasonable way. Then we set up the mimetic spectral element method by introducing projection operators, discrete operators and basis functions. The reduction operator reduces differential forms to co-chains associated with chains. Then, with basis functions, the reconstruction operator reforms the co-chains and results in discrete forms. The reduction operator and the reconstruction operator constitute the projection operator. Furthermore, we analyze the performance of the projection operator acting on differential operators such as exterior derivative, wedge product, interior product, inner product and Hodge star operator, then sequentially derive discrete forms of them. Using discrete differential forms and discrete operators, we set up our mimetic framework (the mimetic spectral element method), and with it, we can easily discrete complicated equations.

After setting up the mimetic spectral element method, we apply it to Euler equations. First, Euler equations are rewritten with inner oriented forms and outer oriented variables respectively. Meanwhile we prove the conservation laws of Euler equations under these new forms. Secondly, by analyzing the expressions of the kinetic energy and helicity in the mimetic framework and the discrete spaces, we decide to make the dual grid and primal grid to be one. In addition, because of our periodic boundary conditions and the fact that degrees of freedom strongly depend on the distribution of cells, we choose to use the weak form in wedge product for inner Euler and use the weak form in inner product for outer Euler. Then, the mimetic spectral element method is applied to the weak inner Euler and weak outer Euler. Two semi-discretized systems are obtained.

With these semi-discretized systems, we are not able to preserve mass, kinetic energy and helicity yet because only a part of properties of Euler equations are kept in either the discrete inner Euler or discrete outer Euler, and each of the two discrete forms of Euler equations

can not satisfy conservation laws individually. So we have to set up interactions between the discrete inner Euler and discrete outer Euler to make use of their properties simultaneously. With the interactions given in Section 4.3, we finally successfully construct a spatially mass-, kinetic energy- and helicity-preserving scheme. Together with the temporal discretization, a fully discretized system is obtained. The resulting scheme is then tested by a periodic flow, which shows that the scheme does satisfy the conservation laws and some other important properties like the divergence free flow condition and the relation that inner vorticity is the exterior derivative (curl) of inner velocity.

## 6.1 Conclusions

In summary, this project is a successful one and some important conclusions are listed as follow:

- First, compared to the existing mass, kinetic energy and helicity conserved schemes, for example, see [31, 44], the structure-preserving mimetic spectral element method has natural advantage for constructing schemes which conserve multiple invariants. This is because that the discretization error which may destroy the conservation laws at the discrete level is eliminated as much as possible.
- Both inner and outer oriented velocity and vorticity are required to express the discrete kinetic energy and helicity. Meanwhile, to preserve them simultaneously, the space of discrete inner oriented velocity  $(L^2\tilde{\Lambda}_h^1(\Omega; \tilde{C}_1))$  need to be identical with that of discrete outer oriented vorticity  $(L^2\Lambda_h^1(\Omega; C_1))$ , and the space of discrete inner oriented vorticity  $(L^2\tilde{\Lambda}_h^2(\Omega; \tilde{C}_2))$  need to be identical with that of discrete inner oriented velocity  $(L^2\Lambda_h^2(\Omega; C_2))$ . Therefore, two dual grids with the primal grid totally coinciding with the dual grid need to be employed.
- Because of the duality between the primal and dual grid we employ, the spaces of discrete forms are not compatible for direct Hodge star computation. Therefore, to obtain both inner and outer oriented forms, both the inner Euler and outer Euler should be discretized and computed.
- At the discrete level, only some properties of Euler equations at the continuous level are conserved for either inner Euler or outer Euler, to preserve both discrete kinetic energy and helicity, we need to set up interactions between the discrete weak inner Euler and the discrete weak outer Euler to make use of these properties together.

## 6.2 Recommendations

This project is a first try of applying the mimetic spectral element method to develop mass-, kinetic energy- and helicity-preserving schemes. However, because of the time constraint, there is still a lot of work left incomplete, and many aspects of our research can be improved. Here in this last section, we will give some advises to the ones who want to carry on research related to this project about what can be done to improve and complete this project.

- First, the computational domain in this project is very simple, a unit 3-cube  $[-1, 1]^3$ . However, real flows rarely have such simple flow domains. To make our scheme applicable to real flow cases, the approach of applying our scheme to complex flow domains should be developed. Although the method that allows the application of the mimetic spectral element method on arbitrary domains is already well developed as we said in Chapter 3, for example, see [17, 25, 26, 38], applying that method to our scheme still is a challenge because we compute two differently oriented Euler simultaneously, which is totally different from any existing mimetic spectral discretization schemes.
- Secondly, for the time derivative terms, the explicit forward Euler which is the last accurate Runge-Kutta method (of order 1) is used. Higher order Runge-kutta methods, like The symplectic Euler (of order 2) or the famous 4th order Runge-Kutta methods, will help a lot. In addition, the time integration developed by Palha et al. [41] can also be a good option. Further, time staggered schemes based on the interactions constructed between the discrete inner and outer Euler may benefit the computation significantly.
- Thirdly, as we can see from the appendix, discretizations we used for convection terms, like  $\iota_u \tilde{\omega}^{(2)}$  and  $\iota_u \tilde{u}^{(1)}$ , are extremely complicated. Basically, we use brute force according to the definition of the interior product to discretize these convection terms. A direct result is that the matrices representing these convections terms are huge. Therefore, the computation becomes very expensive. Essentially, the interior product is a metric-free operator like the exterior derivative which has the metric-free discrete counterpart coboundary (incidence matrix). However, by now, no metric-free discrete counterpart for the interior product is found. Developing a metric-free discrete counterpart for the interior product is of great value and will be a great challenge.
- Fourthly, an important aspect for developing a new scheme is the error analysis which is missed in this project. As we can see from Fig. 5.6, the unphysical fluctuation increases over time, which will eventually result in divergence if the computation time is long enough. Clear error analysis can help us understand the reason of this instability. In addition, understanding the source of error will significantly benefit the development of better schemes based on the scheme given in this project.

Furthermore, the application of our helicity preserved scheme on the investigation of turbulence can be another field of great value. All in all, what we already done just covered a small part of this interesting field which is of great potential.

## Reference

- [1] A. Arakawa. Computational design for long-term numerical integration of the equations of fluid motion: two-dimensional incompressible flow. Part I. *Journal of Computational Physics*, 135(2):103–114, 1997.
- [2] P. Bochev and M. Gerritsma. A spectral mimetic least-squares method. *Computers & Mathematics with Applications*, 68(11):1480–1502, 2014.
- [3] M. Bouman, A. Palha, J. Kreeft, and M. Gerritsma. A conservative spectral element method for curvilinear domains. In *Spectral and High Order Methods for Partial Differential Equations*, pages 111–119. Springer, 2011.
- [4] F. Brezzi, K. Lipnikov, M. Shashkov, and V. Simoncini. A new discretization methodology for diffusion problems on generalized polyhedral meshes. *Computer Methods in Applied Mechanics and Engineering*, 196(37):3682–3692, 2007.
- [5] K. Brix, C. Canuto, and W. Dahmen. Legendre-gauss-lobatto grids and associated nested dyadic grids. *arXiv preprint arXiv:1311.0028*, 2013.
- [6] J. C. Campbell and M. Shashkov. A tensor artificial viscosity using a mimetic finite difference algorithm. *Journal of Computational Physics*, 172(2):739–765, 2001.
- [7] L. B. Da Veiga, V. Gyrya, K. Lipnikov, and G. Manzini. Mimetic finite difference method for the Stokes problem on polygonal meshes. *Journal of Computational Physics*, 228(19):7215–7232, 2009.
- [8] D. J. D. de Ruijter. Energy, vorticity and enstrophy conserving mimetic spectral method for the Euler equation. 2013.
- [9] T. Frankel. *The geometry of physics: an introduction*. Cambridge University Press, 2011.

- [10] M. Gerritsma. Edge functions for spectral element methods. In *Spectral and High Order Methods for Partial Differential Equations*, pages 199–207. Springer, 2011.
- [11] M. Gerritsma. An introduction to a compatible spectral discretization method. *Mechanics of Advanced Materials and Structures*, 19(1-3):48–67, 2012.
- [12] M. Gerritsma, M. Bouman, and A. Palha. Least-squares spectral element method on a staggered grid. In *Large-Scale Scientific Computing*, pages 653–661. Springer, 2010.
- [13] M. Gerritsma, R. Hiemstra, J. Kreeft, A. Palha, P. Rebelo, and D. Toshniwal. The geometric basis of numerical methods. In *Spectral and High Order Methods for Partial Differential Equations-ICOSAHOM 2012*, pages 17–35. Springer, 2014.
- [14] V. Gyrya and K. Lipnikov. High-order mimetic finite difference method for diffusion problems on polygonal meshes. *Journal of Computational Physics*, 227(20):8841–8854, 2008.
- [15] H. Heumann. *Eulerian and semi-Lagrangian methods for advection-diffusion of differential forms*. PhD thesis, Diss., Eidgenössische Technische Hochschule ETH Zürich, Nr. 19608, 2011, 2011.
- [16] R. Hiemstra and M. Gerritsma. High order methods with exact conservation properties. In *Spectral and High Order Methods for Partial Differential Equations-ICOSAHOM 2012*, pages 285–295. Springer, 2014.
- [17] R. R. Hiemstra, D. Toshniwal, R. H. M. Huijsmans, and M. Gerritsma. High order geometric methods with exact conservation properties. *Journal of Computational Physics*, 257:1444–1471, 2014.
- [18] J. Hyman, J. Morel, M. Shashkov, and S. Steinberg. Mimetic finite difference methods for diffusion equations. *Computational Geosciences*, 6(3-4):333–352, 2002.
- [19] J. Hyman and M. Shashkov. Adjoint operators for the natural discretizations of the divergence, gradient and curl on logically rectangular grids. *Applied Numerical Mathematics*, 25(4):413–442, 1997.
- [20] J. Hyman and M. Shashkov. Natural discretizations for the divergence, gradient, and curl on logically rectangular grids. *Computers & Mathematics with Applications*, 33(4):81–104, 1997.
- [21] J. Hyman and M. Shashkov. Approximation of boundary conditions for mimetic finite-difference methods. *Computers & Mathematics with Applications*, 36(5):79–99, 1998.
- [22] J. Hyman and M. Shashkov. Mimetic discretizations for Maxwell’s equations. *Journal of Computational Physics*, 151(2):881–909, 1999.
- [23] J. Hyman and M. Shashkov. The orthogonal decomposition theorems for mimetic finite difference methods. *SIAM Journal on Numerical Analysis*, 36(3):788–818, 1999.

- [24] J. Hyman, M. Shashkov, and S. Steinberg. The numerical solution of diffusion problems in strongly heterogeneous non-isotropic materials. *Journal of Computational Physics*, 132(1):130–148, 1997.
- [25] J. Kreeft. *Mimetic spectral element method; a discretization of geometry and physics*. TU Delft, Delft University of Technology, 2013.
- [26] J. Kreeft and M. Gerritsma. Mixed mimetic spectral element method for Stokes flow: A pointwise divergence-free solution. *Journal of Computational Physics*, 240:284–309, 2013.
- [27] J. Kreeft and M. Gerritsma. Higher-order compatible discretization on hexahedrals. In *Spectral and High Order Methods for Partial Differential Equations-ICOSAHOM 2012*, pages 311–323. Springer, 2014.
- [28] J. Kreeft, A. Palha, and M. Gerritsma. Mimetic framework on curvilinear quadrilaterals of arbitrary order. *arXiv preprint arXiv:1111.4304*, 2011.
- [29] Y. Kuznetsov, K. Lipnikov, and M. Shashkov. The mimetic finite difference method on polygonal meshes for diffusion-type problems. *Computational Geosciences*, 8(4):301–324, 2004.
- [30] K. Lipnikov, M. Shashkov, and D. Svyatskiy. The mimetic finite difference discretization of diffusion problem on unstructured polyhedral meshes. *Journal of Computational Physics*, 211(2):473–491, 2006.
- [31] J. Liu and W. Wang. Energy and helicity preserving schemes for hydro-and magnetohydro-dynamics flows with symmetry. *Journal of Computational Physics*, 200(1):8–33, 2004.
- [32] J. Liu and W. Wang. Convergence analysis of the energy and helicity preserving scheme for axisymmetric flows. *SIAM Journal on Numerical Analysis*, 44(6):2456–2480, 2006.
- [33] A. N. Lowan, N. Davids, A. Levenson, et al. Table of the zeros of the legendre polynomials of order 1–16 and the weight coefficients for Gauss’ mechanical quadrature formula. *Bulletin of the American Mathematical Society*, 48(10):739–743, 1942.
- [34] L. Margolin, M. Shashkov, and P. K. Smolarkiewicz. A discrete operator calculus for finite difference approximations. *Computer methods in applied mechanics and engineering*, 187(3):365–383, 2000.
- [35] H.K. Moffatt and A. Tsinober. Helicity in laminar and turbulent flow. *Annual review of fluid mechanics*, 24(1):281–312, 1992.
- [36] A. Natale. A compatible discretization approach for the incompressible Euler equations. 2013.

- [37] M. Olshanskii and L. G. Rebholz. Note on helicity balance of the Galerkin method for the 3d Navier-Stokes equations. *Computer Methods in Applied Mechanics and Engineering*, 199(17):1032–1035, 2010.
- [38] A. Palha. *High order mimetic discretization; development and application to Laplace and advection problems in arbitrary quadrilaterals*. TU Delft, Delft University of Technology, 2013.
- [39] A. Palha and M. Gerritsma. Mimetic least-squares spectral/hp finite element method for the Poisson equation. In *Large-Scale Scientific Computing*, pages 662–670. Springer, 2010.
- [40] A. Palha and M. Gerritsma. Spectral element approximation of the hodge-star operator in curved elements. In *Spectral and High Order Methods for Partial Differential Equations*, pages 283–291. Springer, 2011.
- [41] A. Palha, P. P. Rebelo, and M. Gerritsma. Mimetic spectral element advection. In *Spectral and High Order Methods for Partial Differential Equations-ICOSAHOM 2012*, pages 325–335. Springer, 2014.
- [42] A. Palha, P. P. Rebelo, R. Hiemstra, J. Kreeft, and M. Gerritsma. Physics-compatible discretization techniques on single and dual grids, with application to the Poisson equation of volume forms. *Journal of Computational Physics*, 257:1394–1422, 2014.
- [43] P. P. Rebelo, A. Palha, and M. Gerritsma. Mixed mimetic spectral element method applied to Darcy’s problem. In *Spectral and High Order Methods for Partial Differential Equations-ICOSAHOM 2012*, pages 373–382. Springer, 2014.
- [44] L. G. Rebholz. An energy-and helicity-conserving finite element scheme for the Navier-Stokes equations. *SIAM Journal on Numerical Analysis*, 45(4):1622–1638, 2007.
- [45] D. Rufat, G. Mason, P. Mullen, and M. Desbrun. The chain collocation method: A spectrally accurate calculus of forms. *Journal of Computational Physics*, 257:1352–1372, 2014.
- [46] D. Toshniwal, R. H. M. Huijsmans, and M. Gerritsma. A geometric approach towards momentum conservation. In *Spectral and High Order Methods for Partial Differential Equations-ICOSAHOM 2012*, pages 393–402. Springer, 2014.

## Appendix: Discretizations

In a Gauss-Lobatto-Legendre grid with  $N$  line segment on each direction, from Section 3.3 we know the discrete forms are expanded as:

*Discrete inner 0-forms, the inner oriented pressure (associated with points):*

$$\tilde{p}^{(0)} = \sum_{i=0}^N \sum_{j=0}^N \sum_{k=0}^N \tilde{p}_{i,j,k} \phi_i^0(x) \phi_j^0(y) \phi_k^0(z), \quad (\text{A.0.1})$$

with vector proxy  $\tilde{p}^{(0)}$ :

$$\tilde{p}^{(0)} = \varphi(\mathcal{R}\tilde{p}^{(0)}) = \left\{ \tilde{p}_1, \tilde{p}_2, \dots, \tilde{p}_l, \dots, \tilde{p}_{(N+1)^3} \right\}^T,$$

where  $\tilde{p}_l = \tilde{p}_{i,j,k}, l = i + 1 + j(N + 1) + k(N + 1)^2, i, j, k = 0 : N$ . We use  $M : N$  means  $M, M + 1, M + 2, \dots, N$ .

*Discrete inner 1-forms, inner oriented velocity (associated with lines):*

$$\begin{aligned} \tilde{u}^{(1)} = & \sum_{i=1}^N \sum_{j=0}^N \sum_{k=0}^N \tilde{u}_{i,j,k}^x \phi_i^1(x) \phi_j^0(y) \phi_k^0(z) dx \\ & + \sum_{i=0}^N \sum_{j=1}^N \sum_{k=0}^N \tilde{u}_{i,j,k}^y \phi_i^0(x) \phi_j^1(y) \phi_k^0(z) dy \\ & + \sum_{i=0}^N \sum_{j=0}^N \sum_{k=1}^N \tilde{u}_{i,j,k}^z \phi_i^0(x) \phi_j^0(y) \phi_k^1(z) dz, \end{aligned} \quad (\text{A.0.2})$$

with vector proxy  $\tilde{\mathbf{u}}^{(1)}$ :

$$\begin{aligned}\tilde{\mathbf{u}}^{(1)} &= \varphi(\mathcal{R}\tilde{\mathbf{u}}^{(1)}) = \{\tilde{\mathbf{u}}^x, \tilde{\mathbf{u}}^y, \tilde{\mathbf{u}}^z\}^T : \\ \tilde{\mathbf{u}}^x &= \left\{ \tilde{u}_1^x, \tilde{u}_2^x, \dots, \tilde{u}_l^x, \dots, \tilde{u}_{N(N+1)^2}^x \right\} ; \\ \tilde{\mathbf{u}}^y &= \left\{ \tilde{u}_1^y, \tilde{u}_2^y, \dots, \tilde{u}_m^y, \dots, \tilde{u}_{N(N+1)^2}^y \right\} ; \\ \tilde{\mathbf{u}}^z &= \left\{ \tilde{u}_1^z, \tilde{u}_2^z, \dots, \tilde{u}_n^z, \dots, \tilde{u}_{N(N+1)^2}^z \right\} ,\end{aligned}\tag{A.0.3}$$

where  $\tilde{u}_l^x = \tilde{u}_{i,j,k}^x$ ;  $\tilde{u}_m^y = \tilde{u}_{i,j,k}^y$ ;  $\tilde{u}_n^z = \tilde{u}_{i,j,k}^z$ :

$$\begin{cases} l = i + jN + kN(N+1) & i = 1 : N; \quad j = 0 : N; \quad k = 0 : N \\ m = i + 1 + (j-1)(N+1) + kN(N+1) & i = 0 : N; \quad j = 1 : N; \quad k = 0 : N \\ n = i + 1 + j(N+1) + (k-1)(N+1)^2 & i = 0 : N; \quad j = 0 : N; \quad k = 1 : N \end{cases} .$$

*Discrete inner 2-forms, inner oriented vorticity (associated with faces):*

$$\begin{aligned}\tilde{\omega}^{(2)} &= \sum_{i=0}^N \sum_{j=1}^N \sum_{k=1}^N \tilde{\omega}_{i,j,k}^x \phi_i^0(x) \phi_j^1(y) \phi_k^1(z) dy \wedge dz \\ &+ \sum_{i=1}^N \sum_{j=0}^N \sum_{k=1}^N \tilde{\omega}_{i,j,k}^y \phi_i^1(x) \phi_j^0(y) \phi_k^1(z) dz \wedge dx \\ &+ \sum_{i=1}^N \sum_{j=1}^N \sum_{k=0}^N \tilde{\omega}_{i,j,k}^z \phi_i^1(x) \phi_j^1(y) \phi_k^0(z) dx \wedge dy ,\end{aligned}\tag{A.0.4}$$

with vector proxy  $\tilde{\omega}^{(2)}$ :

$$\begin{aligned}\tilde{\omega}^{(2)} &= \varphi(\mathcal{R}\tilde{\omega}^{(2)}) = \{\tilde{\omega}^x, \tilde{\omega}^y, \tilde{\omega}^z\}^T : \\ \tilde{\omega}^x &= \left\{ \tilde{\omega}_1^x, \tilde{\omega}_2^x, \dots, \tilde{\omega}_l^x, \dots, \tilde{\omega}_{N^2(N+1)}^x \right\} ; \\ \tilde{\omega}^y &= \left\{ \tilde{\omega}_1^y, \tilde{\omega}_2^y, \dots, \tilde{\omega}_m^y, \dots, \tilde{\omega}_{N^2(N+1)}^y \right\} ; \\ \tilde{\omega}^z &= \left\{ \tilde{\omega}_1^z, \tilde{\omega}_2^z, \dots, \tilde{\omega}_n^z, \dots, \tilde{\omega}_{N^2(N+1)}^z \right\} ,\end{aligned}\tag{A.0.5}$$

where  $\tilde{\omega}_l^x = \tilde{\omega}_{i,j,k}^x$ ;  $\tilde{\omega}_m^y = \tilde{\omega}_{i,j,k}^y$ ;  $\tilde{\omega}_n^z = \tilde{\omega}_{i,j,k}^z$ :

$$\begin{cases} l = i + 1 + (j-1)(N+1) + (k-1)N(N+1) & i = 0 : N; \quad j = 1 : N; \quad k = 1 : N \\ m = i + jN + (k-1)N(N+1) & i = 1 : N; \quad j = 0 : N; \quad k = 1 : N \\ n = i + (j-1)N + kN^2 & i = 1 : N; \quad j = 1 : N; \quad k = 0 : N \end{cases} .$$

*Discrete outer 3-forms, outer oriented pressure (associated with volumes):*

$$p^{(3)} = \sum_{i=1}^N \sum_{j=1}^N \sum_{k=1}^N p_{i,j,k} \phi_i^1(x) \phi_j^1(y) \phi_k^1(z) dx \wedge dy \wedge dz, \quad (\text{A.0.6})$$

with vector proxy  $\mathbf{p}^{(3)}$ :

$$\mathbf{p}^{(3)} = \varphi(\mathcal{R}p^{(3)}) = \{p_1, p_2, \dots, p_l, \dots, p_{N^3}\}^T,$$

where  $p_l = p_{i,j,k}$ ,  $l = i + (j - 1)N + (k - 1)N^2$ ,  $i, j, k = 1 : N$ .

*Discrete outer 2-forms, outer oriented velocity (associated with faces):*

$$\begin{aligned} u^{(2)} &= \sum_{i=0}^N \sum_{j=1}^N \sum_{k=1}^N u_{i,j,k}^x \phi_i^0(x) \phi_j^1(y) \phi_k^1(z) dy \wedge dz \\ &+ \sum_{i=1}^N \sum_{j=0}^N \sum_{k=1}^N u_{i,j,k}^y \phi_i^1(x) \phi_j^0(y) \phi_k^1(z) dz \wedge dx \\ &+ \sum_{i=1}^N \sum_{j=1}^N \sum_{k=0}^N u_{i,j,k}^z \phi_i^1(x) \phi_j^1(y) \phi_k^0(z) dx \wedge dy, \end{aligned} \quad (\text{A.0.7})$$

with vector proxy  $\mathbf{u}^{(2)}$ :

$$\mathbf{u}^{(2)} = \varphi(\mathcal{R}u^{(2)}) = \{\mathbf{u}^x, \mathbf{u}^y, \mathbf{u}^z\}^T : \quad (\text{A.0.8})$$

$$\mathbf{u}^x = \{u_1^x, u_2^x, \dots, u_l^x, \dots, u_{N^2(N+1)}^x\};$$

$$\mathbf{u}^y = \{u_1^y, u_2^y, \dots, u_m^y, \dots, u_{N^2(N+1)}^y\};$$

$$\mathbf{u}^z = \{u_1^z, u_2^z, \dots, u_n^z, \dots, u_{N^2(N+1)}^z\},$$

where  $u_l^x = u_{i,j,k}^x$ ;  $u_m^y = u_{i,j,k}^y$ ;  $u_n^z = u_{i,j,k}^z$ :

$$\begin{cases} l = i + 1 + (j - 1)(N + 1) + (k - 1)N(N + 1) & i = 0 : N; \quad j = 1 : N; \quad k = 1 : N \\ m = i + jN + (k - 1)N(N + 1) & i = 1 : N; \quad j = 0 : N; \quad k = 1 : N \\ n = i + (j - 1)N + kN^2 & i = 1 : N; \quad j = 1 : N; \quad k = 0 : N \end{cases}.$$

Discrete outer 1-forms, outer oriented vorticity (associated with lines):

$$\begin{aligned}
\omega^{(1)} &= \sum_{i=1}^N \sum_{j=0}^N \sum_{k=0}^N \omega_{i,j,k}^x \phi_i^1(x) \phi_j^0(y) \phi_k^0(z) dx \\
&+ \sum_{i=0}^N \sum_{j=1}^N \sum_{k=0}^N \omega_{i,j,k}^y \phi_i^0(x) \phi_j^1(y) \phi_k^0(z) dy \\
&+ \sum_{i=0}^N \sum_{j=0}^N \sum_{k=1}^N \omega_{i,j,k}^z \phi_i^0(x) \phi_j^0(y) \phi_k^1(z) dz ,
\end{aligned} \tag{A.0.9}$$

with vector proxy  $\omega^{(1)}$ :

$$\begin{aligned}
\omega^{(1)} &= \varphi(\mathcal{R}\omega^{(1)}) = \{\omega^x, \omega^y, \omega^z\}^T : \\
\omega^x &= \{\omega_1^x, \tilde{u}_2^x, \dots, \omega_l^x, \dots, \omega_{N(N+1)^2}^x\} ; \\
\omega^y &= \{\omega_1^y, \omega_2^y, \dots, \tilde{u}_m^y, \dots, \omega_{N(N+1)^2}^y\} ; \\
\omega^z &= \{\omega_1^z, \omega_2^z, \dots, \omega_n^z, \dots, \omega_{N(N+1)^2}^z\} ,
\end{aligned} \tag{A.0.10}$$

where  $\omega_l^x = \omega_{i,j,k}^x$ ;  $\omega_m^y = \omega_{i,j,k}^y$ ;  $\omega_n^z = \omega_{i,j,k}^z$ :

$$\begin{cases} l = i + jN + kN(N + 1) & i = 1 : N; \quad j = 0 : N; \quad k = 0 : N \\ m = i + 1 + (j - 1)(N + 1) + kN(N + 1) & i = 0 : N; \quad j = 1 : N; \quad k = 0 : N \\ n = i + 1 + j(N + 1) + (k - 1)(N + 1)^2 & i = 0 : N; \quad j = 0 : N; \quad k = 1 : N \end{cases} .$$

In addition, we will use  $\Phi_{a,b,\dots,c}^{\alpha,\beta,\dots,\gamma}$  to represent integrals given as

$$\Phi_{a,b,\dots,c}^{\alpha,\beta,\dots,\gamma} = \int_{-1}^1 \phi_a^\alpha(x) \phi_b^\beta(x) \cdots \phi_c^\gamma(x) dx . \tag{A.0.11}$$

## A.1 Inner Euler discretization

The fully discretized inner Euler is given as

$$\left\{ \begin{aligned} \frac{1}{\Delta t} \int_{\Omega} \tilde{u}_{n+1}^{(1)} \wedge \sigma^{(2)} - \frac{1}{\Delta t} \int_{\Omega} \tilde{u}_n^{(1)} \wedge \sigma^{(2)} + \int_{\Omega} l_u \tilde{\omega}_n^{(2)} \wedge \sigma^{(2)} - \int_{\Omega} \tilde{p}_{0,n}^{(0)} \wedge d\sigma^{(2)} &= 0 \\ \frac{1}{\Delta t} \int_{\Omega} \tilde{\omega}_{n+1}^{(2)} \wedge \zeta^{(1)} - \frac{1}{\Delta t} \int_{\Omega} \tilde{\omega}_n^{(2)} \wedge \zeta^{(1)} + \int_{\Omega} l_u \tilde{\omega}_n^{(2)} \wedge d\zeta^{(1)} &= 0 , \\ \left( \tilde{u}_{n+1}^{(1)}, d\phi^{(0)} \right)_{\Omega} &= 0 \end{aligned} \right. , \tag{A.1.1}$$

and its matrix form is

$$\begin{pmatrix} \frac{1}{\Delta t} \hat{\mathbb{M}}^{(1)} & \emptyset & \mathbb{E}^{(2,3)} \hat{\mathbb{M}}^{(0)} \\ \emptyset & \frac{1}{\Delta t} \hat{\mathbb{M}}^{(2)} & \emptyset \\ \mathbb{M}^{(1)} \mathbb{E}^{(1,0)} & \emptyset & \emptyset \end{pmatrix} \begin{pmatrix} \tilde{\mathbf{u}}_{n+1} \\ \tilde{\boldsymbol{\omega}}_{n+1} \\ \tilde{\mathbf{p}}_n \end{pmatrix} = \begin{pmatrix} \frac{1}{\Delta t} \hat{\mathbb{M}}^{(1)} \tilde{\mathbf{u}}_n - \mathbb{A} + \frac{1}{2} \mathbb{B} \\ \frac{1}{\Delta t} \hat{\mathbb{M}}^{(2)} \tilde{\boldsymbol{\omega}}_n - \mathbb{E}^{(1,2)} \mathbb{A} \\ \mathbf{0} \end{pmatrix}. \quad (\text{A.1.2})$$

### A.1.1 Mass matrix $\hat{\mathbb{M}}^{(0)}$

Matrix  $\hat{\mathbb{M}}^{(0)}$  results from term  $\int_{\Omega} \tilde{\mathbf{p}}^{(0)} \wedge d\sigma^{(2)}$ .

When  $\lambda^{(3)} = \phi_a^1(x) \phi_b^1(y) \phi_c^1(z) dx \wedge dy \wedge dz$  where  $a = 1 : N, b = 1 : N, c = 1 : N$ ,

$$\int_{\Omega} \tilde{\mathbf{p}}^{(0)} \wedge \lambda^{(3)} = \sum_{i=0}^N \sum_{j=0}^N \sum_{k=0}^N \tilde{p}_{i,j,k} \int_{-1}^1 \phi_i^0(x) \phi_a^1(x) dx \int_{-1}^1 \phi_j^0(y) \phi_b^1(y) dy \int_{-1}^1 \phi_k^0(z) \phi_c^1(z) dz. \quad (\text{A.1.3})$$

Therefore

$$\hat{\mathbb{M}}_{(r,s)}^{(0)} = \Phi_{i,a}^{0,1} \Phi_{j,b}^{0,1} \Phi_{k,c}^{0,1}, \quad (\text{A.1.4})$$

$$\begin{cases} r = a + (b-1)N + (c-1)N^2 & a = 1 : N, b = 1 : N, c = 1 : N \\ s = i + 1 + j(N+1) + k(N+1)^2 & i = 0 : N, j = 0 : N, k = 0 : N \end{cases}. \quad (\text{A.1.5})$$

### A.1.2 Mass matrix $\hat{\mathbb{M}}^{(1)}$

Matrix  $\hat{\mathbb{M}}^{(1)}$  results from term  $\int_{\Omega} \tilde{\mathbf{u}}^{(1)} \wedge \sigma^{(2)}$ .

When  $\sigma^{(2)} = \phi_a^0(x) \phi_b^1(y) \phi_c^1(z) dy \wedge dz$  where  $a = 0 : N, b = 1 : N, c = 1 : N$ ,

$$\int_{\Omega} \tilde{\mathbf{u}}^{(1)} \wedge \sigma^{(2)} = \sum_{i=1}^N \sum_{j=0}^N \sum_{k=0}^N \tilde{u}_{i,j,k}^{\xi} \Phi_{i,a}^{0,1} \Phi_{j,b}^{0,1} \Phi_{k,c}^{0,1}. \quad (\text{A.1.6})$$

When  $\sigma^{(2)} = \phi_a^1(x) \phi_b^0(y) \phi_c^1(z) dz \wedge dx$  where  $a = 1 : N, b = 0 : N, c = 1 : N$ ,

$$\int_{\Omega} \tilde{\mathbf{u}}^{(1)} \wedge \sigma^{(2)} = \sum_{i=1}^N \sum_{j=0}^N \sum_{k=0}^N \tilde{u}_{i,j,k}^{\xi} \Phi_{i,a}^{0,1} \Phi_{b,j}^{0,1} \Phi_{k,c}^{0,1}. \quad (\text{A.1.7})$$

When  $\sigma^{(2)} = \phi_a^1(x) \phi_b^1(y) \phi_c^0(z) dx \wedge dy$  where  $a = 1 : N, b = 1 : N, c = 0 : N$ ,

$$\int_{\Omega} \tilde{\mathbf{u}}^{(1)} \wedge \sigma^{(2)} = \sum_{i=1}^N \sum_{j=0}^N \sum_{k=0}^N \tilde{u}_{i,j,k}^{\xi} \Phi_{i,a}^{0,1} \Phi_{j,b}^{0,1} \Phi_{c,k}^{0,1}. \quad (\text{A.1.8})$$

Therefore

$$\hat{\mathbb{M}}^{(1)} = \begin{pmatrix} \hat{\mathbb{M}}^{11} & \mathbf{0} & \mathbf{0} \\ \mathbf{0} & \hat{\mathbb{M}}^{12} & \mathbf{0} \\ \mathbf{0} & \mathbf{0} & \hat{\mathbb{M}}^{13} \end{pmatrix}, \quad (\text{A.1.9})$$

where

$$\hat{\mathbb{M}}_{r,s}^{11} = \Phi_{a,i}^{0,1} \Phi_{j,b}^{0,1} \Phi_{k,c}^{0,1}, \quad (\text{A.1.10})$$

$$\begin{cases} r = a + 1 + (b - 1)(N + 1) + (c - 1)N(N + 1) & a = 0 : N, b = 1 : N, c = 1 : N \\ s = i + jN + kN(N + 1) & i = 1 : N, j = 0 : N, k = 0 : N \end{cases}; \quad (\text{A.1.11})$$

$$\hat{\mathbb{M}}_{r,s}^{12} = \Phi_{i,a}^{0,1} \Phi_{b,j}^{0,1} \Phi_{k,c}^{0,1}, \quad (\text{A.1.12})$$

$$\begin{cases} r = a + bN + (c - 1)N(N + 1) & a = 1 : N, b = 0 : N, c = 1 : N \\ s = i + 1 + (j - 1)(N + 1) + kN(N + 1) & i = 0 : N, j = 1 : N, k = 0 : N \end{cases}; \quad (\text{A.1.13})$$

$$\hat{\mathbb{M}}_{r,s}^{13} = \Phi_{i,a}^{0,1} \Phi_{j,b}^{0,1} \Phi_{c,k}^{0,1}, \quad (\text{A.1.14})$$

$$\begin{cases} r = a + (b - 1)N + cN^2 & a = 1 : N, b = 1 : N, c = 0 : N \\ s = i + 1 + j(N + 1) + (k - 1)(N + 1)^2 & i = 0 : N, j = 0 : N, k = 1 : N \end{cases}. \quad (\text{A.1.15})$$

### A.1.3 Mass matrix $\hat{\mathbb{M}}^{(2)}$

Matrix  $\hat{\mathbb{M}}^{(2)}$  results from term  $\int_{\Omega} \tilde{\omega}^{(2)} \wedge \zeta^{(1)}$ .

When  $\zeta^{(1)} = \phi_a^1(x) \phi_b^0(y) \phi_c^0(z) dx$  where  $a = 1 : N, b = 0 : N, c = 0 : N$ ,

$$\int_{\Omega} \tilde{\omega}^{(2)} \wedge \zeta^{(1)} = \sum_{i=0}^N \sum_{j=1}^N \sum_{k=1}^N \tilde{\omega}_{i,j,k}^{\xi} \Phi_{i,a}^{0,1} \Phi_{b,j}^{0,1} \Phi_{c,k}^{0,1}. \quad (\text{A.1.16})$$

When  $\zeta^{(1)} = \phi_a^0(x) \phi_b^1(y) \phi_c^0(z) dy$  where  $a = 0 : N, b = 1 : N, c = 0 : N$ ,

$$\int_{\Omega} \tilde{\omega}^{(2)} \wedge \zeta^{(1)} = \sum_{i=1}^N \sum_{j=0}^N \sum_{k=1}^N \tilde{\omega}_{i,j,k}^{\eta} \Phi_{a,i}^{0,1} \Phi_{j,b}^{0,1} \Phi_{c,k}^{0,1}. \quad (\text{A.1.17})$$

When  $\zeta^{(1)} = \phi_a^0(x) \phi_b^0(y) \phi_c^1(z) dz$  where  $a = 0 : N, b = 0 : N, c = 1 : N$ ,

$$\int_{\Omega} \tilde{\omega}^{(2)} \wedge \zeta^{(1)} = \sum_{i=1}^N \sum_{j=1}^N \sum_{k=0}^N \tilde{\omega}_{i,j,k}^{\eta} \Phi_{a,i}^{0,1} \Phi_{b,j}^{0,1} \Phi_{k,c}^{0,1}. \quad (\text{A.1.18})$$

Therefore

$$\hat{\mathbb{M}}^2 = \begin{pmatrix} \tilde{\mathbb{M}}^{21} & \mathbf{0} & \mathbf{0} \\ \mathbf{0} & \tilde{\mathbb{M}}^{22} & \mathbf{0} \\ \mathbf{0} & \mathbf{0} & \tilde{\mathbb{M}}^{23} \end{pmatrix}, \quad (\text{A.1.19})$$

where

$$\hat{\mathbb{M}}_{r,s}^{21} = \Phi_{i,a}^{0,1} \Phi_{b,j}^{0,1} \Phi_{c,k}^{0,1}, \quad (\text{A.1.20})$$

$$\begin{cases} r = a + bN + cN(N+1) & a = 1 : N, b = 0 : N, c = 0 : N \\ s = i + 1 + (j-1)(N+1) + (k-1)N(N+1) & i = 0 : N, j = 1 : N, k = 1 : N \end{cases}; \quad (\text{A.1.21})$$

$$\hat{\mathbb{M}}_{r,s}^{22} = \Phi_{a,i}^{0,1} \Phi_{j,b}^{0,1} \Phi_{c,k}^{0,1}, \quad (\text{A.1.22})$$

$$\begin{cases} r = a + 1 + (b-1)(N+1) + cN(N+1) & a = 0 : N, b = 1 : N, c = 0 : N \\ s = i + jN + (k-1)N(N+1) & i = 1 : N, j = 0 : N, k = 1 : N \end{cases}; \quad (\text{A.1.23})$$

$$\hat{\mathbb{M}}_{r,s}^{23} = \Phi_{a,i}^{0,1} \Phi_{b,j}^{0,1} \Phi_{k,c}^{0,1}, \quad (\text{A.1.24})$$

$$\begin{cases} r = a + 1 + b(N+1) + (c-1)(N+1)^2 & a = 0 : N, b = 0 : N, c = 1 : N \\ s = i + (j-1)N + kN^2 & i = 1 : N, j = 1 : N, k = 0 : N \end{cases}. \quad (\text{A.1.25})$$

### A.1.4 Matrix $\mathbb{A}$

Matrix  $\mathbb{A}$  comes from term  $\int_{\Omega} \iota_{\mathbf{u}} \tilde{\omega}^{(2)} \wedge \sigma^{(2)}$  and from Section 4.3, we know that

$$\begin{aligned} \mathbf{u} &= \left( \star \mathbf{u}^{(2)} \right)^{\sharp} = \sum_{i=0}^N \sum_{j=1}^N \sum_{k=1}^N u_{i,j,k}^x \phi_i^0(x) \phi_j^1(y) \phi_k^1(z) \frac{\partial}{\partial x} \\ &\quad + \sum_{i=1}^N \sum_{j=0}^N \sum_{k=1}^N u_{i,j,k}^y \phi_i^1(x) \phi_j^0(y) \phi_k^1(z) \frac{\partial}{\partial y} \\ &\quad + \sum_{i=1}^N \sum_{j=1}^N \sum_{k=0}^N u_{i,j,k}^z \phi_i^1(x) \phi_j^1(y) \phi_k^0(z) \frac{\partial}{\partial z}, \end{aligned} \quad (\text{A.1.26})$$

$$\begin{aligned} \iota_{\mathbf{u}} \tilde{\omega}^{(2)} &= + \sum_{i=1}^N \sum_{j=1}^N \sum_{k=0}^N \sum_{l=1}^N \sum_{m=0}^N \sum_{n=1}^N u_{i,j,k}^z \tilde{\omega}_{l,m,n}^y \phi_i^1(x) \phi_j^1(y) \phi_k^0(z) \phi_l^1(x) \phi_m^0(y) \phi_n^1(z) dx \\ &\quad - \sum_{i=1}^N \sum_{j=0}^N \sum_{k=1}^N \sum_{l=1}^N \sum_{m=1}^N \sum_{n=0}^N u_{i,j,k}^y \tilde{\omega}_{l,m,n}^z \phi_i^1(x) \phi_j^0(y) \phi_k^1(z) \phi_l^1(x) \phi_m^1(y) \phi_n^0(z) dx \\ &\quad + \sum_{i=0}^N \sum_{j=1}^N \sum_{k=1}^N \sum_{l=1}^N \sum_{m=1}^N \sum_{n=0}^N u_{i,j,k}^x \tilde{\omega}_{l,m,n}^z \phi_i^0(x) \phi_j^1(y) \phi_k^1(z) \phi_l^1(x) \phi_m^1(y) \phi_n^0(z) dy \\ &\quad - \sum_{i=1}^N \sum_{j=1}^N \sum_{k=0}^N \sum_{l=0}^N \sum_{m=1}^N \sum_{n=1}^N u_{i,j,k}^z \tilde{\omega}_{l,m,n}^x \phi_i^1(x) \phi_j^1(y) \phi_k^0(z) \phi_l^0(x) \phi_m^1(y) \phi_n^1(z) dy \\ &\quad + \sum_{i=1}^N \sum_{j=0}^N \sum_{k=1}^N \sum_{l=0}^N \sum_{m=1}^N \sum_{n=1}^N u_{i,j,k}^y \tilde{\omega}_{l,m,n}^x \phi_i^1(x) \phi_j^0(y) \phi_k^1(z) \phi_l^0(x) \phi_m^1(y) \phi_n^1(z) dz \\ &\quad - \sum_{i=0}^N \sum_{j=1}^N \sum_{k=1}^N \sum_{l=1}^N \sum_{m=0}^N \sum_{n=1}^N u_{i,j,k}^x \tilde{\omega}_{l,m,n}^y \phi_i^0(x) \phi_j^1(y) \phi_k^1(z) \phi_l^1(x) \phi_m^0(y) \phi_n^1(z) dz, \end{aligned} \quad (\text{A.1.27})$$

When  $\sigma^{(2)} = \phi_a^0(x) \phi_b^1(y) \phi_c^1(z) dy \wedge dz$  where  $a = 0 : N, b = 1 : N, c = 1 : N$ ,

$$\begin{aligned} \int_{\Omega} \sigma^{(2)} \wedge \iota_{\mathbf{u}} \tilde{\omega}^{(2)} &= \\ &+ \sum_{i=1}^N \sum_{j=1}^N \sum_{k=0}^N \sum_{l=1}^N \sum_{m=0}^N \sum_{n=1}^N u_{i,j,k}^z \tilde{\omega}_{l,m,n}^y \int_{-1}^1 \phi_i^1(x) \phi_l^1(x) \phi_a^0(x) dx \int_{-1}^1 \phi_j^1(y) \phi_m^0(y) \phi_b^1(y) dy \int_{-1}^1 \phi_k^0(z) \phi_n^1(z) \phi_c^1(z) dz \\ &- \sum_{i=1}^N \sum_{j=0}^N \sum_{k=1}^N \sum_{l=1}^N \sum_{m=1}^N \sum_{n=0}^N u_{i,j,k}^y \tilde{\omega}_{l,m,n}^z \int_{-1}^1 \phi_i^1(x) \phi_l^1(x) \phi_a^0(x) dx \int_{-1}^1 \phi_j^0(y) \phi_m^1(y) \phi_b^1(y) dy \int_{-1}^1 \phi_k^1(z) \phi_n^0(z) \phi_c^1(z) dz \\ &= \\ &+ \sum_{i=1}^N \sum_{j=1}^N \sum_{k=0}^N \sum_{l=1}^N \sum_{m=0}^N \sum_{n=1}^N u_{i,j,k}^z \tilde{\omega}_{l,m,n}^y \Phi_{a,i,l}^{0,1,1} \Phi_{m,j,b}^{0,1,1} \Phi_{k,n,c}^{0,1,1} \\ &- \sum_{i=1}^N \sum_{j=0}^N \sum_{k=1}^N \sum_{l=1}^N \sum_{m=1}^N \sum_{n=0}^N u_{i,j,k}^y \tilde{\omega}_{l,m,n}^z \Phi_{a,i,l}^{0,1,1} \Phi_{j,m,b}^{0,1,1} \Phi_{n,k,c}^{0,1,1}. \end{aligned} \quad (\text{A.1.28})$$

When  $\sigma^{(2)} = \phi_a^1(x)\phi_b^0(y)\phi_c^1(z)dz \wedge dx$  where  $a = 1 : N, b = 0 : N, c = 1 : N$ ,

$$\begin{aligned}
& \int_{\Omega} \sigma^{(2)} \wedge l_{\mathbf{u}} \tilde{\omega}^{(2)} = \\
& + \sum_{i=0}^N \sum_{j=1}^N \sum_{k=1}^N \sum_{l=1}^N \sum_{m=1}^N \sum_{n=0}^N u_{i,j,k}^x \tilde{\omega}_{l,m,n}^z \int_{-1}^1 \phi_i^0(x)\phi_l^1(x)\phi_a^1(x)dx \int_{-1}^1 \phi_j^1(y)\phi_m^1(y)\phi_b^0(y)dy \int_{-1}^1 \phi_k^1(z)\phi_n^0(z)\phi_c^1(z)dz \\
& - \sum_{i=1}^N \sum_{j=1}^N \sum_{k=0}^N \sum_{l=0}^N \sum_{m=1}^N \sum_{n=1}^N u_{i,j,k}^z \tilde{\omega}_{l,m,n}^x \int_{-1}^1 \phi_i^1(x)\phi_l^0(x)\phi_a^1(x)dx \int_{-1}^1 \phi_j^1(y)\phi_m^1(y)\phi_b^0(y)dy \int_{-1}^1 \phi_k^0(z)\phi_n^1(z)\phi_c^1(z)dz \\
& = \\
& + \sum_{i=0}^N \sum_{j=1}^N \sum_{k=1}^N \sum_{l=1}^N \sum_{m=1}^N \sum_{n=0}^N u_{i,j,k}^x \tilde{\omega}_{l,m,n}^z \Phi_{i,l,a}^{0,1,1} \Phi_{b,j,m}^{0,1,1} \Phi_{n,k,c}^{0,1,1} \\
& - \sum_{i=1}^N \sum_{j=1}^N \sum_{k=0}^N \sum_{l=0}^N \sum_{m=1}^N \sum_{n=1}^N u_{i,j,k}^z \tilde{\omega}_{l,m,n}^x \Phi_{l,i,a}^{0,1,1} \Phi_{b,j,m}^{0,1,1} \Phi_{k,n,c}^{0,1,1}.
\end{aligned} \tag{A.1.29}$$

When  $\sigma^{(2)} = \phi_a^1(x)\phi_b^1(y)\phi_c^0(z)dx \wedge dy$  where  $a = 1 : N, b = 1 : N, c = 0 : N$ ,

$$\begin{aligned}
& \int_{\Omega} \sigma^{(2)} \wedge l_{\mathbf{u}} \tilde{\omega}^{(2)} = \\
& + \sum_{i=1}^N \sum_{j=0}^N \sum_{k=1}^N \sum_{l=0}^N \sum_{m=1}^N \sum_{n=1}^N u_{i,j,k}^y \tilde{\omega}_{l,m,n}^x \int_{-1}^1 \phi_i^1(x)\phi_l^0(x)\phi_a^1(x)dx \int_{-1}^1 \phi_j^0(y)\phi_m^1(y)\phi_b^1(y)dy \int_{-1}^1 \phi_k^1(z)\phi_n^1(z)\phi_c^0(z)dz \\
& - \sum_{i=0}^N \sum_{j=1}^N \sum_{k=1}^N \sum_{l=1}^N \sum_{m=0}^N \sum_{n=1}^N u_{i,j,k}^x \tilde{\omega}_{l,m,n}^y \int_{-1}^1 \phi_i^0(x)\phi_l^1(x)\phi_a^1(x)dx \int_{-1}^1 \phi_j^1(y)\phi_m^0(y)\phi_b^1(y)dy \int_{-1}^1 \phi_k^1(z)\phi_n^1(z)\phi_c^0(z)dz \\
& = \\
& + \sum_{i=1}^N \sum_{j=0}^N \sum_{k=1}^N \sum_{l=0}^N \sum_{m=1}^N \sum_{n=1}^N u_{i,j,k}^y \tilde{\omega}_{l,m,n}^x \Phi_{l,i,a}^{0,1,1} \Phi_{j,m,b}^{0,1,1} \Phi_{c,k,n}^{0,1,1} \\
& - \sum_{i=0}^N \sum_{j=1}^N \sum_{k=1}^N \sum_{l=1}^N \sum_{m=0}^N \sum_{n=1}^N u_{i,j,k}^x \tilde{\omega}_{l,m,n}^y \Phi_{i,l,a}^{0,1,1} \Phi_{m,j,b}^{0,1,1} \Phi_{c,k,n}^{0,1,1}.
\end{aligned} \tag{A.1.30}$$

Therefore, term  $\int_{\Omega} \sigma^{(2)} \wedge l_{\mathbf{u}} \tilde{\omega}^{(2)}$  can be expressed in matrix form as

$$\mathbb{A} = \begin{pmatrix} \mathbf{0} & \cdots & \mathbf{0} & -\mathbb{A}_1^1 \tilde{\omega}^z & \cdots & -\mathbb{A}_{\mu}^1 \tilde{\omega}^z & +\mathbb{A}_1^2 \tilde{\omega}^y & \cdots & +\mathbb{A}_{\mu}^2 \tilde{\omega}^y \\ +\mathbb{A}_1^3 \tilde{\omega}^z & \cdots & +\mathbb{A}_{\mu}^3 \tilde{\omega}^z & \mathbf{0} & \cdots & \mathbf{0} & -\mathbb{A}_1^4 \tilde{\omega}^x & \cdots & -\mathbb{A}_{\mu}^4 \tilde{\omega}^x \\ -\mathbb{A}_1^5 \tilde{\omega}^y & \cdots & -\mathbb{A}_{\mu}^5 \tilde{\omega}^y & +\mathbb{A}_1^6 \tilde{\omega}^x & \cdots & +\mathbb{A}_{\mu}^6 \tilde{\omega}^x & \mathbf{0} & \cdots & \mathbf{0} \end{pmatrix} \mathbf{u}^{(2)}, \tag{A.1.31}$$

where  $\mu = N^2(N+1)$  and

$$\mathbb{A}_{r,(s,t)}^1 = \Phi_{a,i,l}^{0,1,1} \Phi_{j,m,b}^{0,1,1} \Phi_{n,k,c}^{0,1,1}, \tag{A.1.32}$$

with

$$\begin{cases} t = l + (m - 1)N + nN^2 & l = 1 : N, m = 1 : N, n = 0 : N \\ s = a + 1 + (b - 1)(N + 1) + (c - 1)N(N + 1) & a = 0 : N, b = 1 : N, c = 1 : N \\ r = i + jN + (k - 1)N(N + 1) & i = 1 : N, j = 0 : N, k = 1 : N \end{cases} \quad (\text{A.1.33})$$

$$\mathbb{A}_{r,(s,t)}^2 = \Phi_{a,i,l}^{0,1,1} \Phi_{m,j,b}^{0,1,1} \Phi_{k,n,c}^{0,1,1}, \quad (\text{A.1.34})$$

with

$$\begin{cases} t = l + mN + (n - 1)N(N + 1) & l = 1 : N, m = 0 : N, n = 1 : N \\ s = a + 1 + (b - 1)(N + 1) + (c - 1)N(N + 1) & a = 0 : N, b = 1 : N, c = 1 : N \\ r = i + (j - 1)N + kN^2 & i = 1 : N, j = 1 : N, k = 0 : N \end{cases} \quad (\text{A.1.35})$$

$$\mathbb{A}_{r,(s,t)}^3 = \Phi_{i,l,a}^{0,1,1} \Phi_{b,j,m}^{0,1,1} \Phi_{n,k,c}^{0,1,1}, \quad (\text{A.1.36})$$

with

$$\begin{cases} t = l + (m - 1)N + nN^2 & l = 1 : N, m = 1 : N, n = 0 : N \\ s = a + bN + (c - 1)N(N + 1) & a = 1 : N, b = 0 : N, c = 1 : N \\ r = i + 1 + (j - 1)(N + 1) + (k - 1)N(N + 1) & i = 0 : N, j = 1 : N, k = 1 : N \end{cases} \quad (\text{A.1.37})$$

$$\mathbb{A}_{r,(s,t)}^4 = \Phi_{l,i,a}^{0,1,1} \Phi_{b,j,m}^{0,1,1} \Phi_{k,n,c}^{0,1,1}, \quad (\text{A.1.38})$$

with

$$\begin{cases} t = l + 1 + (m - 1)(N + 1) + (n - 1)N(N + 1) & l = 0 : N, m = 1 : N, n = 1 : N \\ s = a + bN + (c - 1)N(N + 1) & a = 1 : N, b = 0 : N, c = 1 : N \\ r = i + (j - 1)N + kN^2 & i = 1 : N, j = 1 : N, k = 0 : N \end{cases} \quad (\text{A.1.39})$$

$$\mathbb{A}_{r,(s,t)}^5 = \Phi_{i,l,a}^{0,1,1} \Phi_{m,j,b}^{0,1,1} \Phi_{c,k,n}^{0,1,1}, \quad (\text{A.1.40})$$

with

$$\begin{cases} t = l + mN + (n - 1)N(N + 1) & l = 1 : N, m = 0 : N, n = 1 : N \\ s = a + (b - 1)N + cN^2 & a = 1 : N, b = 1 : N, c = 0 : N \\ r = i + 1 + (j - 1)(N + 1) + (k - 1)N(N + 1) & i = 0 : N, j = 1 : N, k = 1 : N \end{cases} \quad (\text{A.1.41})$$

$$\mathbb{A}_{r,(s,t)}^6 = \Phi_{l,i,a}^{0,1,1} \Phi_{j,m,b}^{0,1,1} \Phi_{c,k,n}^{0,1,1}, \quad (\text{A.1.42})$$

with

$$\begin{cases} t = l + 1 + (m - 1)(N + 1) + (n - 1)N(N + 1) & l = 0 : N, m = 1 : N, n = 1 : N \\ s = a + (b - 1)N + cN^2 & a = 1 : N, b = 1 : N, c = 0 : N \\ r = i + jN + (k - 1)N(N + 1) & i = 1 : N, j = 0 : N, k = 1 : N \end{cases} \quad (\text{A.1.43})$$

### A.1.5 Matrix B

Matrix B comes from term  $\int_{\Omega} l_{\mathbf{u}} \star \mathbf{u}^{(2)} \wedge d\sigma^{(2)}$ ,

$$\begin{aligned} l_{\mathbf{u}} \star \mathbf{u}^{(2)} &= \sum_{i=0}^N \sum_{j=1}^N \sum_{k=1}^N u_{i,j,k}^x \sum_{l=0}^N \sum_{m=1}^N \sum_{n=1}^N u_{l,m,n}^x \phi_i^0(x) \phi_j^1(y) \phi_k^1(z) \phi_l^0(x) \phi_m^1(y) \phi_n^1(z) \\ &+ \sum_{i=1}^N \sum_{j=0}^N \sum_{k=1}^N u_{i,j,k}^y \sum_{l=1}^N \sum_{m=0}^N \sum_{n=1}^N u_{l,m,n}^y \phi_i^1(x) \phi_j^0(y) \phi_k^1(z) \phi_l^1(x) \phi_m^0(y) \phi_n^1(z) \\ &+ \sum_{i=1}^N \sum_{j=1}^N \sum_{k=0}^N u_{i,j,k}^z \sum_{l=1}^N \sum_{m=1}^N \sum_{n=0}^N u_{l,m,n}^z \phi_i^1(x) \phi_j^1(y) \phi_k^0(z) \phi_l^1(x) \phi_m^1(y) \phi_n^0(z). \end{aligned} \quad (\text{A.1.44})$$

When  $\lambda^{(3)} = \phi_a^1(x) \phi_b^1(y) \phi_c^1(z) dx \wedge dy \wedge dz$  where  $a = 1 : N, b = 1 : N, c = 1 : N$ ,

$$\begin{aligned} &\int_{\Omega} \lambda^{(3)} \wedge l_{\mathbf{u}} \star \mathbf{u}^{(2)} = \\ &+ \sum_{i=0}^N \sum_{j=1}^N \sum_{k=1}^N u_{i,j,k}^x \sum_{l=0}^N \sum_{m=1}^N \sum_{n=1}^N u_{l,m,n}^x \int_{-1}^1 \phi_i^0(x) \phi_l^0(x) \phi_a^1(x) dx \int_{-1}^1 \phi_j^1(y) \phi_m^1(y) \phi_b^1(y) dy \int_{-1}^1 \phi_k^1(z) \phi_n^1(z) \phi_c^1(z) dz \\ &+ \sum_{i=1}^N \sum_{j=0}^N \sum_{k=1}^N u_{i,j,k}^y \sum_{l=1}^N \sum_{m=0}^N \sum_{n=1}^N u_{l,m,n}^y \int_{-1}^1 \phi_i^1(x) \phi_l^1(x) \phi_a^1(x) dx \int_{-1}^1 \phi_j^0(y) \phi_m^0(y) \phi_b^1(y) dy \int_{-1}^1 \phi_k^1(z) \phi_n^1(z) \phi_c^1(z) dz \\ &+ \sum_{i=1}^N \sum_{j=1}^N \sum_{k=0}^N u_{i,j,k}^z \sum_{l=1}^N \sum_{m=1}^N \sum_{n=0}^N u_{l,m,n}^z \int_{-1}^1 \phi_i^1(x) \phi_l^1(x) \phi_a^1(x) dx \int_{-1}^1 \phi_j^1(y) \phi_m^1(y) \phi_b^1(y) dy \int_{-1}^1 \phi_k^0(z) \phi_n^0(z) \phi_c^1(z) dz \\ &= \\ &+ \sum_{i=0}^N \sum_{j=1}^N \sum_{k=1}^N u_{i,j,k}^x \sum_{l=0}^N \sum_{m=1}^N \sum_{n=1}^N u_{l,m,n}^x \Phi_{i,l,a}^{0,0,1} \Phi_{j,m,b}^{1,1,1} \Phi_{k,n,c}^{1,1,1} \\ &+ \sum_{i=1}^N \sum_{j=0}^N \sum_{k=1}^N u_{i,j,k}^y \sum_{l=1}^N \sum_{m=0}^N \sum_{n=1}^N u_{l,m,n}^y \Phi_{i,l,a}^{1,1,1} \Phi_{j,m,b}^{0,0,1} \Phi_{k,n,c}^{1,1,1} \\ &+ \sum_{i=1}^N \sum_{j=1}^N \sum_{k=0}^N u_{i,j,k}^z \sum_{l=1}^N \sum_{m=1}^N \sum_{n=0}^N u_{l,m,n}^z \Phi_{i,l,a}^{1,1,1} \Phi_{j,m,b}^{1,1,1} \Phi_{k,n,c}^{0,0,1}. \end{aligned} \quad (\text{A.1.45})$$

Therefore, we obtain

$$\begin{aligned} \mathbb{B} &= \left( \mathbb{B}_1^1 \mathbf{u}^x \quad \cdots \quad \mathbb{B}_\mu^1 \mathbf{u}^x \right) \mathbf{u}^x \\ &+ \left( \mathbb{B}_1^2 \mathbf{u}^y \quad \cdots \quad \mathbb{B}_\mu^2 \mathbf{u}^y \right) \mathbf{u}^y \\ &+ \left( \mathbb{B}_1^3 \mathbf{u}^z \quad \cdots \quad \mathbb{B}_\mu^3 \mathbf{u}^z \right) \mathbf{u}^z, \end{aligned} \quad (\text{A.1.46})$$

where  $\mu = N^2(N+1)$  and

$$\mathbb{B}_{r,(s,t)}^1 = \Phi_{i,l,a}^{0,0,1} \Phi_{j,m,b}^{1,1,1} \Phi_{k,n,c}^{1,1,1}, \quad (\text{A.1.47})$$

with

$$\begin{cases} t = l + 1 + (m-1)(N+1) + (n-1)N(N+1) & l = 0 : N, m = 1 : N, n = 1 : N \\ s = a + (b-1)N + (c-1)N^2 & a = 1 : N, b = 1 : N, c = 1 : N \\ r = i + 1 + (j-1)(N+1) + (k-1)N(N+1) & i = 0 : N, j = 1 : N, k = 1 : N \end{cases} \quad (\text{A.1.48})$$

$$\mathbb{B}_{r,(s,t)}^2 = \Phi_{i,l,a}^{1,1,1} \Phi_{j,m,b}^{0,0,1} \Phi_{k,n,c}^{1,1,1}, \quad (\text{A.1.49})$$

with

$$\begin{cases} t = l + mN + (n-1)N(N+1) & l = 1 : N, m = 0 : N, n = 1 : N \\ s = a + (b-1)N + (c-1)N^2 & a = 1 : N, b = 1 : N, c = 1 : N \\ r = i + jN + (k-1)N(N+1) & i = 1 : N, j = 0 : N, k = 1 : N \end{cases} \quad (\text{A.1.50})$$

$$\mathbb{B}_{r,(s,t)}^3 = \Phi_{i,l,a}^{1,1,1} \Phi_{j,m,b}^{1,1,1} \Phi_{k,n,c}^{0,0,1}, \quad (\text{A.1.51})$$

with

$$\begin{cases} t = l + (m-1)N + nN^2 & l = 1 : N, m = 1 : N, n = 0 : N \\ s = a + (b-1)N + (c-1)N^2 & a = 1 : N, b = 1 : N, c = 1 : N \\ r = i + (j-1)N + kN^2 & i = 1 : N, j = 1 : N, k = 0 : N \end{cases} \quad (\text{A.1.52})$$

## A.2 Outer Euler discretization

In terms of the outer Euler, the fully discretized form is given as

$$\begin{cases} -\frac{1}{\Delta t} \left( u_{n+1}^{(2)}, \sigma^{(2)} \right)_\Omega + \frac{1}{\Delta t} \left( u_n^{(2)}, \sigma^{(2)} \right)_\Omega - \int_\Omega \sigma^{(2)} \wedge \iota_u \tilde{\omega}_n^{(2)} + \left( p_{0,n}^{(3)}, d\sigma^{(2)} \right)_\Omega = 0 \\ -\frac{1}{\Delta t} \left( \tilde{\omega}_{n+1}^{(2)}, \zeta^{(1)} \right)_\Omega + \frac{1}{\Delta t} \left( \tilde{\omega}_n^{(2)}, \zeta^{(1)} \right)_\Omega - \int_\Omega d\zeta \wedge \iota_u \tilde{\omega}_n^{(2)} = 0 \\ \left( du_{n+1}^{(2)}, \tau^{(3)} \right)_\Omega = 0 \end{cases}, \quad (\text{A.2.1})$$

which is expressed in matrix form as

$$\begin{pmatrix} \frac{1}{\Delta t} \mathbb{M}^{(1)} & \emptyset & \mathbb{E}^{(2,3)} \mathbb{M}^{(3)} \\ \emptyset & \frac{1}{\Delta t} \mathbb{M}^{(2)} & \emptyset \\ \mathbb{M}^{(3)} \mathbb{E}^{(3,2)} & \emptyset & \emptyset \end{pmatrix} \begin{pmatrix} u_{n+1}^{(2)} \\ \omega_{n+1}^{(1)} \\ p_n^{(3)} \end{pmatrix} = \begin{pmatrix} \frac{1}{\Delta t} \mathbb{M}^{(1)} u_n^{(2)} - \mathbb{A} + \frac{1}{2} \mathbb{B} \\ \frac{1}{\Delta t} \mathbb{M}^{(2)} \omega_n^{(1)} - \mathbb{E}^{(1,2)} \mathbb{A} \\ \mathbf{0} \end{pmatrix}. \quad (\text{A.2.2})$$

**A.2.1 Mass matrix  $\mathbb{M}^{(1)}$** 

$$\mathbb{M}^{(1)} = \begin{pmatrix} \mathbb{M}^{11} & \mathbf{0} & \mathbf{0} \\ \mathbf{0} & \mathbb{M}^{12} & \mathbf{0} \\ \mathbf{0} & \mathbf{0} & \mathbb{M}^{13} \end{pmatrix}. \quad (\text{A.2.3})$$

$$\begin{aligned} \mathbb{M}_{r,s}^{11} &= \int_{-1}^1 \phi_i^1(x) \phi_l^1(x) dx \int_{-1}^1 \phi_j^0(y) \phi_m^0(y) dy \int_{-1}^1 \phi_k^0(z) \phi_n^0(z) dz \\ &= \Phi_{i,l}^{1,1} \Phi_{j,m}^{0,0} \Phi_{k,n}^{0,0}, \end{aligned} \quad (\text{A.2.4})$$

with

$$\begin{cases} r = i + jN + kN(N+1) & i = 1 : N, j = 0 : N, k = 0 : N \\ s = l + mN + nN(N+1) & l = 1 : N, m = 0 : N, n = 0 : N \end{cases}. \quad (\text{A.2.5})$$

$$\begin{aligned} \mathbb{M}_{r,s}^{12} &= \int_{-1}^1 \phi_i^0(x) \phi_l^0(x) dx \int_{-1}^1 \phi_j^1(y) \phi_m^1(y) dy \int_{-1}^1 \phi_k^0(z) \phi_n^0(z) dz \\ &= \Phi_{i,l}^{0,0} \Phi_{j,m}^{1,1} \Phi_{k,n}^{0,0}, \end{aligned} \quad (\text{A.2.6})$$

with

$$\begin{cases} r = i + 1 + (j-1)(N+1) + kN(N+1) & i = 0 : N, j = 1 : N, k = 0 : N \\ s = l + 1 + (m-1)(N+1) + nN(N+1) & l = 0 : N, m = 1 : N, n = 0 : N \end{cases}. \quad (\text{A.2.7})$$

$$\begin{aligned} \mathbb{M}_{r,s}^{13} &= \int_{-1}^1 \phi_i^0(x) \phi_l^0(x) dx \int_{-1}^1 \phi_j^0(y) \phi_m^0(y) dy \int_{-1}^1 \phi_k^1(z) \phi_n^1(z) dz \\ &= \Phi_{i,l}^{0,0} \Phi_{j,m}^{0,0} \Phi_{k,n}^{1,1}, \end{aligned} \quad (\text{A.2.8})$$

with

$$\begin{cases} r = i + 1 + j(N+1) + (k-1)(N+1)^2 & i = 0 : N, j = 0 : N, k = 1 : N \\ s = l + 1 + m(N+1) + (n-1)(N+1)^2 & l = 0 : N, m = 0 : N, n = 1 : N \end{cases}. \quad (\text{A.2.9})$$

**A.2.2 Mass matrix  $\mathbb{M}^{(2)}$** 

$$\mathbb{M}^{(2)} = \begin{pmatrix} \mathbb{M}^{21} & \mathbf{0} & \mathbf{0} \\ \mathbf{0} & \mathbb{M}^{22} & \mathbf{0} \\ \mathbf{0} & \mathbf{0} & \mathbb{M}^{23} \end{pmatrix}. \quad (\text{A.2.10})$$

$$\begin{aligned} \mathbb{M}_{r,s}^{21} &= \int_{-1}^1 \phi_i^0(x) \phi_l^0(x) dx \int_{-1}^1 \phi_j^1(y) \phi_m^1(y) dy \int_{-1}^1 \phi_k^1(z) \phi_n^1(z) dz \\ &= \Phi_{i,l}^{0,0} \Phi_{j,m}^{1,1} \Phi_{k,n}^{1,1}, \end{aligned} \quad (\text{A.2.11})$$

with

$$\begin{cases} r = i + 1 + (j - 1)(N + 1) + (k - 1)N(N + 1) & i = 0 : N, j = 1 : N, k = 1 : N \\ s = l + 1 + (m - 1)(N + 1) + (n - 1)N(N + 1) & l = 0 : N, m = 1 : N, k = 1 : N \end{cases} \quad (\text{A.2.12})$$

$$\begin{aligned} \mathbb{M}_{r,s}^{22} &= \int_{-1}^1 \phi_i^1(x) \phi_l^1(x) dx \int_{-1}^1 \phi_j^0(y) \phi_m^0(y) dy \int_{-1}^1 \phi_k^1(z) \phi_n^1(z) dz \\ &= \Phi_{i,l}^{1,1} \Phi_{j,m}^{0,0} \Phi_{k,n}^{1,1}, \end{aligned} \quad (\text{A.2.13})$$

with

$$\begin{cases} r = i + jN + (k - 1)N(N + 1) & i = 1 : N, j = 0 : N, k = 1 : N \\ s = l + mN + (n - 1)N(N + 1) & l = 1 : N, m = 0 : N, n = 1 : N \end{cases} \quad (\text{A.2.14})$$

$$\begin{aligned} \mathbb{M}_{r,s}^{23} &= \int_{-1}^1 \phi_i^1(x) \phi_l^1(x) dx \int_{-1}^1 \phi_j^1(y) \phi_m^1(y) dy \int_{-1}^1 \phi_k^0(z) \phi_n^0(z) dz \\ &= \Phi_{i,l}^{1,1} \Phi_{j,m}^{1,1} \Phi_{k,n}^{0,0}, \end{aligned} \quad (\text{A.2.15})$$

with

$$\begin{cases} r = i + (j - 1)N + kN^2 & i = 1 : N, j = 1 : N, k = 0 : N \\ s = l + (m - 1)N + nN^2 & l = 1 : N, m = 1 : N, n = 0 : N \end{cases} \quad (\text{A.2.16})$$

### A.2.3 Mass matrix $\mathbb{M}^{(3)}$

$$\begin{aligned} \mathbb{M}_{r,s}^{(3)} &= \int_{-1}^1 \phi_i^1(x) \phi_l^1(x) dx \int_{-1}^1 \phi_j^1(y) \phi_n^1(y) dy \int_{-1}^1 \phi_k^1(z) \phi_m^1(z) dz \\ &= \Phi_{i,l}^{1,1} \Phi_{j,m}^{1,1} \Phi_{k,n}^{1,1}, \end{aligned} \quad (\text{A.2.17})$$

with

$$\begin{cases} r = i + (j - 1)N + (k - 1)N^2 & i = 1 : N, j = 1 : N, k = 1 : N \\ s = l + (m - 1)N + (n - 1)N^2 & l = 1 : N, m = 1 : N, n = 1 : N \end{cases} \quad (\text{A.2.18})$$



